5-1993

A Mechanistic Approach to Modeling Habitat Needs of Drift-Feeding Salmonids

R. Craig Addley
Utah State University

A MECHANISTIC APPROACH TO MODELING HABITAT NEEDS OF DRIFT-FEEDING SALMONIDS

by

R. Craig Addley

A thesis submitted in partial fulfillment
of the requirements for the degree

of

MASTER OF SCIENCE

in

Civil and Environmental Engineering

Approved:

UTAH STATE UNIVERSITY
Logan, Utah

1993

CONTENTS

Page

LIST OF TABLES iv

LIST OF FIGURES v

ABSTRACT ix

INTRODUCTION 1

BACKGROUND (LITERATURE REVIEW) 4

DRIFT-FEEDING MODEL DESCRIPTION 7

General predation cycle 7
Net energy intake model overview 8
Calculating gross energy intake (GEI) 8
Calculating energy losses 15
Calculating energy costs 15
Complete net energy intake (NEI) equation 16
Model assumptions 17

INPUT COMPONENTS OF THE NEI MODEL 19

Reaction distance 19
Swimming velocity 22
Swimming cost 25
Feeding foray cost 26
Assimilation losses and digestion costs 27
Maximum daily food consumption 28
Maximum capture rate 30
Prey capture probability 32
Drift density 33
Drift size 35
Drift dry weight and energy content 37
Uniform drift density assumption 37
Variable water column velocity 38

FIELD VALIDATION 41

Methods and assumptions 41
Results and discussion for data set one 45
Results and discussion for data set two 63

SENSITIVITY ANALYSIS 71

Methods and assumptions 71
Results and discussion 72

SUPPLEMENTARY SENSITIVITY/SIMULATION ANALYSIS 84

Methods and assumptions 84
Results and discussion 84

DISCUSSION 113

General discussion 113
Predictions and insights from the model 115
Engineering significance (application of the model) . . 118
Recommendations 120

REFERENCES 121

APPENDIX 129

SENSITIVITY ANALYSIS GRAPHS 130

LIST OF TABLES

Table		Page
1	Daytime drift densities and relative percentages of aquatic invertebrate taxa in St. Charles Creek, Idaho, during the summer	34
2	Size composition of daytime drifting aquatic invertebrates in St. Charles Creek, Idaho	36
3	Equations used in the net energy intake (NEI) model . .	44

LIST OF FIGURES

Figure		Page
1	Schematic representation of the mechanisms of prey capture for stream-dwelling salmonids	10
2	Representation of the maximum capture distance (MCD) of a fish in all directions on the plane perpendicular to the fish's axis	12
3	The relationship between prey length and reaction distance	21
4	Relationship between fish length, temperature, and swimming velocity	23
5	Relationship between 60-minute sustained swimming velocity, fish length, and temperature for sockeye salmon	24
6	Comparison of the swimming cost equation derived by Stewart (1980) and actual rainbow trout swimming cost data from Rao (1968)	26
7	Relationship between maximum energy intake and temperature	29
8	Comparison of maximum capture rate given the time to complete a prey capture foray	31
9	Length-frequency distributions of drifting invertebrates in three separate reaches of St. Charles Creek, Idaho	36
10	Plot of the A and B coefficients derived for the empirical velocity equation (equation 29)	40
11	Frequency histogram of the available habitat in St. Charles Creek, Idaho	45
12	Frequency histogram of the number of cutthroat trout observed at each total depth/mean velocity combination in St. Charles Creek, Idaho	47
13	Frequency histogram of the number of cutthroat trout observed at each total depth/mean velocity combination in St. Charles Creek, Idaho	48
14	Frequency histogram of the number of cutthroat trout observed at each total depth/mean velocity combination in St. Charles Creek, Idaho	49

15 Frequency histogram of the number of cutthroat trout observed at each total depth/mean velocity combination in St. Charles Creek, Idaho 50

16 Calculated preference of cutthroat trout in St. Charles Creek, Idaho, for each total depth/mean velocity combination 51

17 Calculated preference of cutthroat trout in St. Charles Creek, Idaho, for each total depth/mean velocity combination 52

18 Calculated preference of cutthroat trout in St. Charles Creek, Idaho, for each total depth/mean velocity combination 53

19 Calculated preference of cutthroat trout in St. Charles Creek, Idaho, for each total depth/mean velocity combination 54

20 NEI modeled at each total depth and mean column velocity combination for 30 mm trout at 12°C. 57

21 NEI modeled at each total depth and mean column velocity combination for 50 mm trout at 12°C. 58

22 NEI modeled at each total depth and mean column velocity combination for 100 mm trout at 12°C. 59

23 NEI modeled at each total depth and mean column velocity combination for 200 mm trout at 12°C. 60

24 Correlation between relative fish preference (# fish/available habitat, scaled between 0 and 1.0) and percent of maximum NEI predicted by the NEI model (in 10% increments) for each of the different size classes of fish combined (10-39, 40-69, 70-159, 160-490 mm) 61

25 Correlation between relative fish preference (# fish/available habitat, scaled between 0 and 1.0) and percent of maximum NEI predicted by the NEI model (in 10% increments) for each of the different size classes of fish separately 62

26 Modeled NEI and observed fish locations at Station 60 (a run) in St. Charles Creek 64

27 Modeled NEI and observed fish locations at Station 60 (a run) in St. Charles Creek 65

28 Modeled NEI and observed fish locations at Station 59 (a pool) in St. Charles Creek 66

29 Modeled NEI and observed fish locations at Station 50 (a run) in St. Charles Creek 67

30 Modeled NEI and observed fish locations at Station 48 (a pool) in St. Charles Creek 68

31 Correlation between relative fish preference (# fish/available habitat, scaled between 0 and 1.0) and percent of maximum NEI predicted by the NEI model (in 10% increments) for all stations combined (Station 60, 59, 50, and 48) 70

32 Baseline NEI surface used for sensitivity analysis . . . 73

33 Percent change (sensitivity) of the volume under the NEI surface to 10% changes of each parameter used to model the NEI surface 74

34 Percent change (sensitivity) of the NEI centroid for the volume under the NEI surface to 10% changes of each parameter used to model the NEI surface 75

35 Percent change (sensitivity) of the depth centroid for the volume under the baseline NEI surface to 10% changes of each model parameter 76

36 Percent change (sensitivity) of the velocity centroid for the volume under the NEI surface to 10% changes of each parameter used to model the NEI surface 77

37 Plot of gross energy intake (GEI), NEI, and swimming cost for a 25 mm fish over a range of mean velocities at a total depth of 45 cm 86

38 Plot of gross energy intake (GEI), NEI, and swimming cost for a 50 mm fish over a range of mean velocities at a total depth of 45 cm 87

39 Plot of gross energy intake (GEI), NEI, and swimming cost for a 100 mm fish over a range of mean velocities at a total depth of 50 cm 88

40 Plot of gross energy intake (GEI), NEI, and swimming cost for a 200 mm fish over a range of mean velocities at a total depth of 65 cm 89

41 Plot of gross energy intake (GEI), NEI, and swimming cost for a 150 mm fish over a range of mean velocities at a total depth of 60 cm 90

42 Plot of gross energy intake (GEI), NEI, and swimming cost for a 200 mm fish over a range of total depths at a mean velocity of 45 cm/s 91

43 Modeled NEI for a 150 mm fish at a drift density of 0 prey/100 m^3 and a temperature of 12°C 93

44 Modeled NEI for a 150 mm fish at a drift density of 50 prey/100 m^3 and a temperature of 12°C 94

45 Modeled NEI for a 150 mm fish at a drift density of 100 prey/100 m^3 and a temperature of 12°C 95

46 Modeled NEI for a 150 mm fish at a drift density of 400 prey/100 m^3 and a temperature of 12°C 96

47 Modeled NEI for a 150 mm fish at a drift density of 1000 prey/100 m^3 and a temperature of 12°C 97

48 Modeled NEI for a 200 mm fish at a temperature of 3°C and a drift density of 400 prey/100 m^3 98

49 Modeled NEI for a 200 mm fish at a temperature of 9°C and a drift density of 400 prey/100 m^3 99

50 Modeled NEI for a 200 mm fish at a temperature of 17°C and a drift density of 400 prey/100 m^3 100

51 Modeled NEI for a 150 mm fish at a reaction distance of 37.8 cm, a temperature of 12°C, and a drift density of 400 prey/100 m^3 102

52 Modeled NEI for a 150 mm fish at a reaction distance of 65.2 cm, a temperature of 12°C, and a drift density of 400 prey/100 m^3 103

53 Modeled NEI for a 150 mm fish at a reaction distance of 96.6 cm, a temperature of 12°C, and a drift density of 400 prey/100 m^3 104

54 Satiation time versus hourly consumption rate (GEI) for 25 mm fish at temperatures of 4, 8, 12, and 17.8°C . 106

55 Satiation time versus hourly consumption rate (GEI) for 50 mm fish at temperatures of 4, 8, 12, and 17.8°C 107

56 Satiation time versus hourly consumption rate (GEI) for 100 mm fish at temperatures of 4, 8, 12, and 17.8°C 108

57 Satiation time versus hourly consumption rate (GEI) for 200 mm fish at temperatures of 4, 8, 12, and 17.8°C 109

58 The effect of fish size on satiation time 111

59 The effect of temperature on satiation time for a 200 mm fish 112

ABSTRACT

A Mechanistic Approach to Modeling Habitat Needs
of Drift-Feeding Salmonids

by

R. Craig Addley, Master of Science
Utah State University, 1993

Major Professor: Dr. Thomas B. Hardy
Department: Civil and Environmental Engineering

A mechanistic model is developed to determine the habitat needs of drift-feeding stream salmonids from the direct cause-and-effect relationships of environmental and physiological variables on net energy intake (NEI). The model determines NEI by subtracting energy costs (basal metabolism, swimming cost, digestion cost) and losses (egestion and excretion) from the gross energy intake obtained as a result of simulated prey capture. The prey capture portion of the model utilizes components of the predation model of C.S. Holling and the prey capture model of N.F. Hughes and L.M. Dill to determine the rate of prey capture (gross energy intake) as a function of fish size, water velocity, water depth, water temperature, and the amount of drift. Physiological input parameters for the model are estimated from the literature.

Two separate validation tests of the model's ability to predict stream habitat use of trout, primarily cutthroat trout (*Oncorhynchus clarki*), in St. Charles Creek, Idaho, are presented. In both cases, the NEI model closely predicts the

stream habitat that different size classes of fish utilize. The validation tests provide strong evidence that drift-feeding fish utilize stream habitats that provide high rates of NEI as determined by the model.

Sensitivity and simulation analyses of the model are used to identify the most important input parameters and to illustrate in terms of energetics why drift-feeding fish utilize various habitats. Model simulations explain why fish utilize deeper and faster habitats as they get larger and why they utilize slower habitats in the winter. In addition, it is shown that streams with high drift rates should theoretically provide more usable salmonid habitat than similar streams with lower drift rates.

(151 pages)

INTRODUCTION

At present, over 70 models or methods have been used throughout the United States to determine appropriate instream flow requirements or characterize the quality of aquatic fish habitat in streams (EA Engineering, Science, and Technology, Inc., 1986). Although several of these methods have been developed for generalized applications, few have met with broad success. At the present time, the Instream Flow Incremental Methodology (IFIM) is the most widely applied method and is required or preferred in 24 states and Canadian provinces (Reiser, Wesche, and Estes, 1989). Although this method has been "institutionalized" to a large degree, it remains broadly unvalidated. Furthermore, it has been criticized for its lack of demonstrable correlation to fish standing crop biomass or population dynamics (Orth and Maughan, 1982; Scott and Shirvell, 1987).

One of the primary motivations for developing habitat models for stream-dwelling fish stems from the urgent need of lotic ecologists to understand the habitat needs of stream fish and be able to predict the effects of stream alterations on stream fisheries. Streams and rivers are particularly vulnerable to anthropogenic disturbances and many of the world's rivers and streams have been, or are in the process of being, subjected to extensive dam building, diking, channelization, clearing of woody debris, and dewatering (Power et al., 1988). In order to rationally assess or predict the impacts of such disturbances on stream fisheries, it is essential to understand what biotic and abiotic factors are important to fish and the mechanisms by which they affect individual fish and ultimately fish populations.

The purpose of this research was to develop a mechanistic stream habitat model for drift-feeding salmonids and evaluate it using cutthroat trout (*Oncorhynchus clarki*). The model is an individual-based, mechanistic model of net energy intake (NEI) that can be used to explain and predict habitat needs of drift-feeding fish in terms of fitness attained through energy acquisition and growth. The rationale for developing a *mechanistic* model is twofold: (1) an accurate mechanistic model would be capable of predicting habitat needs from direct cause-and-effect relationships of environmental variables under existing or altered flow regimes, and (2) a mechanistic model would have the potential to *explain* empirical (observed) patterns of habitat use by stream-dwelling salmonids. The rationale for developing a model of NEI is that fish should, and often do, select and utilize habitats that provide high rates of NEI (Fausch, 1984; Townsend and Winfield, 1985; Wilzbach, 1985; Stephens and Krebs, 1986; Hughes, 1991). Ware (1982) argued that NEI (surplus power in his paper) is an analogue of fitness and that natural selection has operated such that fish behavior (and fish morphology) is correlated to the acquisition of increased NEI, which in turn results in increased fitness.

The model developed in this paper is designed to provide a conceptually sound method of quantifying NEI in streams for individual drift-feeding fish. The model design assumes that NEI of individual fish is the primary factor that determines habitat utilization in drift-feeding fish and that biotic and abiotic variables in streams that influence habitat suitability for drift-feeding salmonids do so solely through their direct or

indirect effects on NEI. Because of these assumptions, the model fails to address a number of other factors that can affect habitat suitability/utilization. Because the model addresses only NEI, it fails to address behaviors other than those related to feeding energetics, and because the model is individual-based, it fails to account for the results of intra- and interspecific competition and predation. Nevertheless, the working hypothesis of this paper is that if NEI can be quantified, then the effects of NEI and other factors (e.g., cover for predation avoidance) on habitat utilization/suitability can more readily be elucidated and/or quantified.

BACKGROUND (LITERATURE REVIEW)

A significant amount of fisheries literature shows that NEI is an important factor controlling habitat utilization of salmonids. A number of authors have found that drift-feeding salmonids choose and defend specific locations in streams that provide high NEI (Jenkins, 1969; Chapman and Bjornn, 1969; Everest and Chapman, 1972; Fausch, 1984; Hill, 1989; Hughes and Dill, 1990). These locations are typically areas with low focal velocity where swimming costs are low, yet near high velocities where large amounts of drifting food is available. Research has also shown that drift-feeding salmonids form linear dominance hierarchies, where larger (more dominate) fish defend the best net energy sites and smaller (less dominate) fish are forced to occupy less energetically optimum sites (Fausch, 1984; Hughes, 1991).

Three authors to date have attempted to quantify NEI and the effects of NEI on microhabitat choice. Fausch (1984) used a measure of drift energy available (number of prey items available to be ingested) minus swimming costs incurred maintaining stream position to calculate potential profit (potential net energy intake) for salmonids in an artificial stream channel. Fausch used the amount of drift passing through a pie-shaped "window" at the highest velocity within two body lengths of the fish as a measure of available drift energy. The energy cost of swimming at a given focal velocity was calculated from equations developed by Stewart (1980). Fausch found that his measure of potential profit was correlated with the specific growth rate of the fish and with the linear dominance hierarchy of the fish population.

Individuals with the highest potential profit grew at the highest specific growth rate. Additionally, the largest fish defended positions in the stream with the highest potential profit and hence grew the fastest while the smaller fish were forced to use microhabitats with less potential profit and grew at lower specific growth rates.

Hill (1989) and Hill and Grossman (1993) calculated NEI for rainbow trout (*Oncorhynchus mykiss*) by empirically measuring capture success of drifting invertebrates at different current velocities and subtracting swimming cost, assimilation losses, and digestion costs from the gross energy intake (GEI). Hill found that the velocities with the highest predicted NEI closely matched actual velocities used by rainbow trout in Coweeta Creek, North Carolina.

Hughes and Dill (1990) and Hughes (1991) added significantly to the development of a more mechanistic model of potential energy intake. Hughes and Dill modeled potential net energy intake using the mechanisms of prey capture. The swimming speed of the fish and the average velocity of drifting prey items in the water column were used to calculate a maximum capture distance (MCD). Using this MCD, a maximum capture area was derived through which potential prey items would pass. Assuming that all prey items passing through this maximum capture area would be ingested, they calculated potential net energy intake by subtracting swimming cost to maintain position from the gross energy content of prey passing through the capture area. Hughes and Dill (1990) found that their model of potential net energy intake was an excellent predictor of position choice for solitary

Arctic grayling. They found that grayling chose feeding positions in the stream with the highest NEI and that their model was able to predict position choice significantly better than the more simplistic model of Fausch (1984). Hughes (1991) also found that dominant fish occupied the highest NEI sites while smaller fish occupied sequentially less optimum NEI sites.

DRIFT-FEEDING MODEL DESCRIPTION

General predation cycle

Observational descriptions of the drift-feeding behavior of stream salmonids (e.g., Wankowski, 1979; Bachman, 1984) are compatible with the conceptual model of predation developed by Holling (1959; 1966), which separates predation into components of search, encounter, recognition, pursuit, capture, eating, and digestion. This model has been used in the past to analyze feeding behavior in particulate-feeding fish (e.g., Eggers, 1975; Ringler and Brodowski, 1983; Wright and O'Brien, 1984) and is used as the basis for the development of the mechanistic NEI model.

Typical predatory behavior of stream-dwelling salmonids consists of fish holding station in the water current at discrete focal locations they have chosen within their home range. From these focal locations they visually locate prey items and move to intercept them. Home ranges are relatively small, 15 m^2 (Bachman, 1984) to 22 m^2 (Heggenes, Northcote, and Peter, 1991), and the number of feeding locations are few, ca. six (Bachman, 1984). After a prey item has been intercepted, fish return to their feeding locations (sometimes after being swept some distance downstream) and resume visually searching for food. If the amount of drifting food is very low or if it becomes dark, fish may leave their feeding locations and assume positions in areas with low water velocity (resting locations) (Edmundson, Everest, and Chapman, 1968; Campbell and Neuner, 1985; Hughes, 1991).

Net energy intake model overview

The proposed drift-feeding model simulates net energy intake (NEI) by calculating the number of drifting prey that a fish can capture in a given time (gross energy intake) and subtracting energy costs and losses. Energy costs are the metabolic cost incurred during stationary swimming while waiting for prey (SC), the metabolic cost incurred during prey capture (CC), and the cost of digesting prey (F_d). Energy losses are energy lost as nonassimilated gross energy intake (GEI) egested as feces (F) and assimilated GEI excreted as ammonia and urea (U) (i.e., waste products). The balanced energy equation for calculating NEI is as follows:

$$NEI = GEI - SC - CC - F - U - F_d \qquad (1)$$

Calculating gross energy intake (GEI)

Calculation of GEI is accomplished by modeling the mechanism of prey capture for drift-feeding fish (Hughes and Dill, 1990). Fish maintain a holding station in the current while searching for prey. They have a forward-facing hemispherical reaction distance within which prey are seen and recognized (Confer et al., 1978; Luecke and O'Brien, 1981; Dunbrack and Dill, 1984). Sighted prey will be captured (energy intake) if the fish decides to attempt capture and can reach the prey before it is swept past the fish's focal location. The velocity of the water determines the velocity of the prey and the amount of time the fish has to intercept the prey. Prey location (distance from the fish), swimming speed of the fish, and the water velocity that the fish must swim against to maintain station all interact to determine

whether the fish will physically be able to intercept a prey item before it passes the fish. After a prey attack occurs, the fish returns to its focal position to resume searching for prey.

The actual capture of prey is modeled by defining the size of the area within which the fish can reach drifting prey from its focal position before the prey passes the fish. To determine the size of the capture area, the maximum distance the fish can capture a drifting prey item in every direction perpendicular and transverse to the fish (e.g., left, right, up, and down) is calculated using the kinematics of fish locomotion from a fixed focal position and the kinematics of drifting prey.

Calculating maximum capture distance. Figure 1 shows a schematic of the mechanisms of prey capture described by Hughes and Dill (1990). The time it takes the prey item to move past the fish along line segment BC is:

$$TP = \frac{(RD^2 - AC^2)^{1/2}}{V_p} \quad OR \quad TP = \frac{BC}{V_p} \qquad (2)$$

where: TP = time required for the prey item to reach a line perpendicular to the fish's focal point

RD = reaction distance of the fish to the prey item

AC = distance from the fish to the point where the prey item crosses the line perpendicular to the fish

V_p = velocity of the drifting prey item

BC = distance from visual recognition of the prey item to the line perpendicular to the fish

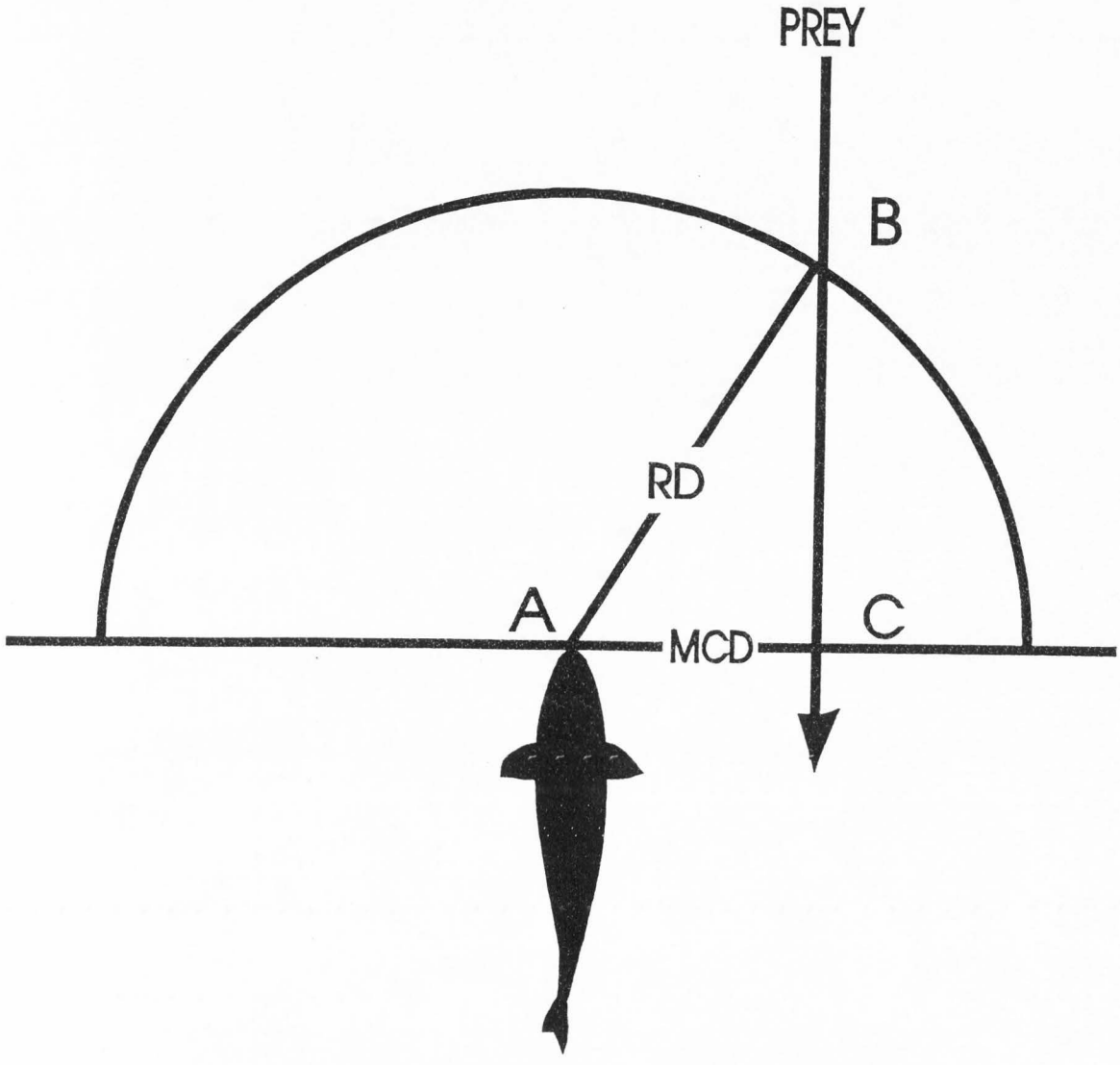

Figure 1. Schematic representation of the mechanisms of prey capture for a stream-dwelling salmonid (plan view). The schematic represents a fish holding station in a stream with a forward facing reaction distance (RD) represented by the arc and line segment AB. To capture a prey item the fish must move distance AC relative to the stream bed before the prey moves distance CB. The maximum distance the fish can capture prey in a given distance is termed the maximum capture distance (MCD) (adapted from Hughes and Dill, 1990).

The time it takes the fish to intercept prey on the perpendicular line AC is:

$$TF = \left(\frac{AC^2}{V_{max}^2 - V_{mean}^2} \right)^{1/2} \qquad OR \qquad TF = \frac{AC}{V_x} \tag{3}$$

where: TF = time it takes fish to intercept prey

V_{max} = maximum velocity the fish will swim to capture prey

V_{mean} = average water velocity between the fish and the capture point on the perpendicular line AC

V_x = velocity component of the fish in the direction of the perpendicular line AC ($V_x = (V_{max}^2 - V_{mean}^2)^{1/2}$)

By using an iterative solution method, the maximum capture distance (MCD) in any direction in the plane perpendicular and transverse to the fish can be calculated by solving for the distance where TF = TP. Figure 2 shows the MCDs for a fish in the plane perpendicular and transverse to the fish. Note that the vertical MCD is shorter than the horizontal MCD. This results from the higher water velocities higher in the water column.

An equation for MCD can also be derived by setting TF = TP (equation 1 = equation 2) and solving for MCD (variable AC):

$$MCD = \sqrt{\frac{RD^2 (V_{max}^2 - V_{mean}^2)}{V_{max}^2 + V_p - V_{mean}^2}} \tag{4}$$

Unfortunately equation 4 is not easily solved. The equation is an implicit equation because V_{mean} is a function of MCD.

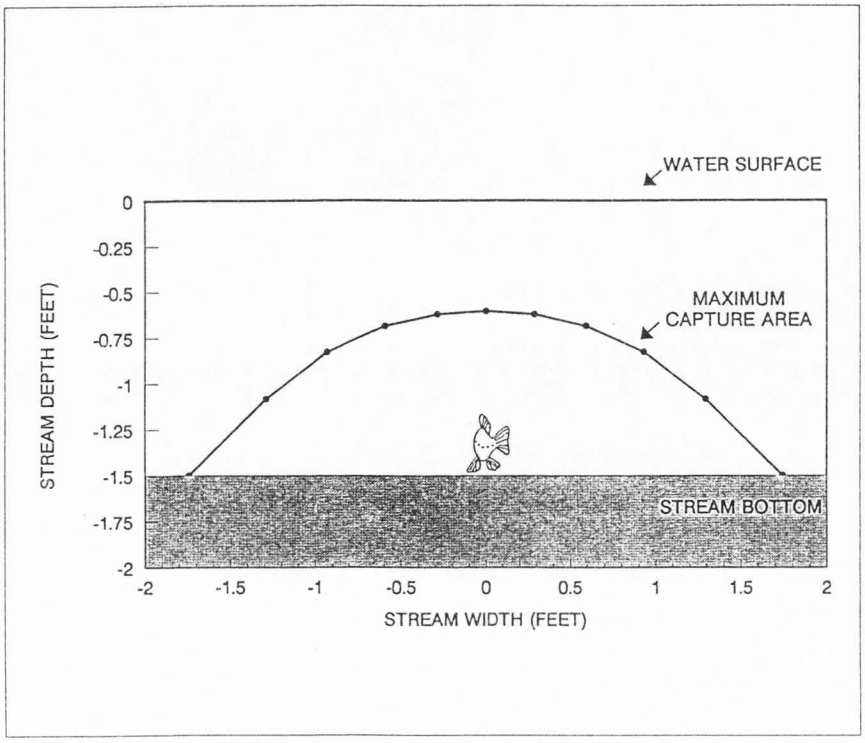

Figure 2. Representation of the maximum capture distance (MCD) of a fish in all directions on the plane perpendicular to the fish's axis. By connecting the MCDs together a maximum capture area (MCA) can be defined. Theoretically, any prey item passing through the MCA can be captured. The shorter MCD in the vertical direction is a function of the faster water velocities higher in the water column.

Equation 4 reduces to the same equation used by Hughes and Dill (1990) for the special case where the water velocity is the same throughout the water column. Hughes and Dill assumed the water velocity throughout the water column equaled the average column velocity. By setting $V_p = V_{mean} = V$, where V is the average column velocity of the water, equation 4 reduces to:

$$MCD = \sqrt{RD^2 - \left(\frac{V \cdot RD}{V_{max}}\right)^2} \qquad (5)$$

Calculating maximum capture area. After calculating MCD in all directions in the plane perpendicular and transverse to the fish using the kinematics of fish locomotion, the topography of the stream, and water velocity throughout the stream, a maximum capture area is calculated. Figure 2 shows that integration of the MCDs forms a maximum capture area (MCA). Any prey item that passes through the MCA can theoretically be captured by the fish.

Gross energy intake. The gross energy intake (GEI) is the total prey energy captured by the fish. GEI can be estimated in an idealized manner by multiplying the MCA by the average water velocity flowing through the MCA to obtain the water flow rate (volume/time) and then multiplying flow rate and drift density (prey/volume) to get the number of prey/time passing through the capture area. The potential number of prey captured are subsequently converted into energy units. Thus:

$$GEI^{*} = \sum_{i=1}^{n} MCA_i \cdot V_{ave\,i} \cdot DD_i \cdot PE_i \qquad (6)$$

where: GEI^{*} = idealized gross energy intake (J/sec)

MCA_i = maximum capture area for the *i*th prey size (m^2)

$V_{ave\,i}$ = average velocity through MCA_i for the *i*th prey size (m/sec)

DD_i = drift density for the *i*th prey size ($prey/m^3$)

PE = energy content of the *i*th prey item (J)

n = number of size classes of prey

This idealized formulation of equation 6 does not account for limits imposed on GEI by time constraints during foraging, the probability that the feeding foray will result in a successful

prey capture (PC), or the digestive capacity of a given size fish. Because fish will miss opportunities to capture prey items while they are making a feeding foray, the real GEI of the fish will be lower than GEI*:

$$GEI^* \geq GEI \tag{7}$$

The maximum number of feeding forays or prey captures (MNC) a fish can make over a time interval is:

$$MNC = \frac{t_a}{t_w + t_f} \tag{8}$$

where t_a is the time step available for feeding (e.g., 1 hr), t_w is the time spent waiting for prey, and t_f is the time required to execute a feeding foray (Bres, 1986). Including the probability that the feeding foray will result in a successful capture (PC) in equation 8 and multiplying the MNC by the energy content of a prey item to obtain gross energy intake (GEI) result in the following equation:

$$GEI = \frac{PE \cdot PC}{t_w + t_f} \tag{9}$$

A complete discussion of calculating the time and probability variables will be provided in following sections. An equation for the time waiting (t_w) variable found in equations 8 and 9, however, is shown here:

$$t_w = \frac{1}{MCA \cdot V_{ave} \cdot DD} \tag{10}$$

It is important to note that equation 9 is equivalent to the disc equation of Holling (1959). By combining equations 9 and 10, the resulting expression for GEI is:

$$GEI = \frac{PE \cdot PC}{\frac{1}{MCA \cdot V_{ave} \cdot DD} + t_f} \qquad (11)$$

Equation 11 rearranged into a form equivalent to the disc equation of Holling (1959) is:

$$GEI = \frac{MCA \cdot V_{ave} \cdot DD \cdot PE \cdot PC}{1 + t_f \cdot MCA \cdot V_{ave} \cdot DD} \qquad (12)$$

where $MCA \cdot V_{ave}$ is the "instantaneous rate of discovery" and t_f is the "handling time."

GEI will also be limited by the amount of food a fish can consume. Maximum consumption is a function of stomach capacity and gastric evacuation rates (Elliott, 1975a). The daily GEI, therefore, must be less than maximum daily consumption (MAXC):

$$GEI \leq MAXC \qquad (13)$$

Calculating energy losses

A fraction of GEI is lost as waste products. Waste products are nonassimilated energy egested as feces (F) and assimilated energy excreted as ammonia and urea (U). Waste losses generally range between 25-30% of GEI (Elliott, 1976).

Calculating energy costs

Energy costs include (1) metabolism while the fish is maintaining position (stationary swimming) and capturing prey, and (2) digestion of food. The energetic costs of food digestion

(F_d) include energy used in deamination of proteins, mechanical digestion, assimilation, and storage (Ney, 1990). Food digestion costs appear to range from 12-16% of the GEI (Brett and Groves, 1979). Metabolic costs are swimming cost (SC), which includes basal metabolic and locomotion costs for maintaining focal location, and capture cost (CC), which includes basal metabolic and locomotion costs expended in capturing prey. Swimming cost (SC) and capture cost (CC) are functions of swimming velocity, acceleration, and temperature. Actual equations to calculate SC and CC are discussed in following sections of the paper.

Complete net energy intake (NEI) equation

Based on the components of the energy balance equation (equation 1) and the prey capture equation (equation 12), the final balanced energy equation for calculating NEI is as follows:

$$NEI_{(energy/time)} = \frac{\sum_{i=1}^{n} MCA_i \cdot V_{ave\ i} \cdot DD_i \cdot PC_i \cdot (E_i - CC_i) - SC}{1 + \sum_{i=1}^{n} t_{f\,i} \cdot MCA_i \cdot V_{ave\ i} \cdot DD_i} \qquad (14)$$

where i represents each size class of prey, SC (swimming cost) and CC (capture cost) are discussed in following sections, and E is the energy gained from a single prey item after the energy losses and food digestion costs are subtracted. Thus:

$$E = PE - F - U - F_d \qquad OR \qquad E \approx 0.58\,PE \qquad (15)$$

where E ≈ 0.58 PE results because energy losses from F, U, and F_d equal approximately 42% of the PE (prey energy) ingested.

It should be noted that equation 14, while derived independently, is nearly identical to equation 3 in Dunbrack and Giguere (1987), which was used to model the bioenergetics of predator movement. The primary difference is that the encounter value λ or $MCA \cdot V_{ave} \cdot DD$ in this model is not strictly a function of reaction distance, but involves the kinematics of fish locomotion.

Model assumptions

The model presented above represents an effort to develop a quantitative model of NEI based on the mechanisms of predation in stream-dwelling salmonids. In this development, the following have been assumed:

(1) That fish habitat choice is based on NEI

(2) That the maximum capture distance is accurately described using fish swimming velocities without including acceleration

(3) That constraining prey capture to the plane perpendicular to the fish is realistic (accurate)

(4) That the density of prey items in the water is constant at all water velocities

(5) That the time constraint on GEI resulting from fish not being able to search for prey while making a feeding foray can be modeled

(6) That the probability of capture is known or obtainable (e.g., capture probability may be a function of water velocity)

(7) That an upper bound on GEI due to satiation of the fish can accurately be modeled

(8) That the water velocity is known throughout the three-dimensional water column

(9) That the unsteady locomotion costs of capturing prey (acceleration and deceleration) can be modeled.

INPUT COMPONENTS OF THE NEI MODEL

In this section the individual input parameters to the NEI model are briefly discussed and quantified. The input components of the model are reaction distance, swimming velocity, swimming cost, assimilation losses and digestion costs, maximum daily consumption, maximum feeding rate, capture efficiency, drift quantity and size, and water velocity. Input parameters were chosen to be as applicable to cutthroat trout as possible; however, because of the paucity of data available, it was necessary to utilize input parameters from research on a wide range of salmonid species.

Reaction distance

The reaction distance of a fish is the distance at which the fish can visually locate a prey item and recognize that it is a prey item. The reaction distance of fish can be visualized as a hemisphere in front of the fish (Confer et al., 1978; Luecke and O'Brien, 1981; Dunbrack and Dill, 1984). The length of the reactive distance increases with increasing illumination and contrast (Confer et al., 1978; Kettle and O'Brien, 1978; Levine, Lobel, and McNichol, 1979; Henderson, 1982; Lazzaro, 1987) and increases with increasing size of prey (e.g., Confer and Blades, 1975; Vinyard and O'Brien, 1976; Confer et al., 1978; Henderson, 1982; Schmidt and O'Brien, 1982; Dunbrack and Dill, 1983). Reaction distance increases with motion of prey items (Ware, 1973; Henderson, 1982) and decreases with increasing water turbidity (Vinyard and O'Brien, 1976; Confer et al., 1978). In addition, larger fish have larger reactive distances than small fish (e.g., Dunbrack and Dill, 1983; Schmidt and O'Brien, 1982).

A number of pertinent reaction distances reported in the literature have been combined in Figure 3. The scatter is largely a function of differing experimental conditions such as different types of prey, different species and sizes of fish, and moving or stationary prey. To get an estimate of reaction distance for the NEI model, an equation was fit to the reaction distance data of Dunbrack and Dill (1983). The data from Dunbrack and Dill were used because they allowed an equation to be fit for different fish sizes; nevertheless, the data are less than desirable because they were only for prey drifting on the surface, the prey sizes were reported in widths instead of lengths, and fish were coho salmon and not cutthroat trout. Figure 3 shows a reaction distance curve for a 150 mm fish based on the empirical data of Dunbrack and Dill (1983) and the theoretical work of Ware (1973) that suggests the prey length-reaction distance relationship should have the form of a second degree polynomial, but Eggers (1977) shows the relationship varies depending on inherent contrast. The reaction distance and prey length equation for the NEI model input is:

$$PL = (RD^2 + 50\ RD)\left(\frac{1 + 5.8\ e^{-0.34\ FL}}{1725}\right) \qquad (16)$$

where: PL = prey length (mm)

RD = reaction distance (cm)

FL = total fish length (mm)

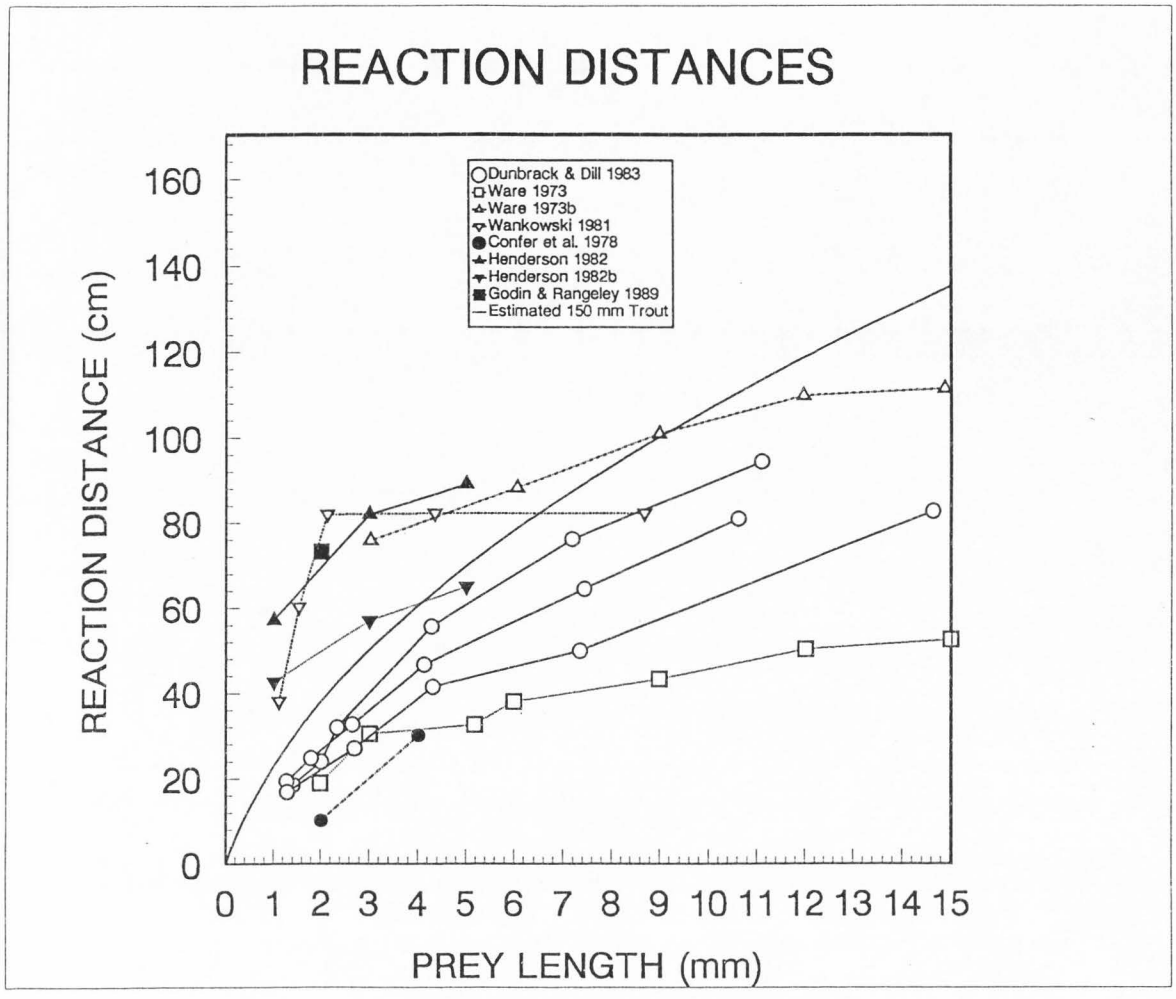

Figure 3. The relationship between prey length and reaction distance. Dunbrack and Dill (1983) 80 mm coho and drifting Plecoptera nymphs at 2160 lux. The prey sizes were reported as widths but converted to lengths via $L=4.925W^{1.203}$ (C. Hawkins, 1992, unpublished data). Ware (1973) 110-140 mm rainbow trout and stationary chicken liver at 10 lux. Ware $(1973)_b$ same as previous but with moving prey. Wankowski (1981) juvenile Atlantic salmon and drifting prey at 2.33 W m^{-1}. Confer et al. (1978) 70-150 mm lake and brook trout and zooplankton at 1450 lux. Confer and Blades (1975) pumpkinseed and zooplankton. Henderson (1982) 180-240 mm cutthroat trout and chicken liver at approximately 100 lux. Henderson $(1982)_b$ same as above except at approximately 2 lux. Godin and Rangeley (1989) 53 mm Atlantic salmon and drifting, cylindrical pieces of euphausiids at 350 lux. The solid line is a reaction distance curve for a 150 mm fish modeled from equation 16 in the text.

Swimming velocity

The velocity that a fish is capable of swimming depends on the size of the fish (Fry and Cox, 1970; Brett and Glass, 1973; Jones, Kiceniuk, and Bamford, 1974; Glova and McInerney, 1977; Beamish, 1978), the water temperature (Brett, Hollands, and Alderdice, 1958; Griffiths and Alderdice, 1972; Brett and Glass, 1973; Glova and McInerney, 1977; Beamish, 1978), the species of fish, the prehistory of the fish (Brett, Hollands, and Alderdice, 1958; Webb, 1975), and the amount of time the velocity must be sustained (Brett, 1964). Figure 4 shows a plot of a number of swimming velocity relationships found in the literature.

For the NEI model, the 60-minute maximum sustained swimming speed for sockeye salmon (Brett and Glass, 1973) is used for both the maximum velocity that fish will swim to maintain position and capture prey. The 60-minute maximum sustained swimming speed is a good estimate of the maximum sustained speed, and the sockeye salmon data are the only salmonid data available that cover a complete range of fish sizes and temperatures. It would be more accurate to use swimming velocity data developed specifically for cutthroat trout and for prey capture, but they are not available. The 60-minute maximum sustained swimming speed equations are:

$$\begin{array}{ll} 2^{\circ}C & \log V_{max} = 0.9053+0.6294 \log T_L \\ 5^{\circ}C & \log V_{max} = 0.9555+0.6243 \log T_L \\ 10^{\circ}C & \log V_{max} = 1.0346+0.6294 \log T_L \\ 15^{\circ}C & \log V_{max} = 1.1289+0.6345 \log T_L \\ 20^{\circ}C & \log V_{max} = 1.1031+0.6293 \log T_L \end{array} \qquad (17)$$

where: V_{max} = maximum sustained swimming speed (cm/s)

T_L = total length (cm)

T = temperature (°C)

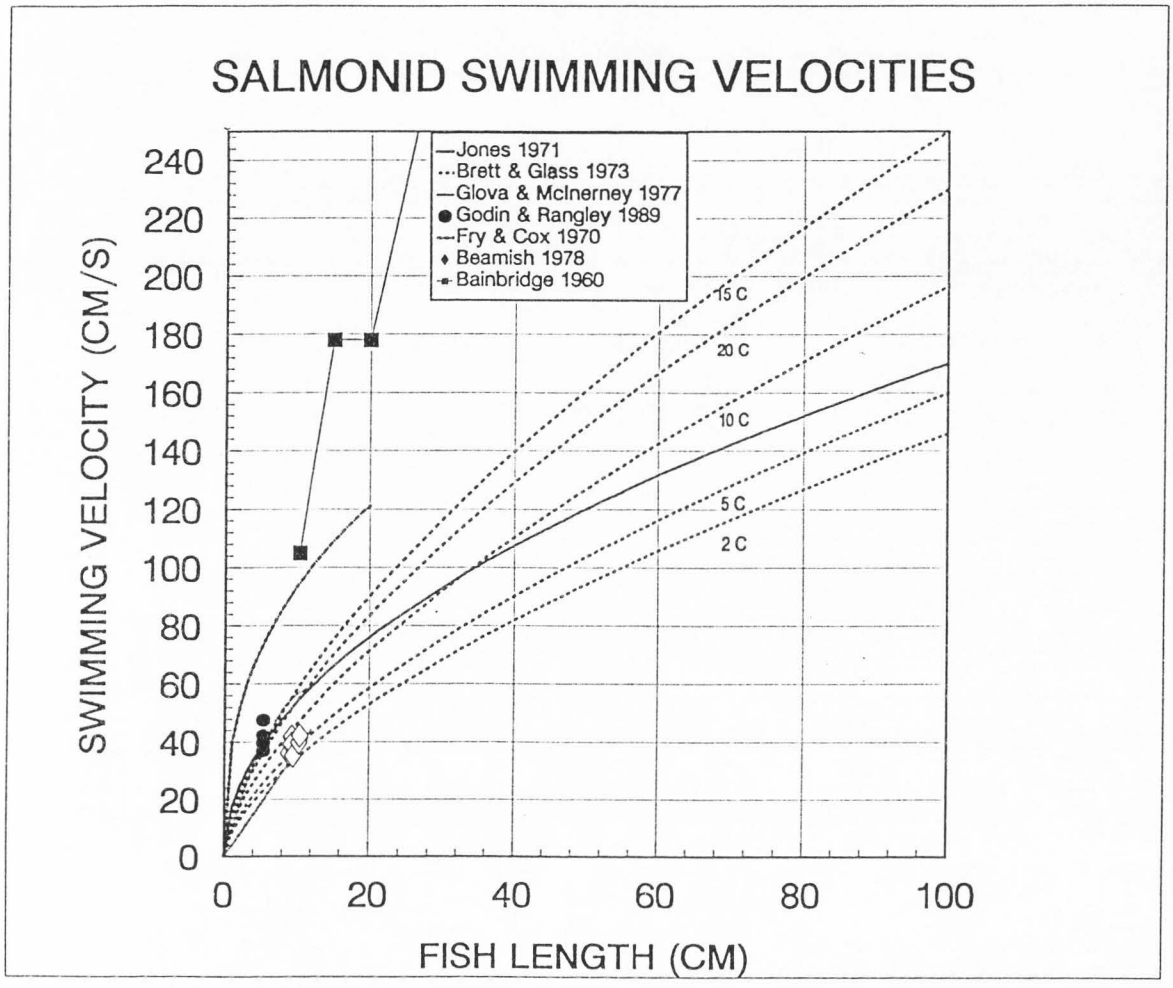

Figure 4. Relationship between fish length (fork and total), temperature, and swimming velocity. Jones (1971) is a general salmonid equation $V=17L^{0.5}$ derived from a review of numerous studies at different temperatures and the assumption $V \propto L^{0.5}$. Brett and Glass (1973) 60-minute maximum sustained velocity (critical velocity) data for sockeye salmon at temperatures of 2, 5, 10, 15 and 20°C. Glova and McInerney (1977) critical velocities of coho salmon at 3 and 18°C, bottom and top line, respectively. Godin and Rangeley (1989) velocity Atlantic salmon used to capture drift at 13°C. Fry and Cox (1970) maximum 1 minute velocities for rainbow trout at 5-15°C. Beamish (1978) 30 to 60-minute maximum sustained velocities of rainbow trout. Bainbridge (1960) 1 second burst velocities for 4 rainbow trout.

To obtain a continuous function, the following equation was derived from the equations of Brett and Glass (1973) using a temperature algorithm described by Kitchell et al. (1974) and is compared to equations 17 in Figure 5:

$$V_{max} = 13.86 \left(\frac{21.42-T}{3.92}\right)^{0.24} e^{0.24\left(1-\left(\frac{21.42-T}{3.92}\right)\right)} TL^{0.63} \qquad (18)$$

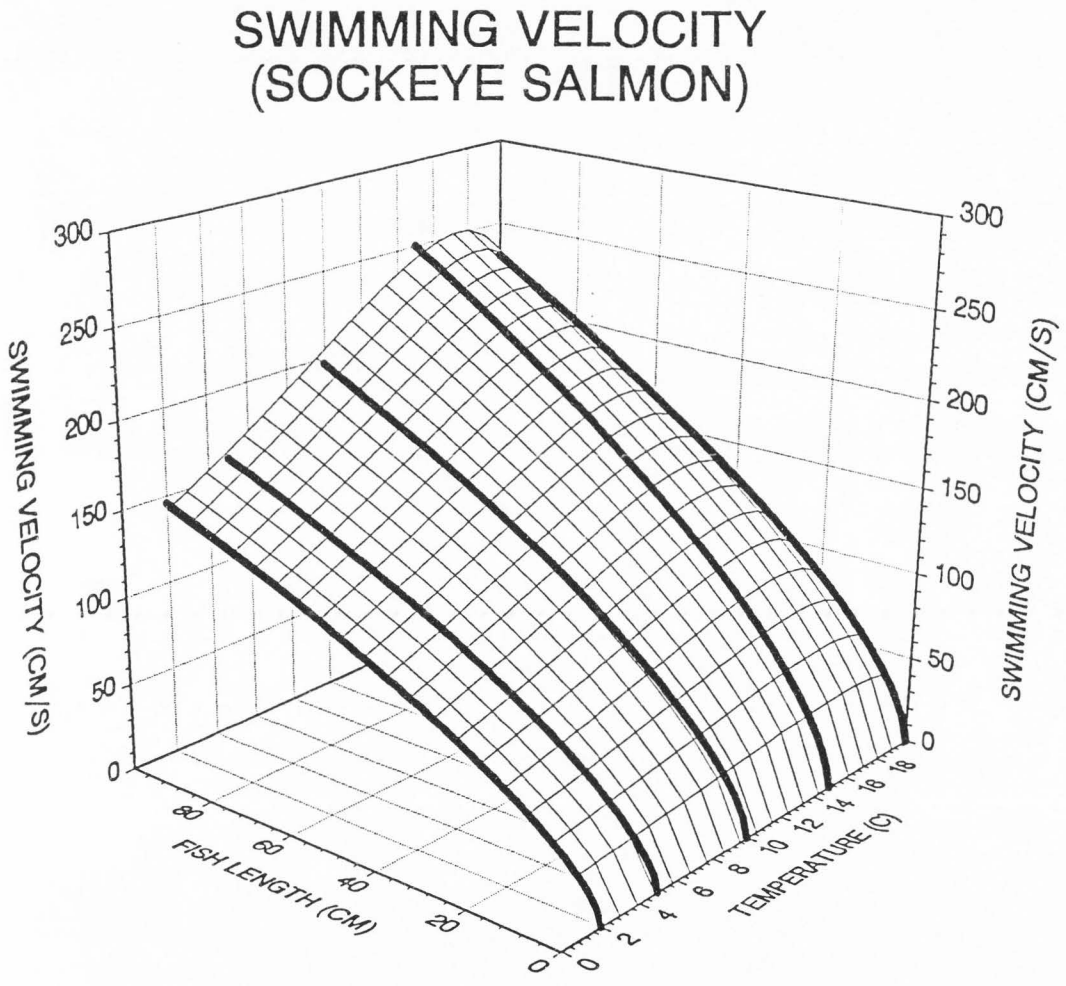

Figure 5. Relationship between 60-minute sustained swimming velocity, fish length, and temperature for sockeye salmon. Heavy lines are regression lines from Brett and Glass (1973)(equations 17), and the surface is equation 18 that was fit to the regression lines.

Swimming cost

The components of swimming cost in this paper are basal metabolism and active metabolism. Basal metabolism is the minimum rate of energy expenditure required to keep the fish alive (i.e., maintenance energy requirements). Active metabolism is the energy utilized for activities that require locomotion such as maintaining position in current. Before any consumed energy can be stored or converted to somatic or gonadal growth, fish must meet energy demands for maintenance and activity (Kitchell, 1983). Swimming cost depends on temperature, fish weight, and swimming velocity (Stewart, 1980).

For the NEI model input, the rainbow trout swimming cost equation developed by Stewart that accounts for both active and basal metabolism was considered the most applicable equation available for cutthroat trout. Stewart (1980) fit the swimming cost equation to the rainbow trout swimming data of Rao (1968). The equation is:

$$R_{U\ (J \cdot hr^{-1})} = 1.4905\, W^{0.784} e^{0.068T} e^{(0.0259-0.0005T)U} \qquad (19)$$

Comparisons of equation 19 and actual rainbow trout swimming cost data for 5 and 15°C (Rao, 1968) are shown in Figure 6.

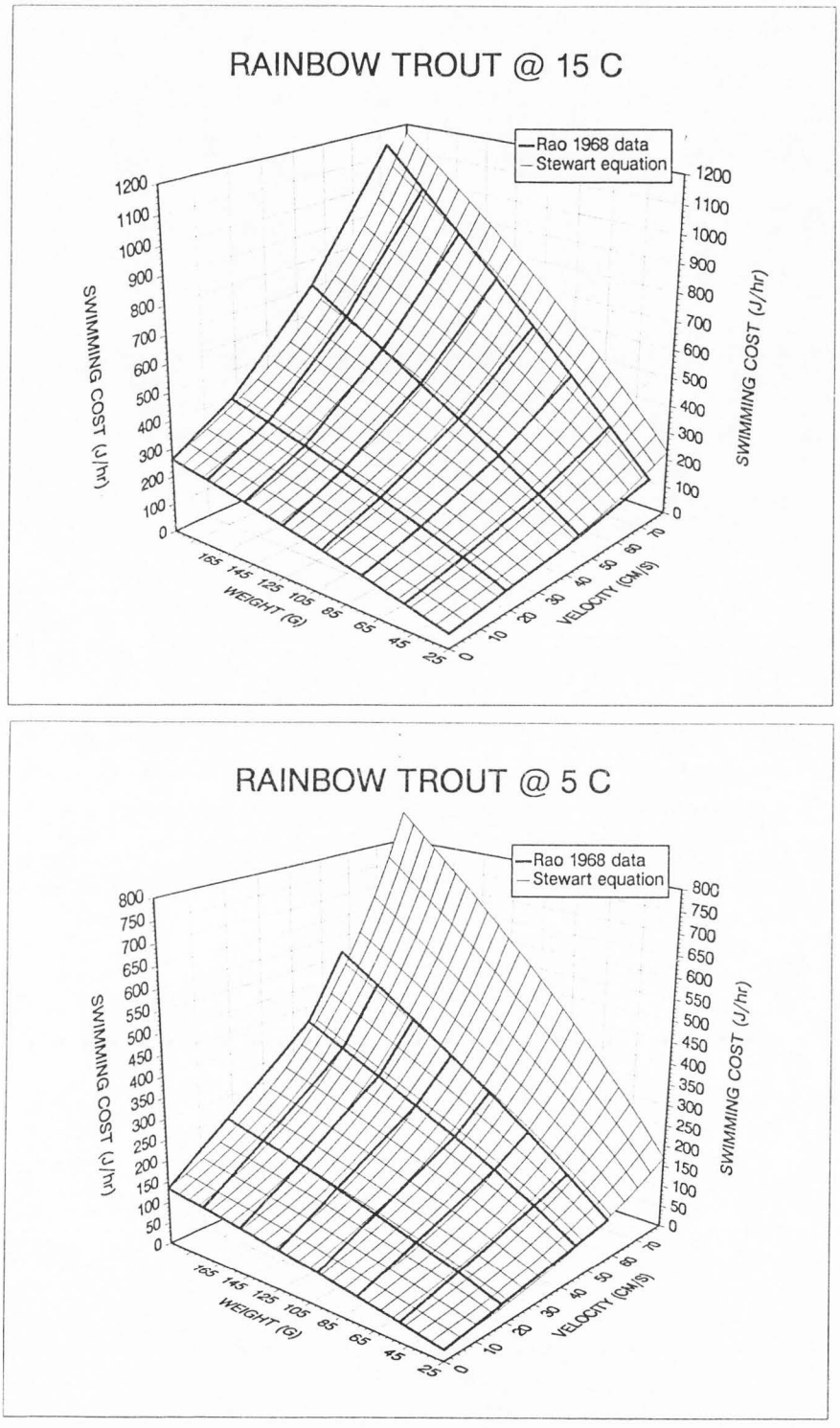

Figure 6. Comparison of the swimming cost equation derived by Stewart (1980) and actual rainbow trout swimming cost data from Rao (1968) at temperatures of 15 and 5°C.

Feeding foray costs

Swimming cost equations are derived for steady-state swimming conditions and do not account for the costs involved in unsteady-state swimming activities such as accelerating and decelerating. Webb (1982) has shown that unsteady swimming is more energetically costly than steady swimming. Brett (1970; cited in Puckett and Dill, 1984) found that 20 seconds of burst speed was equivalent to 15 minutes at the 60-minute maximum sustained metabolism, or 45 times as costly. Puckett and Dill (1984) have shown that burst swimming may be 5-20+ times more expensive than would be expected by extrapolation from empirical swimming speed and oxygen consumption relationships.

For a first approximation of feeding foray costs, it is reasonable to assume that the cost of returning to the feeding location is insignificant compared to the cost of capturing prey (Godin and Rangeley, 1989). It is also reasonable to assume that the time it takes to capture prey is about 1 second and that fish capture prey items at their 60-minute maximum sustained velocity (from 7 to 4.5 body lengths/sec for fish 60 and 200 mm, respectively). Puckett and Dill (1984) and Godin and Rangeley (1989) recorded capture velocities from 3.4 to about 8 or 9 body lengths/sec. For NEI model input, a conservative assumption was made that capture cost (CC) was 6 times greater than steady swimming cost at the same velocity. Therefore, capture cost equals 6 times the sustained swimming cost for 1 second calculated from equations 18 and 19:

$$CC = 6\, R_{vmax} \qquad (20)$$

Assimilation losses and digestion costs

Waste products and food digestion constitute energy losses and costs to fish. Waste products are nonassimilated energy egested as feces (F) and assimilated energy excreted as ammonia and urea (U). For brown trout feeding on invertebrates, waste losses have a complex, nonlinear relation to feeding rate, temperature, and fish size (Elliott, 1976):

$$PF = 0.212\,T^{-0.222}\,e^{0.631\,(c/cmax)}$$
$$PU = 0.0259\,T^{0.580}\,e^{-0.299\,(c/cmax)} \qquad (21)$$

where: PF = Proportion of daily energy intake lost as feces

PU = Proportion of daily energy intake excreted

C = Daily energy consumption

Cmax = Maximum daily consumption (discussed later)

T = Temperature °C

It is feasible, however, to calculate wastes as a fixed proportion of GEI. Waste generally ranges between 25-30% of GEI (Elliott, 1976). The energy costs of food digestion include energy used in deamination of proteins, mechanical digestion, assimilation, and storage (Ney, 1990). Food digestion costs range from 12-16% of the GEI (Brett and Groves, 1979). For NEI model input, energy losses (F and U) are assumed to be 28% of GEI, and cost of food digestion is 14% of GEI (see equation 15).

Maximum daily food consumption

Elliott (1975a; 1975b) studied the satiation requirements and the daily consumption rates of brown trout. He found that single meal satiation and daily consumption rates vary with temperature and size of the fish. Elliott (1975b; 1979) derived mathematical

equations to quantify maximum daily food consumption of gammarids and a variety of other natural trout foods (e.g., *Baetis*, Chironomidae, Oligochaete, *Protonemura*, and *Hydropsyche*). The consumption equations developed by Elliott (1979) for brown trout are:

$$\begin{aligned} 3.8\text{-}6.6^{\circ}C &\qquad C_{max} = 2.902\,W^{0.762}e^{0.418T} \\ 6.6\text{-}13.3^{\circ}C &\qquad C_{max} = 15.018\,W^{0.759}e^{0.171T} \\ 13.3\text{-}17.8^{\circ}C &\qquad C_{max} = 26.433\,W^{0.767}e^{0.126T} \\ 17.8\text{-}21.7^{\circ}C &\qquad C_{max} = 3.241x10^{7}\,W^{0.753}e^{-0.662T} \end{aligned} \tag{22}$$

where C_{max} is maximum consumption (cal day^{-1}), W is fish live weight (g), and T is temperature (°C). These equations show that maximum consumption initially rises rapidly with increased temperature up to 18°C, then decreases dramatically (Figure 7).

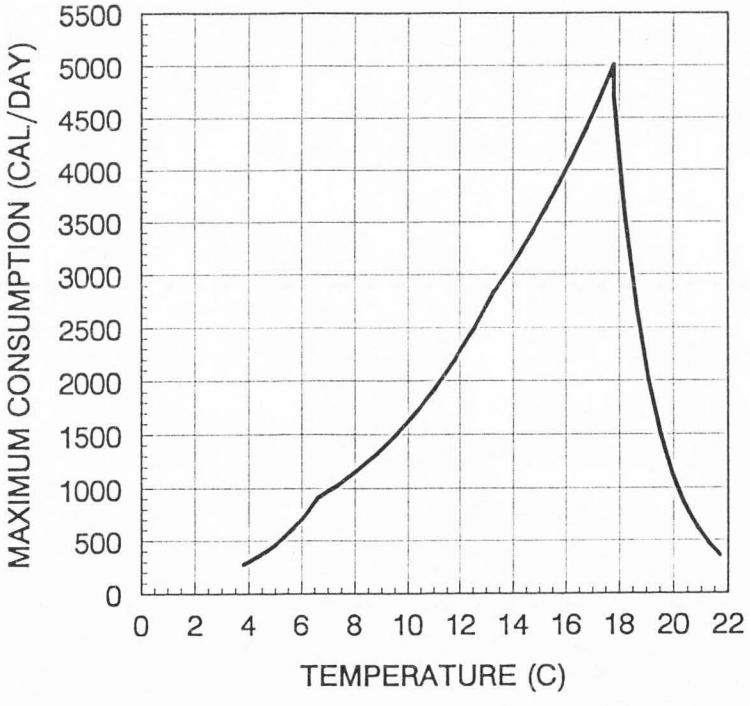

Figure 7. Relationship between maximum energy intake (cal day^{-1}) and temperature (°C) for a 50 gram trout (adapted from Elliott, 1979).

Unfortunately, the shape of the maximum consumption versus temperature curve is not the same as that found for some salmonid studies (Brett, Shelbourn, and Shoop, 1969; Edsall et al., 1974 cited in Stewart, 1980). Part of the discrepancy may result from the fact that different sizes and types of food items are evacuated from the stomach at different rates (Jobling, 1987). However, because the equations from Elliott are developed for small prey types typical of those found in streams, it is assumed that these equations are the most appropriate for the stream NEI model.

Maximum capture rate

The maximum capture rate of drifting invertebrates is limited by the time fish spend waiting to detect a prey item (t_w), the time required to make the feeding foray and begin waiting for another prey item (t_f), and the time available for feeding (t_a). The maximum number of prey captures (MNC) shown previously in equation 8 is:

$$MNC = \frac{t_a}{t_w + t_f} \tag{23}$$

The average amount of time spent waiting for prey (t_w) shown previously in equation 10 is a function of drift density (DD), average water velocity (V_{ave}), and the size of the maximum capture area (MCA). Specifically:

$$t_w = \frac{1}{MCA \cdot V_{ave} \cdot DD} \tag{24}$$

The time require to make a feeding foray (t_f) is composed of the time to recognize the prey (t_{rec}), capture the prey (t_c),

handle the prey (t_h), and return to the feeding location to begin a new search for prey (t_{ret}):

$$t_f = t_{rec} + t_c + t_h + t_{ret} \tag{25}$$

The overall equation for defining maximum number of captures is obtained by combining equations 23, 24, and 25 and is:

$$Maximum\ Captures \leq \frac{t_a}{\frac{1}{MCA \cdot V_{ave} \cdot DD} + t_f} \tag{26}$$

Figure 8 shows the effect of including the feeding foray time constraint of equation 26 on maximum capture rate.

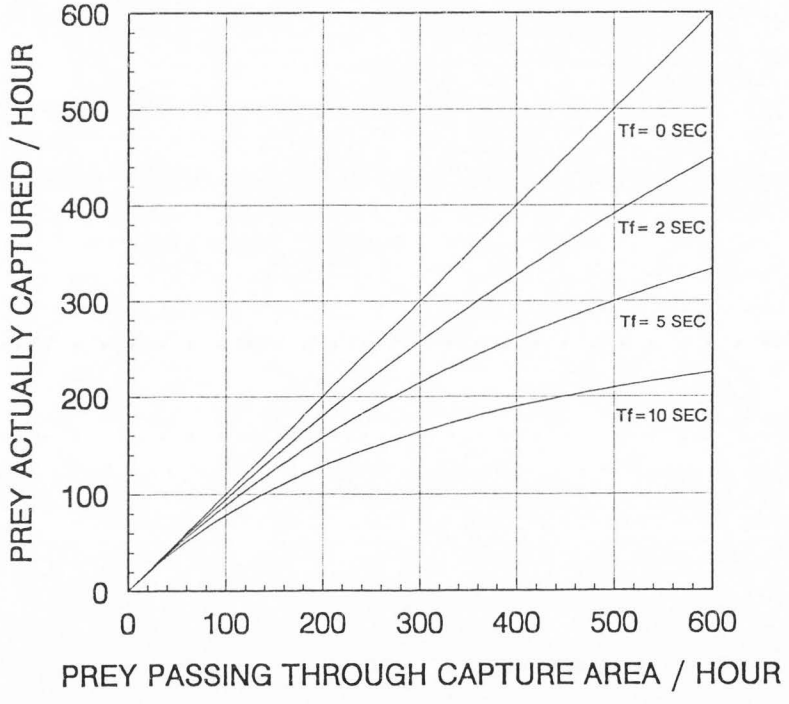

Figure 8. Comparison of maximum capture rate given the time to complete a prey capture foray is 0, 2, 5, and 10 seconds. Note that the case where foray time is 0 results in all prey passing through the fish's MCA being captured.

For the NEI model, the average time waiting for prey (t_w) is calculated from the specific drift density (DD), average water velocity (V_{ave}), and the calculated maximum capture area (MCA). The time to make a feeding foray (t_f) is the sum of its component parts where recognition time (t_{rec}) is considered here to be instantaneous, the time to capture prey (t_c) is about 1 second based on observations by Bachman (1984), handling time (t_h) is considered negligible and/or included in return time, and the time to return to feeding (t_{ret}) is about 4 seconds (Bachman, 1984). As a result, the time to make a feeding foray (t_f) is assumed in the model input to be 5 seconds.

Prey capture probability

Capture probability should be related to (1) the probability of detecting a visible prey, (2) the probability of attacking prey, and (3) the probability of actually capturing/ingesting prey. The probability of detecting a visible prey item is likely to be highest at low velocities and lowest at very high velocities and depend on how cryptic (visible) the prey is (Gendron and Staddon, 1983; Wilzbach, Cummins, and Hall, 1986). The probability of attacking prey and successfully capturing/ingesting prey in relatively slow water is likely 100 percent if the prey are not highly mobile and if the prey are not too small or too large and if the fish is hungry (Dunbrack and Dill, 1983). It is reasonable to assume that both the probability of attack and successful capture/ingestion decrease with increasing velocity.

Due to the lack of empirical data on capture probability, it would be necessary to speculate on the relationship between

probability of capture (P_c) and search rate (water velocity). Gendron and Staddon (1983) proposed a function satisfying the criterion that P_c is high at slow search rates and low at fast search rates that could be used in the NEI model; however, for the sake of simplicity P_c has been set to 1.0 in the model. P_c is retained in the NEI model only for the purpose of keeping the model general for future uses.

Drift density

Allan (1987), in a third order Rocky Mountain stream, found day averages of drift density in June and July of 480 to 650 insects per 100 m^3, with night averages as high as 5400 per 100 m^3 and 24 hr average densities of 1000 to 2000 per 100 m^3. In the fall, September and October, drift densities decreased considerably with day averages of drift density from 100 to 300 per 100 m^3. Night drift densities were five- to tenfold greater than day drift densities in the early season with smaller ratios later in the season. Ephemeroptera were the major component in the drift (60-80% early and 40-50% later; the majority Baetis) followed by Plecoptera, simuliidae, and Chironomidae. Chironomidae were twice as abundant in day drift as night drift, while the other taxa were largely night drifters. Allan (1987) cites other studies that set the typical range of drift density at 10-100 to 500 per 100 m^3 with a maximum recorded record of 17260 per 100 m^3 in the Green River, Utah-Colorado. Wilzbach, Cummins, and Hall (1986) reported the average of dawn, noon, and dusk drift densities in an Oregon stream between 200 and 800 per 100 m^3.

The drift density in the NEI model should be set at the specific densities of the stream site that is being modeled if data are available. In this paper, existing drift density data for St. Charles Creek, Utah, were utilized. Daytime drift density in St. Charles Creek during the summer of 1990 varied according to the gradient of the study reaches. Daytime drift in the low gradient study reach averaged 2600 organisms per 100 m^3, while drift in the medium and high gradient reaches was 430 and 700 per 100 m^3, respectively (R. Black, 1990, unpublished data). These drift densities fall within the general range reported by other studies. Table 1 shows the overall densities and the relative percentages of each taxon.

Table 1. Daytime drift densities and relative percentages of aquatic invertebrate taxa in St. Charles Creek, Idaho, during the summer (R. Black, 1990, unpublished data)

	High Gradient	Medium Gradient	Low Gradient
Total Density (#/100 m^3)	2600	435700	
Number of Samples	46	5012	
% Chironomidae	53	2953	
% *Baetis* spp.	7	3920	
% Simuliidae	5	93	
% Ephemoptera	2	45	
% Diptera	1	12	
% Colleoptera	4	31	
% Trichoptera	1	28	
% Terrestrial	11	33	
% other	16	105	

Drift size

The size of invertebrates in the drift is site dependent. Generally, the most abundant size of invertebrates in the drift of salmonid streams seems to be between 0 and 5 mm. Bannon and Ringler (1986) found in a second order New York stream that the most abundant sizes of drift were between 1 and 4 mm, with most, 30-60%, in the 2 mm size class. The 1 mm size class accounted for 2-20% and 5-18% were in the 4 mm category. A few larger (5-8 mm) organisms were found later in the summer.

Salmonids typically feed only on prey approximately 1 mm or larger (Bannon and Ringler, 1986) and possibly only on prey larger than 2 mm (Bisson, 1978; Skinner, 1985). In addition, fish preferentially consumed large prey items even though they are not abundant. For example, Bannon and Ringler (1986) found that fish disproportionately fed on prey larger than 3 mm even though they were rare in the drift.

In St. Charles Creek, Idaho, the most abundant prey were less than 6 mm. Figure 9 and Table 2 show the percentage of different size classes of prey for three different reaches of the stream (low, medium, and high gradient)(R. Black, 1990, unpublished data). The proportion of drift observed in St. Charles Creek greater than 1 mm was used in the NEI model. In most cases the proportion of drift in each of three size classes (1-3 mm, 3-6 mm, and 6-11 mm) was used for model input (Table 2).

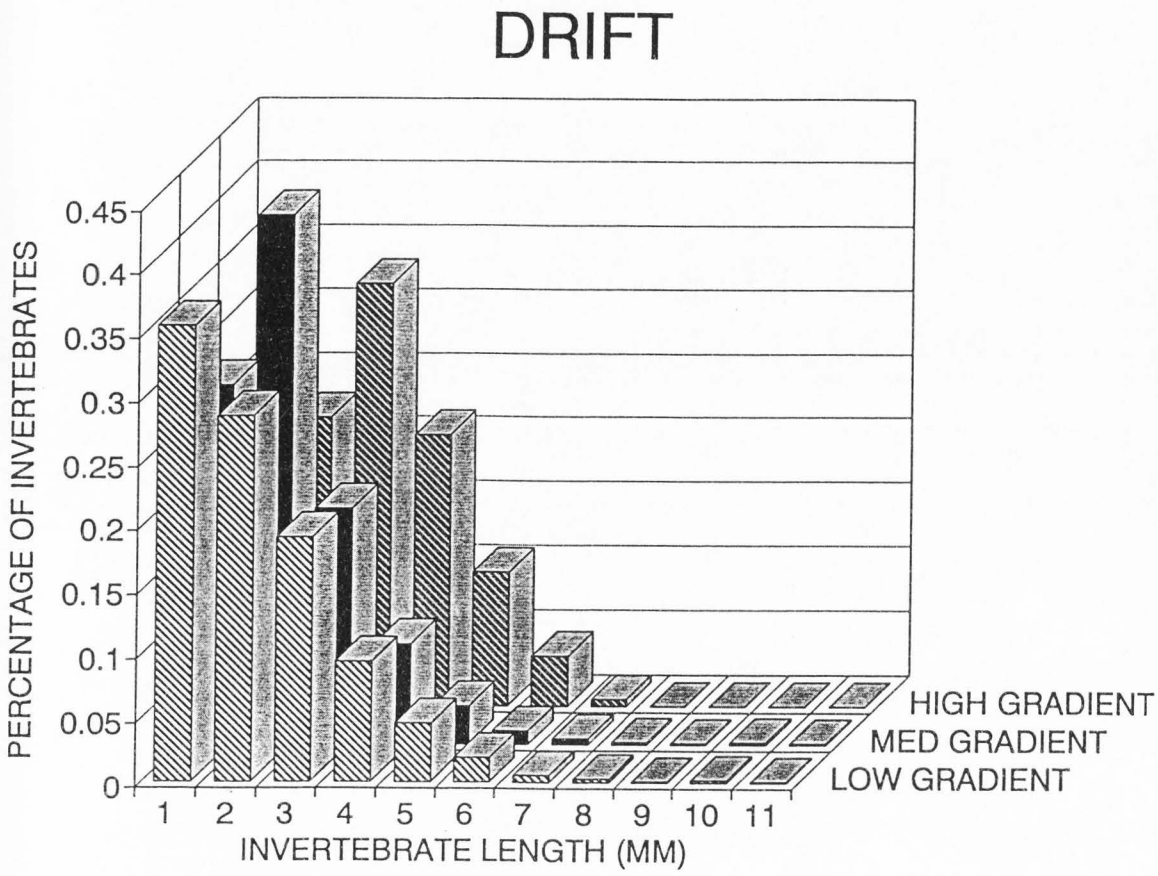

Figure 9. Length-frequency distributions of drifting invertebrates in three separate reaches (high, medium, and low gradient) of St. Charles Creek, Idaho (R. Black, 1990, unpublished data).

Table 2. Size composition of daytime drifting aquatic invertebrates in St. Charles Creek, Idaho (R. Black, 1990, unpublished data)

	Low Gradient	Medium Gradient	High gradient
Number Measured	4620	3400	356
Ave Length > 1mm	2.6 mm	2.3 mm	3.0 mm
Percentages			
% Above 1mm	64	72	91
% 1-3 mm	74	83	60
% 3-6 mm	25	16	39
% 6-11 mm	1	1	1

Drift dry weight and energy content

Drift can be converted to dry weight using the general aquatic invertebrate regression of Smock (1980):

$$W = 0.019 L^{2.46} \quad (27)$$

where W is dry weight (mg) and L is length (mm). Dry weight can subsequently be converted to energy using the relationship 1 g dry weight equals 20,097 joules (4800 calories) (Cummins and Wuycheck, 1971).

For input into the NEI model, prey energy is determined by converting equation 27 to joules:

$$PE_i = 0.3818 L_i^{2.46} \quad (28)$$

where PE_i is energy of the ith prey size in joules and L_i is the ith prey length (mm).

Uniform drift denstiy assumption

An implicit assumption of the proposed drift-feeding model is that drift density is not a function of velocity and is uniform throughout the water column. Several studies (e.g., Waters, 1965; Elliott, 1970; Wankowski and Thorpe, 1979; Irvine and Northcote, 1982; Smith and Li, 1983; Hill, 1989) support the assumption that drift density is not a function of velocity or only a slightly increasing function of velocity (i.e., drift rate is directly proportional to the volume of water flowing through a drift net). Matter and Hopwood (1980), however, have shown that in large streams drift density can be stratified in the water column.

Variable water column velocity

An implicit assumption in the derivation of maximum capture area (MCA) is that the water velocities are known throughout the three-dimensional water column. In practice, it is not feasible to measure water velocities everywhere. Most fisheries investigations measure water velocity at points in the vertical water column where the velocity is typically equal to the average velocity for the total depth (Platts, Megahan, and Minshall, 1983). In most river channels the distributions of velocities in the vertical direction are logarithmic, and the velocity at 0.4 of the water depth from the bottom of the stream is approximately the average water column velocity (Leopold, Wolman, and Miller, 1964). To utilize average velocity measurements in the NEI model, a relationship of the average water velocity to point velocities throughout the water column was required.

There are two approaches available for calculating point velocities throughout the water column from average velocities: (1) theoretical and (2) empirical (Milhouse, 1990). In this thesis the empirical approach is used. The empirical approach utilizes an equation of the form:

$$\frac{V_p}{V_m} = A\left(\frac{D_p}{D}\right)^B \qquad (29)$$

where: D = mean total depth of the stream

D_p = depth at a point

A,B = empirical constants

V_m = mean velocity of the water column

V_p = point velocity in the water column

By measuring a number of point velocities and the corresponding mean velocities in a stream channel, the parameters of equation 29 (i.e., A and B) can be obtained from regression.

There is some uncertainty to be expected from using the approach outlined above. In particular, point velocities near the bottom of the stream may deviate from the calculated velocity because the theory used in the calculations cannot account for the fact that velocities may be slower or faster than expected near bed elements (rocks) (Milhouse, 1990). This problem can cause a person to obtain constants from regression using equation 29 that are not reasonable. Constants obtained by R. Addley (1992, unpublished data) resulted in velocity profiles that did not accurately predict "mean column velocity" (velocity at 0.4 of the water depth from the stream bottom) when, in fact, mean column velocity was one of the primary known values used in the regression. Velocity values near the bottom of the stream that are lower than expected because they are downstream of a bed element (rock) artificially increase both of the constants (A and B) that are derived by regression.

To partially compensate for the above problem, the values of constants A and B of equation 29 can be constrained. From equation 29 it follows that if the mean water column velocity is assumed to be 0.4 of the depth from the bottom of the stream, then when D_p/D equals 0.4, the velocity mean V_m should equal the point velocity V_p. Solving equation 29 for these conditions results in the following equation:

$$\ln(A) = -B \ln(0.4) \qquad (30)$$

For input into the NEI model, empirical constants for equation 29 were estimated from (1) regression of fish focal velocities and mean column velocities collected by L. Jacobsen (1990, unpublished data) on St. Charles Creek, Idaho, (2) from multiple velocity measurements in pools and runs of Blacksmith Fork, Utah (R. Addley, 1992, unpublished data), and (3) from the U.S. Geological Survey empirical relationship of velocity and depth in Rantz et al. (1982). The initial NEI model input constants were chosen to be representative of the values obtained by regression and yet be constrained to fit equation 30 (Figure 10). The initial input constants are A = 1.3 and B = 0.3.

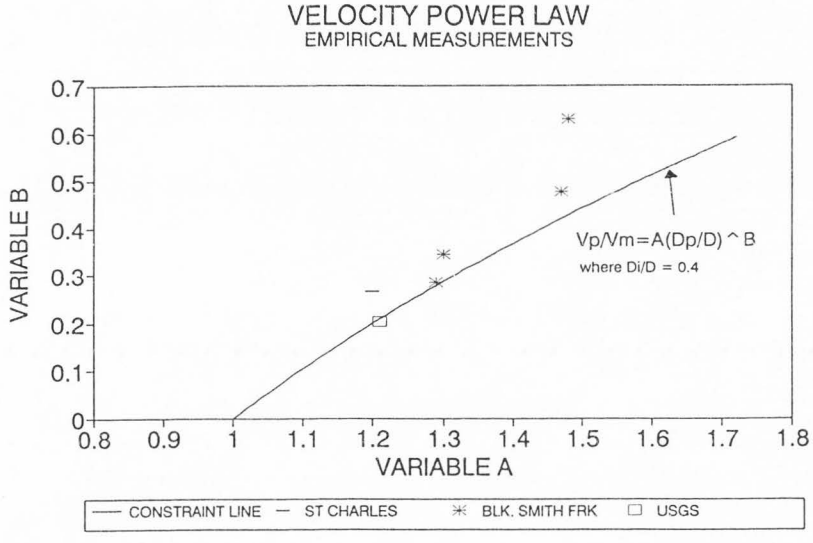

Figure 10. Plot of the A and B coefficients derived for the empirical velocity equation (equation 29). Coefficients were obtained by regression of data from (1) data from St. Charles Creek, Idaho (L. Jacobsen, 1990, unpublished data), (2) data from various locations on the Blacksmith Fork, Utah (R. Addley, 1992, unpublished data), and the empirical depth-velocity relationship from the U.S. Geological Survey (Rantz et al., 1982). Also presented is a line representing the constraint applied to equation 29 (see text for details).

FIELD VALIDATION

Methods and assumptions

NEI model output was tested against two different sets of field data collected in 1989 and 1990 on St. Charles Creek, Idaho. Validation data were obtained independently of data used in constructing the NEI model. The first and largest data set consists of habitat availability measurements and 1400+ microhabitat observations of cutthroat (73%), brook (26%), and rainbow trout (1%) obtained by Lee Jacobsen in St. Charles Creek (Jacobsen, 1993, unpublished). Microhabitat observations were obtained by snorkeling 10% of each habitat type (e.g., pools, runs, glides, riffles) in St. Charles Creek and recording the species and length of each fish as well as microhabitat variables (water depth, average velocity, focal velocity, water temperature, substrate, etc.). The data used in the validation were all collected in the summer. The sizes of fish in the data set range from 10 to 490 mm TL.

To evaluate the NEI model, frequency histograms of the habitat availability and microhabitat utilization data were plotted on a two-dimensional grid of mean water column velocity and depth. Microhabitat utilization data were segregated into four size classes of fish: very small (10-39 mm), small (40-69 mm), intermediate (70-159 mm), and large (160-490 mm). The location and frequency of habitat use of fish in each size class were then plotted on the velocity and depth grid and compared to habitat availability. Manly's Alpha preference index (Krebs, 1989) was used to quantify habitat preference over the grid of depths and velocities, and a Monte-Carlo computer program for chi

square goodness-of-fit testing (Romesburg and Marshall, 1985) was used to determine whether fish used depths and velocities in a nonrandom manner (P = 0.05). In addition, linear correlation was used to determine the relationship between fish size and habitat (depth and velocity) use.

The NEI model was then used to calculate NEI over the same aforementioned grid of depths and velocities for four different sizes of fish (30, 50, 100, 200 mm) that corresponded to the mean length of fish in each of the size categories (10-39, 40-69, 70-159, 160-490 mm). The results of the NEI model predictions for each fish size and the actual microhabitat utilization of each size class of fish were then compared for correspondence. Determination of the correspondence between model predictions and actual habitat use was accomplished by graphical presentation and by rank correlation of modeled NEI quality versus fish utilization.

The second data set used for validation consists of one set of fish positions in two pools (Stations 59 and 48) and two runs (Stations 60 and 50) in St. Charles Creek along with detailed spatial mapping of the depth and water velocity of each pool and run. The station numbers for the pools and runs analyzed correspond to the station numbers in Jacobsen (1993, unpublished). A total of 55 fish positions were mapped in the four stations with 67% of the fish being cutthroat trout, 24% brook trout, and 11% rainbow trout. Fish positions were mapped by snorkeling each station one time in the month of August between 11 and 12:00 am. Immediately following mapping of fish locations, a 0.46 m (1.5 ft) by 0.31 m (1 ft) grid was laid out on each station by placing transects marked by nylon rope every

0.46 m from the beginning of the station to the end with each transect marked off in 0.31 m increments. Total water depth and average water column velocity were measured at each 0.31 m increment of each transect. To test the NEI model, NEI was calculated throughout each station and the model predictions of NEI were graphically compared to the actual locations being utilized by fish. In addition, a computer randomization test (10,000 permutations) was used to determine if fish were using the habitat in a nonrandom manner (Manly, 1991), and Spearman's rank correlation was used to determine rank correlation between the density of fish and modeled NEI.

Model input parameters for the validation tests are shown in Table 3. All input parameters are general values derived previously except for water depth, water velocity, fish size, and drift density. Water depth and velocity were input directly into the model for each depth and velocity combination being modeled. The sizes of fish modeled corresponded to the mean fish sizes in the validation data. Drift density for the first validation data set was set at 400 prey/100 m^3, which was the average daytime drift density in the middle reach of St. Charles Creek (Table 1). Drift density for the second validation data set was set at 209, 149, 106, and 106 prey per 100 m^3 for stations 60, 59, 50, and 48, respectively. These drift densities were the station specific densities found at each site (R. Black, 1990, unpublished data). The size distribution of the drifting invertebrates used in the model corresponded to that in the medium gradient reach of St. Charles Creek (Table 2).

Table 3. Equations used in the net energy intake (NEI) model

Parameter & Units	Equation/Calculation Method	Source and Discussion
NEI_i (joules/hr)	$NEI = \frac{\sum_{i=1}^{n} MCA_i \cdot V_{ave\ i} \cdot DD_i \cdot PC_i \cdot (E_i - CC_i) - SC}{1 + \sum_{i=1}^{n} t_{f\ i} \cdot MCA_i \cdot V_i \cdot DD_i}$	Net energy intake rate based on possible gross energy intake minus energy costs and losses for each prey size i
MCD_{ij} (ft)	$MCD_{ij} = \sqrt{\frac{RD_i^2 (V_{max}^2 - V_{mean_j^2})}{V_{max}^2 + V_p - V_{mean_j^2}}}$	Calculated in the plane transverse and perpendicular to the fish by an iterative computer program where $V_{mean\ j}$ = mean velocity along MCD_{ij} (calculated within the computer program) and RD_i is the reaction distance for prey size i
V_{max} (ft/s)	$V_{max} = 13.86 \left(\frac{21.42 - T}{3.92}\right)^{0.24} e^{0.24\left(1 - \left(\frac{21.42-T}{3.92}\right)\right)} TL^{0.63}$	Maximum sustained fish velocity equation derived from Brett & Glass (1973) T=temperature (°C) TL=total length (cm)
RD_i (ft)	$PL_i = (RD_i^2 + 50\ RD_i)\left(\frac{1 + 5.8\ e^{-.034(FL)}}{1725}\right)$	Reaction distance equation derived from data of Dunbrack & Dill (1983) where PL_i = prey length (mm), RD_i = reaction distance (cm), and FL = total fish length (mm)
MCA_i (ft^2)	Area circumscribed by connecting MCD_is in all directions in the plane transverse and perpendicular to the fish (calculated with a computer program)	Maximum capture area at a location given water depth, water velocity, and channel morphology
$V_{ave\ i}$ (ft/s)	Average water velocity through MCA_i calculated within the computer program	Average velocity in the MCA
DD_i (prey/ft^3)	Site specific emperical data	Daytime drift density in St. Charles Creek, Idaho, for each prey size i (Black 1990, unpublished data)
PC_i	Assume probability of capture equals 1.0	Probability of successful prey capture
E_i (joules/prey)	$0.58\ PE_i$	Energy assimilated (gross energy intake minus 14% for food digestion and 28% for losses due to excretion and feces)
PE_i (joules/prey)	$PE_i = 0.3818\ (PL_i)^{2.46}$	Prey energy derived from Smock (1980) and Cummins & Wuycheck (1971) where PL_i = prey length (mm)
CC_i (joules)	6 times cost of swimming (SC) for one second at V_{max}	First approximation of cost of capturing prey. About 20% of the emperical cost found by Puckett and Dill (1984)
SC (joules/hr)	$R_U = 1.4905\ W^{0.784} e^{0.068T} e^{(0.0259 - 0.0005T)U}$	Stewart (1980) W=weight (gm) T=temp (°C) U=velocity (cm/s)
t_f	Emperically approximated as 5 seconds	Taken from time to complete a feeding foray in Bachman (1984)

Results and discussion for data set one (Jacobsen data)

Habitat availability. A frequency histogram of the depths and mean column velocities of stream habitat available in St. Charles Creek is shown in Figure 11. The largest percentage of habitat available in St. Charles Creek consists of relatively slow, shallow water less than about 50 cm deep with mean velocities less than about 20 cm/s. There is also a large portion of habitat available with depths less than about 70 cm and velocities in the range of 20 to 90 cm/s, but very little habitat is available with depths greater than 70 cm.

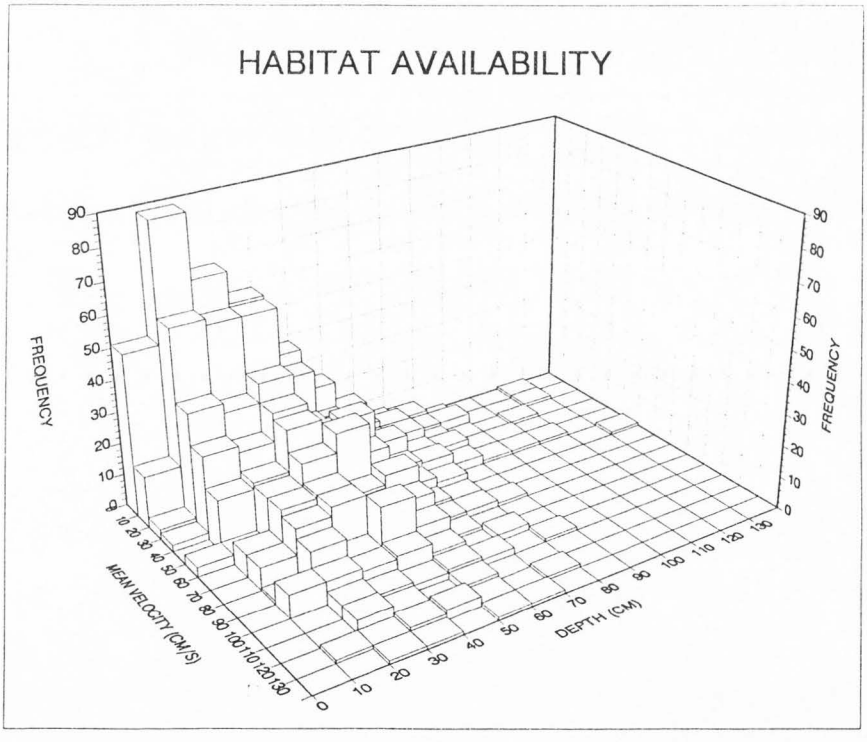

Figure 11. Frequency histogram of the available habitat in St. Charles Creek, Idaho (Jacobsen, 1993, unpublished). Note that this graph is oriented in a different direction than most of the following graphs so that the frequency distribution can clearly be seen.

Habitat utilization. Frequency histograms of the observed fish microhabitat locations for each size class of fish are plotted on a grid of depth and velocity in Figures 12-15. Each size class of fish utilized depth and velocity habitat that differed significantly from the stream habitat available ($P<0.05$) (see Figure 11). Very small fish (10-39 mm) used very slow, shallow habitats similar to the most abundant habitat available (Figure 12), but none of the deeper, faster habitats; and the size classes of fish larger than 39 mm utilized habitats deeper and faster than those that were most abundant (Figures 13-15). In particular, the two largest size classes of fish (Figures 14-15) utilized deep and relatively fast water that was very rare in the stream (see Figure 11).

Habitat preference. Plots of Manly's Alpha preference index show quantitatively the preference of trout in St. Charles Creek for deeper and faster water as they increase in size (Figures 16-19). Manly's Alpha preference index was calculated at the center of each 10 unit by 10 unit combination of depth and velocity. Preference values greater than 0.005 indicate fish utilized a particular habitat more than would be expected given the proportion of that habitat in the stream, and values less than 0.005 indicate avoidance of particular habitats. Comparison of Figures 16-19 shows that small trout preferentially utilized only shallow habitats and that larger fish preferred deep habitats and avoided shallow water. In addition, as fish size increased, they preferred a wider range of water velocities that included velocities up to approximately 65 cm/s for the larger fish.

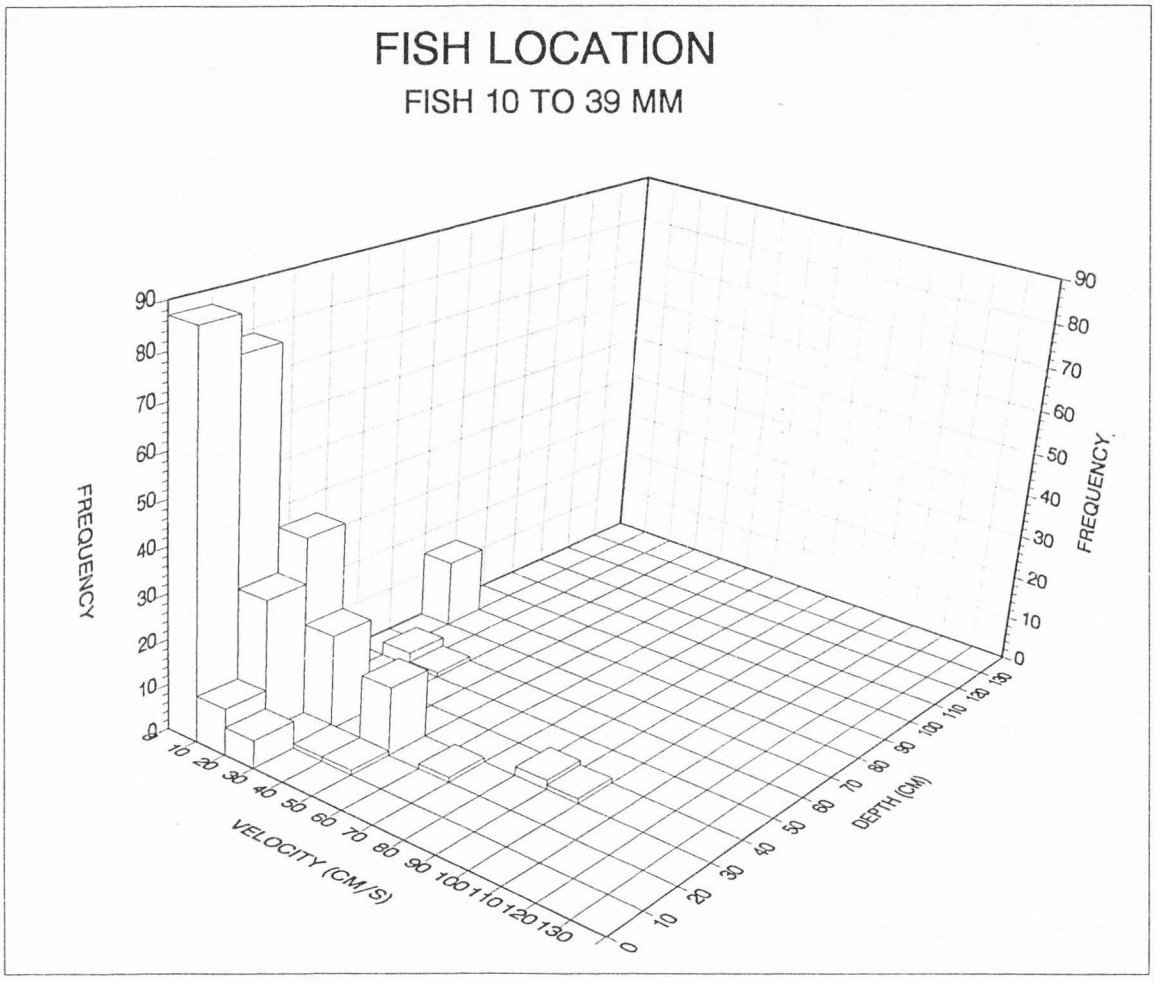

Figure 12. Frequency histogram of the number of cutthroat trout observed at each total depth/ mean velocity combination in St. Charles Creek, Idaho (Jacobsen, 1993,. unpublished). The total number of fish locations plotted is 346. The average size of the fish was 29 mm TL with a range from 10 to 39 mm. Note that this graph is oriented similar to Figure 11.

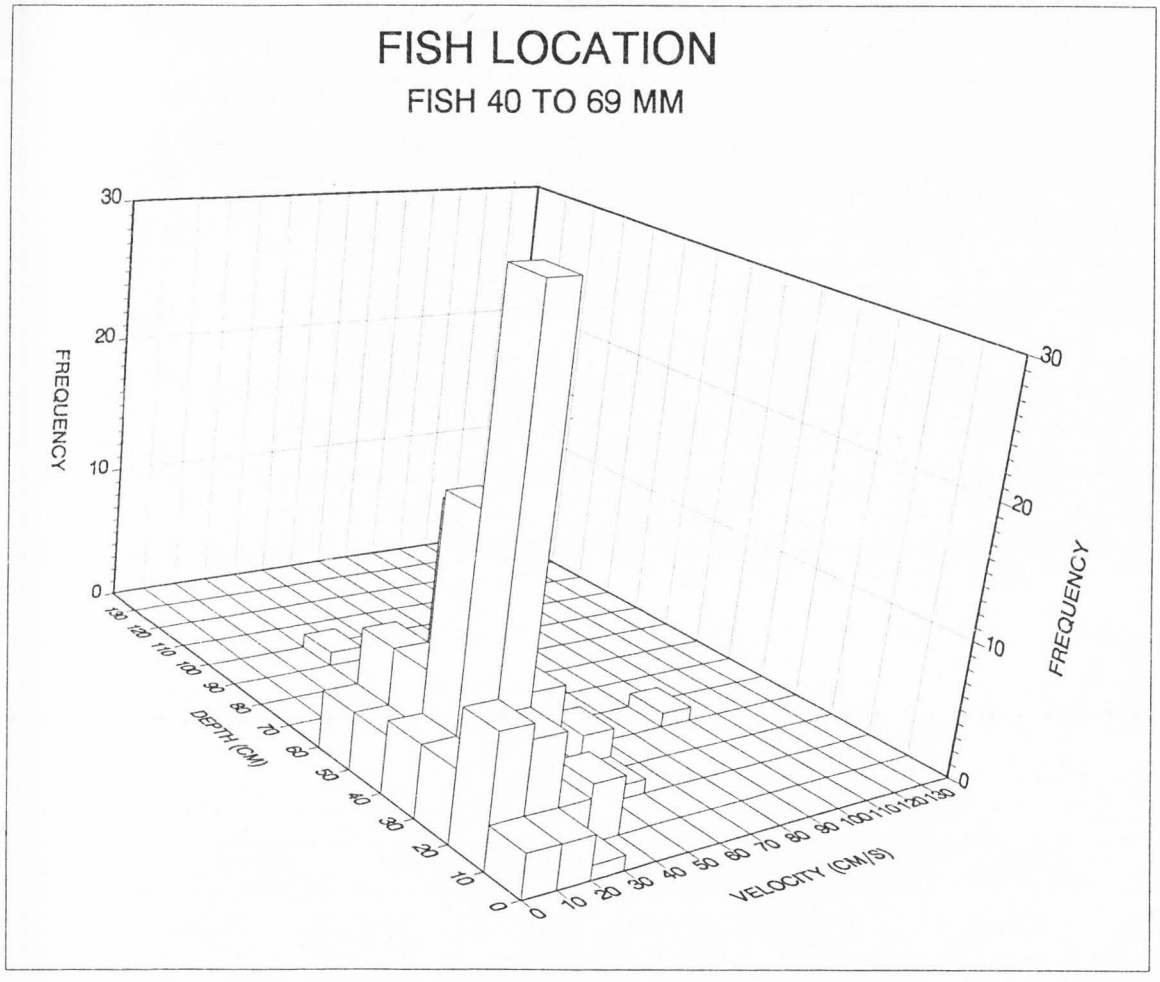

Figure 13. Frequency histogram of the number of cutthroat trout observed at each total depth/ mean velocity combination in St. Charles Creek, Idaho (Jacobsen, 1993, unpublished). The total number of fish locations plotted is 168. The average size of the fish was 49 mm TL with a range from 40 to 69 mm. Note that this graph is oriented different than Figure 11.

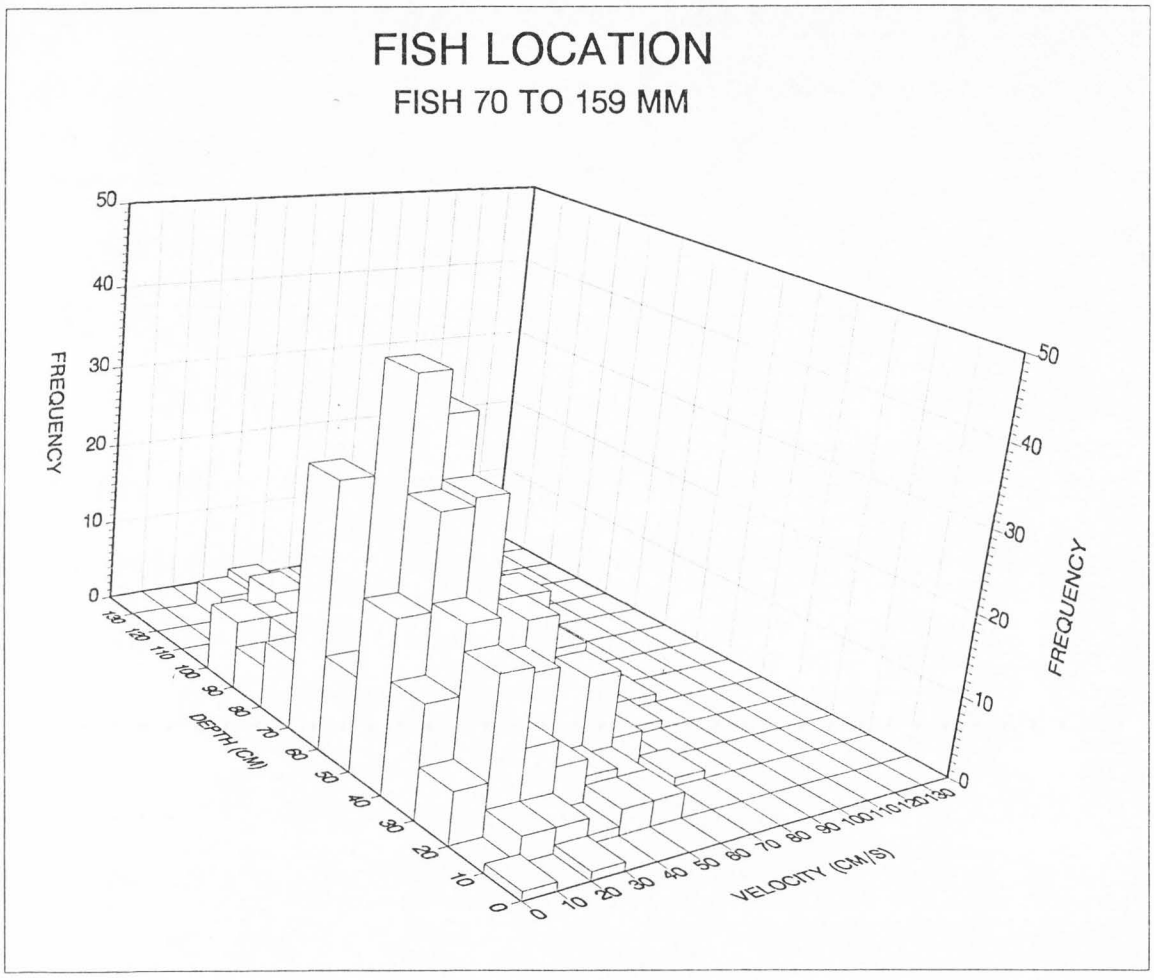

Figure 14. Frequency histogram of the number of cutthroat trout observed at each total depth/ mean velocity combination in St. Charles Creek, Idaho (Jacobsen, 1993, unpublished). The total number of fish locations plotted is 712. The average size of the fish was 106 mm TL with a range from 70 to 159 mm. Note that this graph is oriented different than Figure 11.

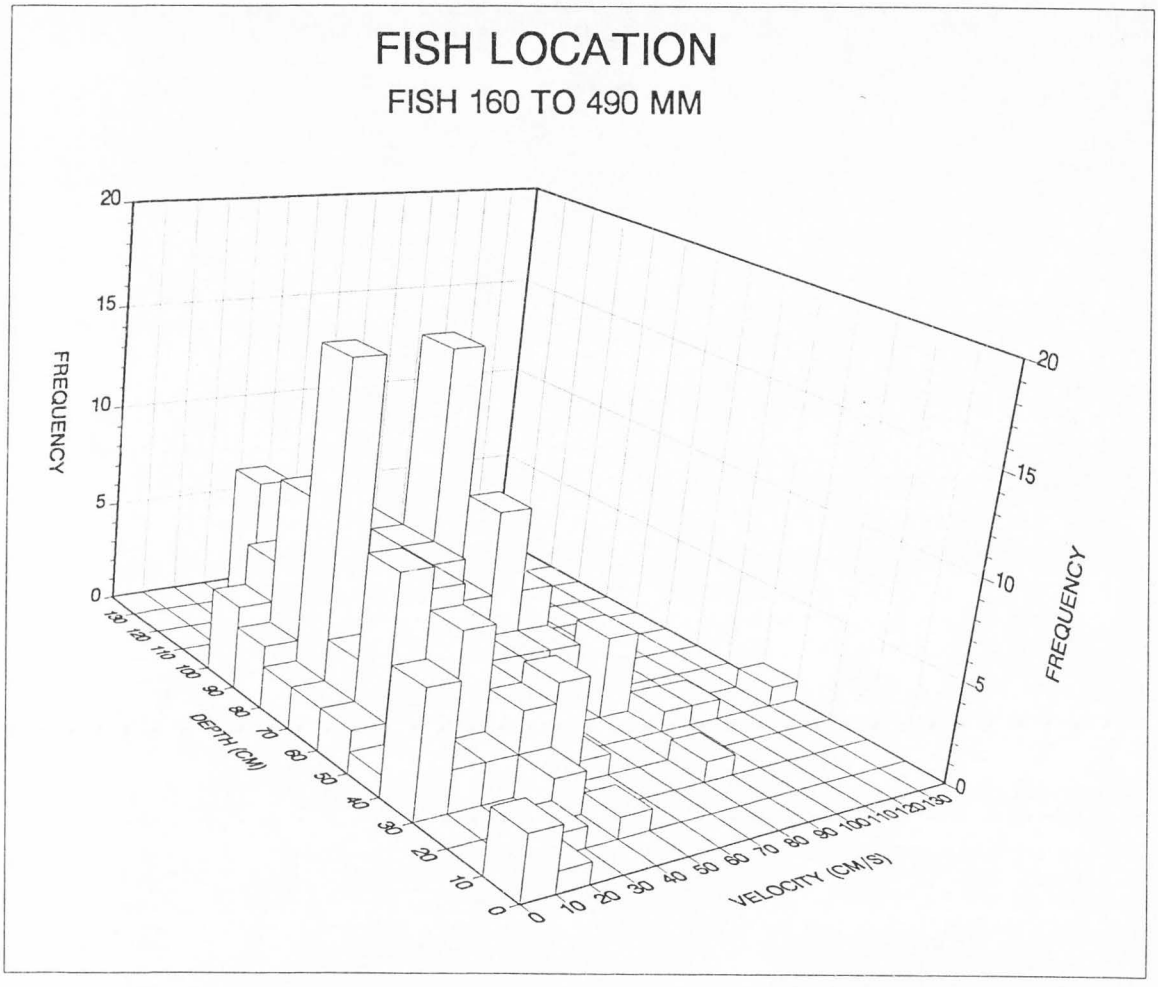

Figure 15. Frequency histogram of the number of cutthroat trout observed at each total depth/ mean velocity combination in St. Charles Creek, Idaho (Jacobsen, 1993, unpublished). The total number of fish locations plotted is 249. The average size of the fish was 209 mm TL with a range from 160 to 490 mm. Note that this graph is oriented different than Figure 11.

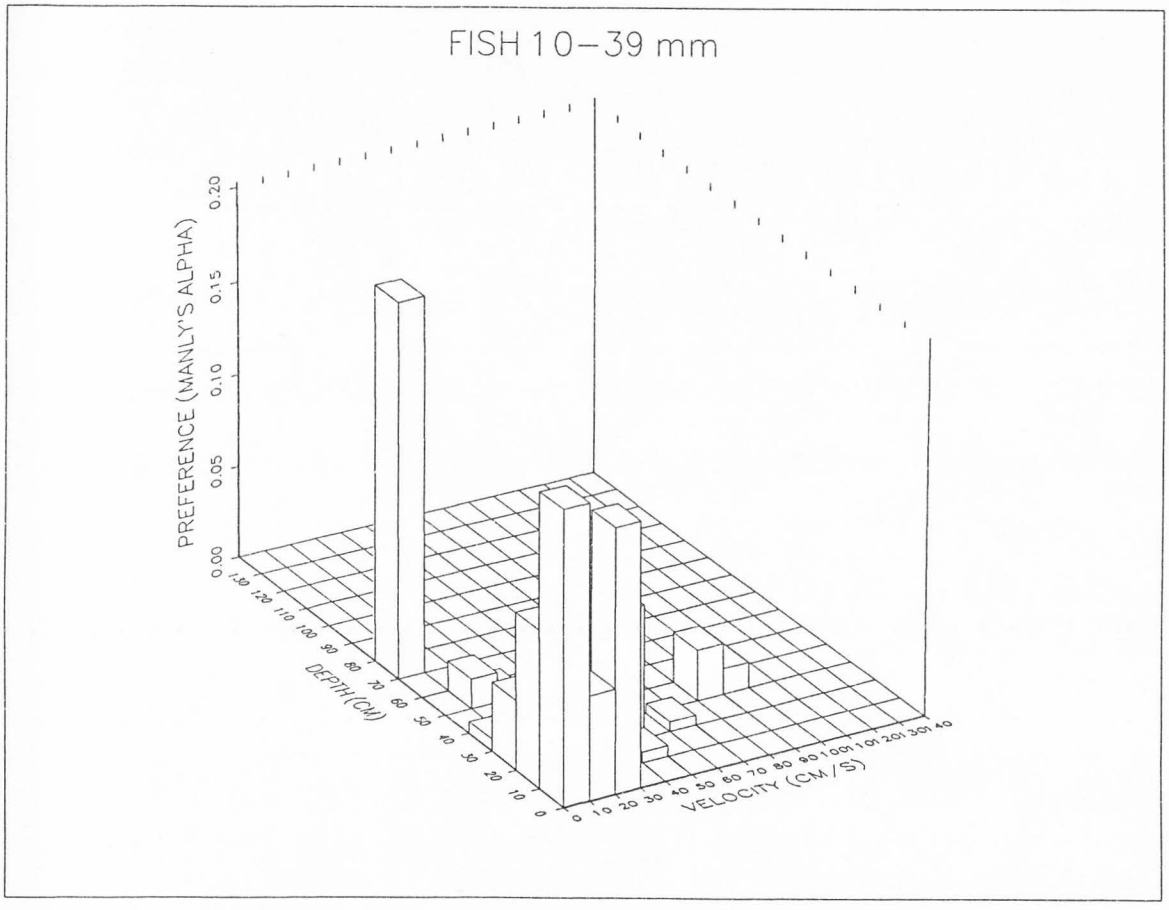

Figure 16. Calculated preference of cutthroat trout in St. Charles Creek, Idaho, for each total depth/ mean velocity combination. The preference function is Manly's Alpha (Krebs, 1989) where values greater than 0.005 (not 0.05, see the Figure) indicate preference and values less than 0.005 indicate avoidance. The lengths of fish plotted range from 10 to 39 cm. Note that this graph is oriented different than Figure 11.

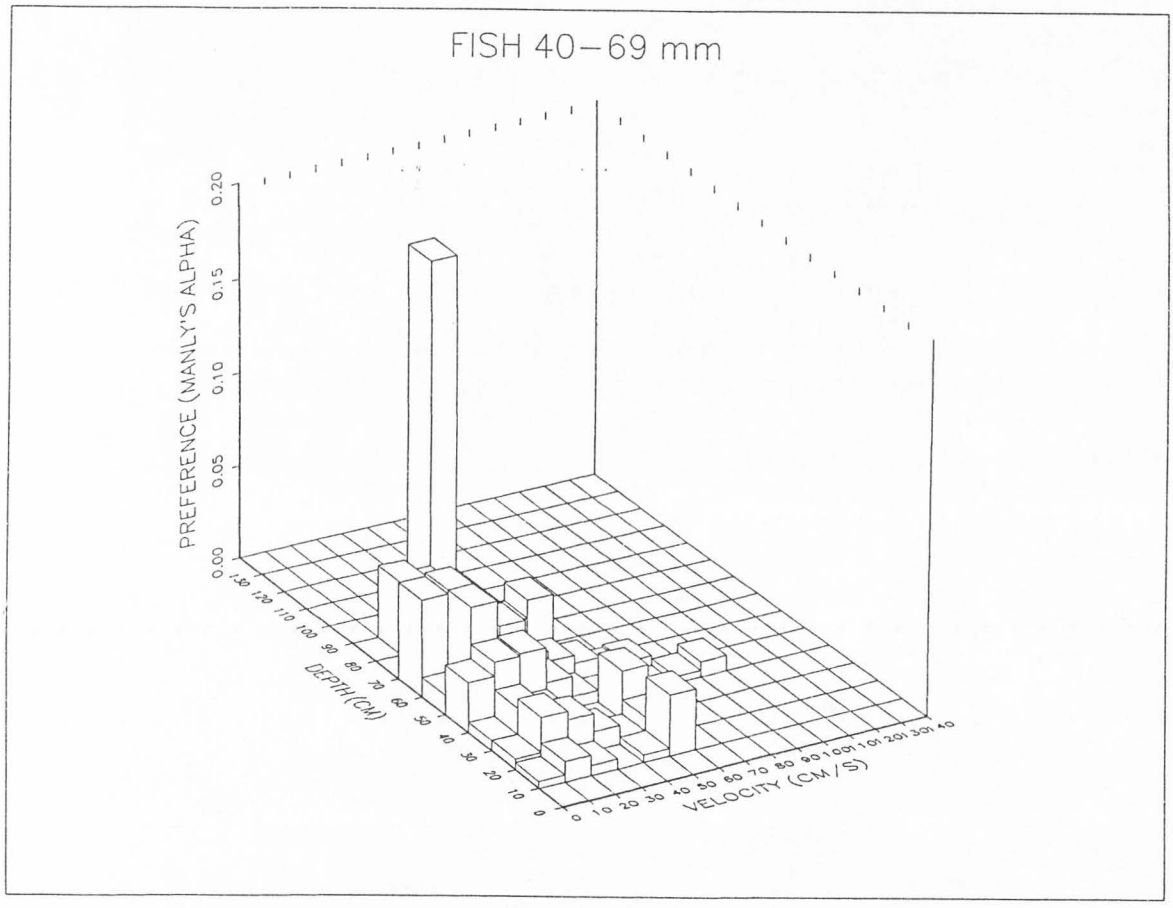

Figure 17. Calculated preference of cutthroat trout in St. Charles Creek, Idaho, for each total depth/ mean velocity combination. The preference function is Manly's Alpha (Krebs, 1989) where values greater than 0.005 (not 0.05, see the Figure) indicate preference and values less than 0.005 indicate avoidance. The lengths of fish plotted range from 40 to 69 cm. Note that this graph is oriented different than Figure 11.

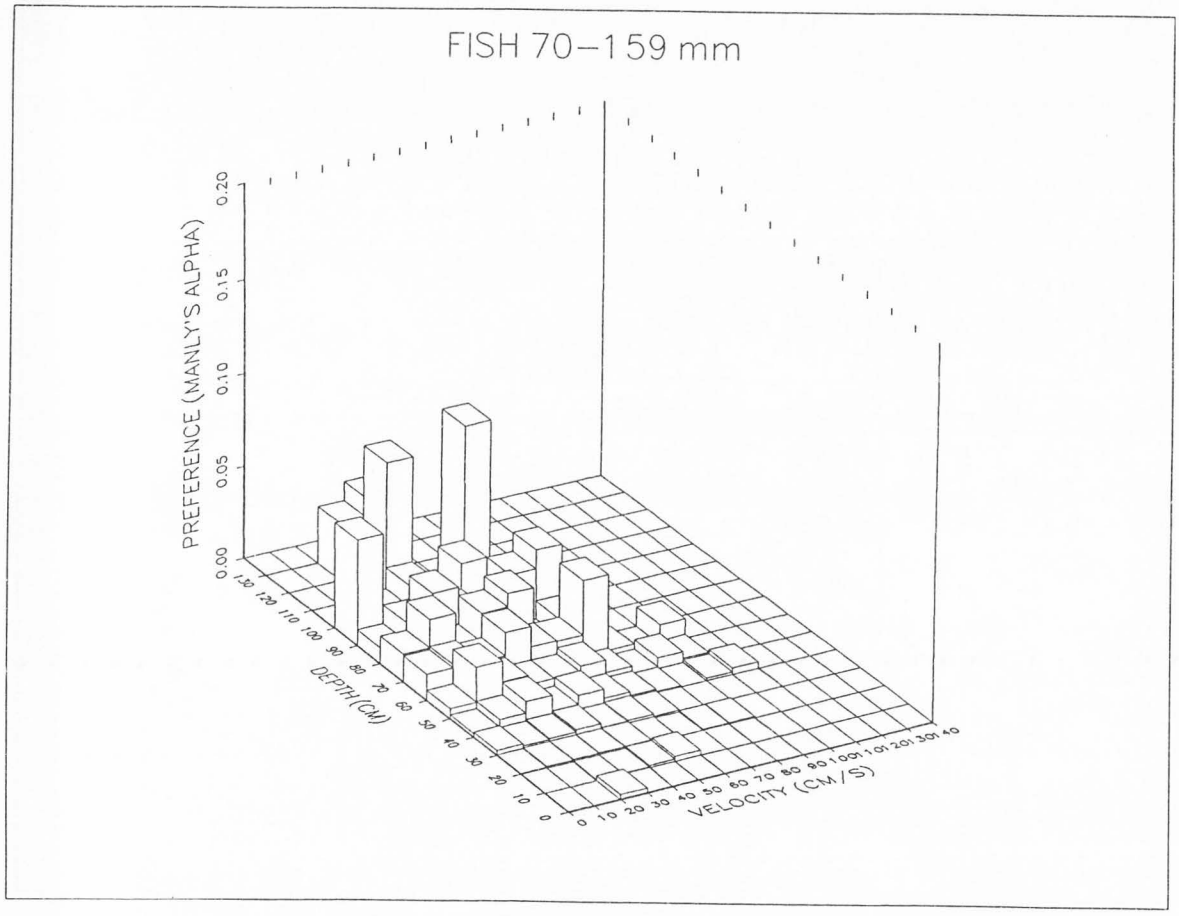

Figure 18. Calculated preference of cutthroat trout in St. Charles Creek, Idaho, for each total depth/ mean velocity combination. The preference function is Manly's Alpha (Krebs, 1989) where values greater than 0.005 (not 0.05, see the Figure) indicate preference and values less than 0.005 indicate avoidance. The lengths of fish plotted range from 70 to 159 cm. Note that this graph is oriented different than Figure 11.

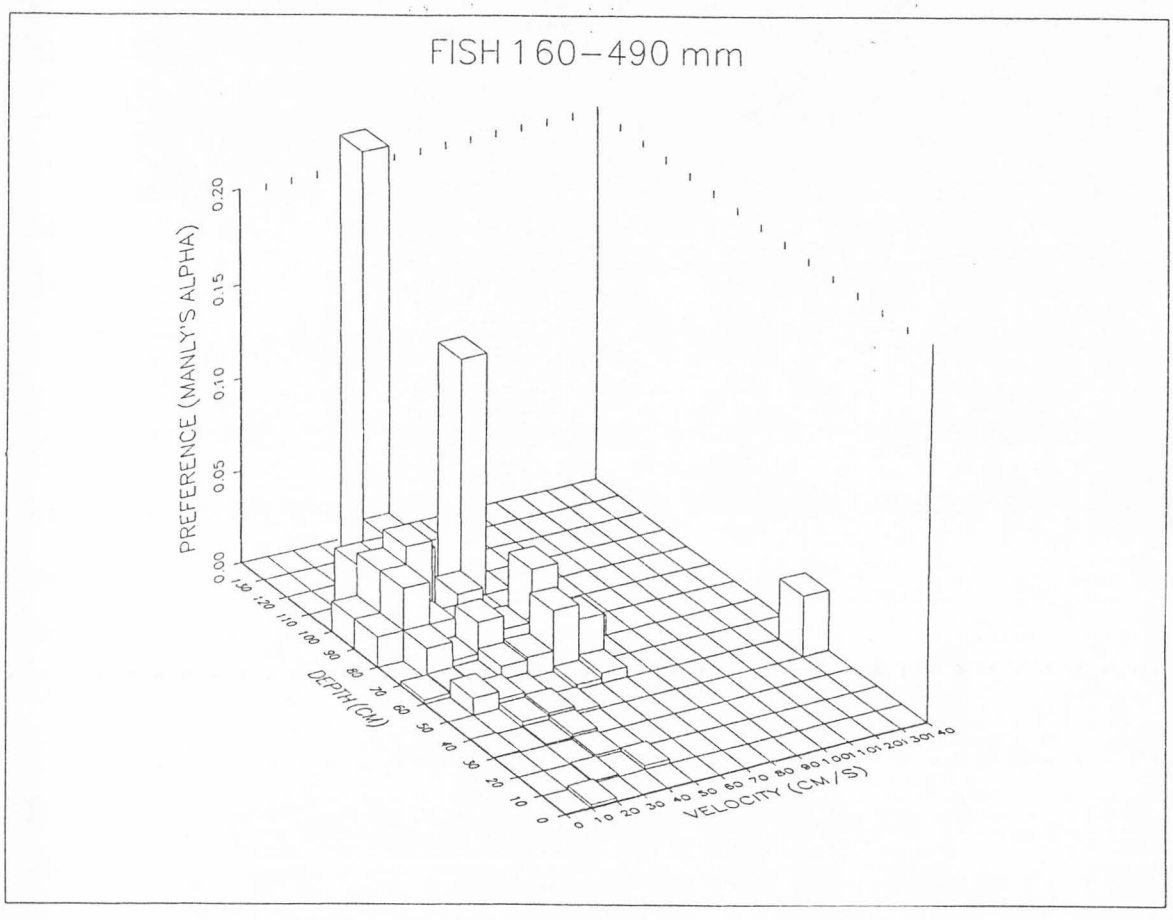

Figure 19. Calculated preference of cutthroat trout in St. Charles Creek, Idaho, for each total depth/ mean velocity combination. The preference function is Manly's Alpha (Krebs, 1989) where values greater than 0.005 (not 0.05, see the Figure) indicate preference and values less than 0.005 indicate avoidance. The lengths of fish plotted range from 160 to 490 cm. Note that this graph is oriented different than Figure 11.

Some of the preference figures (Figures 16-19) show anomalous regions of high preference that result from a small number of fish being located in a region of depths and velocities that is very rare in the habitat availability data in part because the small number of habitat availability measurements left "holes" (unevenness) in the frequency distribution (see Figure 11). For example, Figure 16 shows a peak of high preference at a velocity of 20-30 cm/s and a depth of 0-10 cm that is the result of only nine fish (of 346 total) being located in a region of low habitat availability. Aside from the anomalies, however, the general trends of the data show that different sized fish are preferentially utilizing different depths and velocities.

Fish size versus habitat use. Linear correlation of fish size versus velocity and fish size versus depth showed that increased fish size was significantly correlated the utilization of deeper and faster water. The mean column velocity utilized was positively correlated with fish size, where the slope of the regression line $b_1=0.14$ ($P<0.001$); and the water depths utilized increased with increased fish size $b_1=0.41$ ($P<0.001$).

NEI versus fish location. NEI model predictions of the pattern of depths and velocities that different size fish in St. Charles Creek should be utilizing to obtain high NEI corresponded remarkably well with the pattern of actual depths and velocities being utilized by different sized fish (Figures 20-23). Figure 20 shows a surface plot of NEI for a 30 mm fish (temperature = 12°C and drift density = 400 prey/ 100 m^3) overlaid with the habitat locations of fish ranging from 10 to 39 mm. The majority

of the fish locations occur near the beginning of the highest peak in NEI just outside of the area where the model predicts they should be located. For fish larger than 39 mm, the NEI model predicts that fish should increasingly utilize faster velocities and deeper depths. Figures 21-23 show NEI modeled for fish 50, 100, and 200 mm overlaid with the locations of corresponding size classes of fish. In each of these cases, the majority of the fish locations actually fall within the region of depths and velocities that the NEI model predicts they should.

Spearman's rank correlation test indicates that there is a significant and strong correlation between fish habitat use and the predictions of NEI by the model. The area under each predicted NEI surface was separated into regions of 10% decreasing increments of maximum NEI (e.g., 100-90%, 90-80%, 80-70% of maximum NEI) and rank correlated with the relative preference (# fish/available habitat, scaled between 0 and 1.0) of fish present in each region (Figure 24). For all sizes of fish combined, Spearman's $r_{n=11} = 0.91$ ($P<0.01$). Figure 25 shows the correlation of each size class of fish separately. The rank correlation of the smallest size class of fish (10-39 mm) with the NEI model produces the poorest fit with a Spearman's $r_{n=11} = -0.14$ (also see Figure 20). The other size classes of fish (40-69, 70-159, and 160-490 mm), however, show strong and significant correlations with the NEI model, Spearman's $r_{n=11} = 0.89$, 0.96, and 0.96, respectively ($P<0.01$).

Figure 20. NEI modeled at each total depth and mean column velocity combination for 30 mm trout at 12°C. Actual cutthroat trout depth/velocity locations from St. Charles Creek, Idaho, (Jacobsen, 1993, unpublished) are plotted as circles on the isoplot of the NEI surface. The total number of fish locations plotted is 346. The average size of the fish was 29 mm TL with a range from 10 to 39 mm. Note that this graph is oriented different than Figure 11.

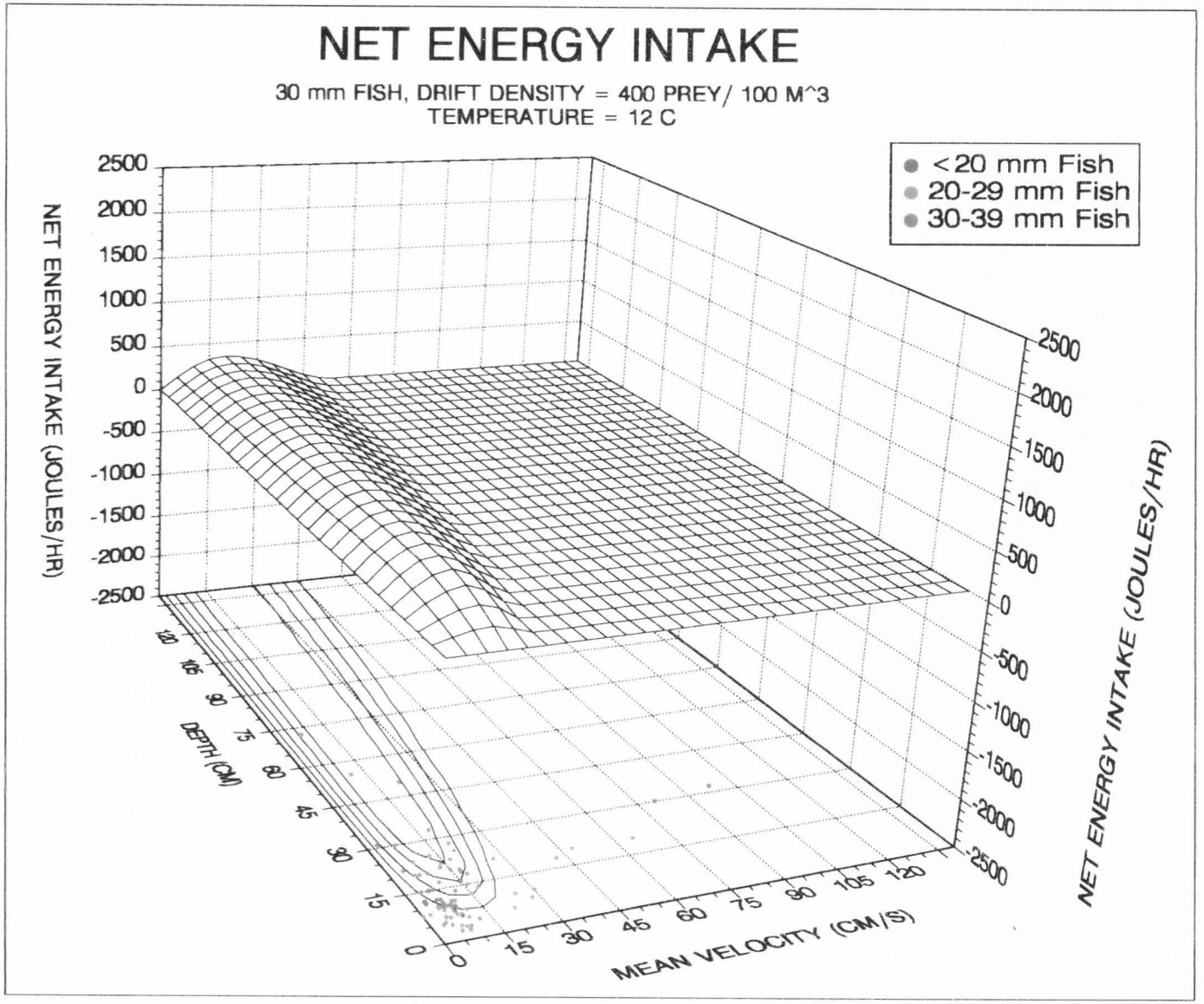
NET ENERGY INTAKE
30 mm FISH, DRIFT DENSITY = 400 PREY/ 100 M^3
TEMPERATURE = 12 C
< 20 mm Fish
20-29 mm Fish
30-39 mm Fish
NET ENERGY INTAKE (JOULES/HR)
2500
2000
1500
1000
500
0
-500
-1000
-1500
-2000
-2500
DEPTH (CM)
0
15
30
45
60
75
90
105
120
MEAN VELOCITY (CM/S)
NET ENERGY INTAKE (JOULES/HR)

Figure 21. NEI modeled at each total depth and mean column velocity combination for 50 mm trout at 12°C. Actual cutthroat trout depth/velocity locations from St. Charles Creek, Idaho, (Jacobsen, 1993, unpublished) are plotted as circles on the isoplot of the NEI surface. The total number of fish locations plotted is 168. The average size of the fish was 49 mm TL with a range from 40 to 69 mm. Note that this graph is oriented different than Figure 11.

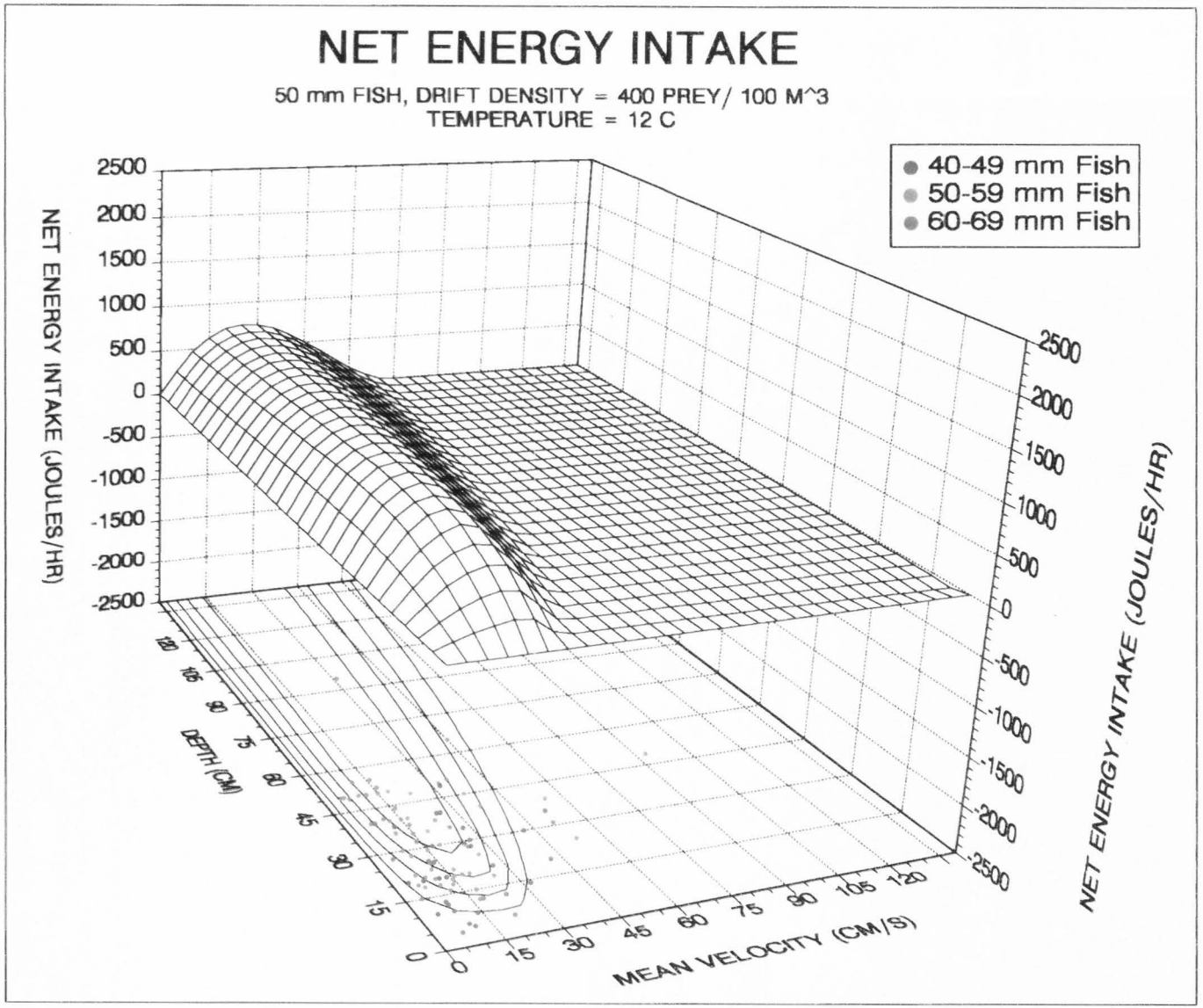
NET ENERGY INTAKE
50 mm FISH, DRIFT DENSITY = 400 PREY/ 100 M^3
TEMPERATURE = 12 C
40-49 mm Fish
50-59 mm Fish
60-69 mm Fish
NET ENERGY INTAKE (JOULES/HR)
2500
2000
1500
1000
500
0
-500
-1000
-1500
-2000
-2500
DEPTH (CM)
0
15
30
45
60
75
90
105
120
MEAN VELOCITY (CM/S)
NET ENERGY INTAKE (JOULES/HR)

Figure 22. NEI modeled at each total depth and mean column velocity combination for 100 mm trout at 12°C. Actual cutthroat trout depth/velocity locations from St. Charles Creek, Idaho, (Jacobsen, 1993, unpublished) are plotted as circles on the isoplot of the NEI surface. The total number of fish locations plotted is 712. The average size of the fish was 106 mm TL with a range from 70 to 159 mm. Note that this graph is oriented different than Figure 11.

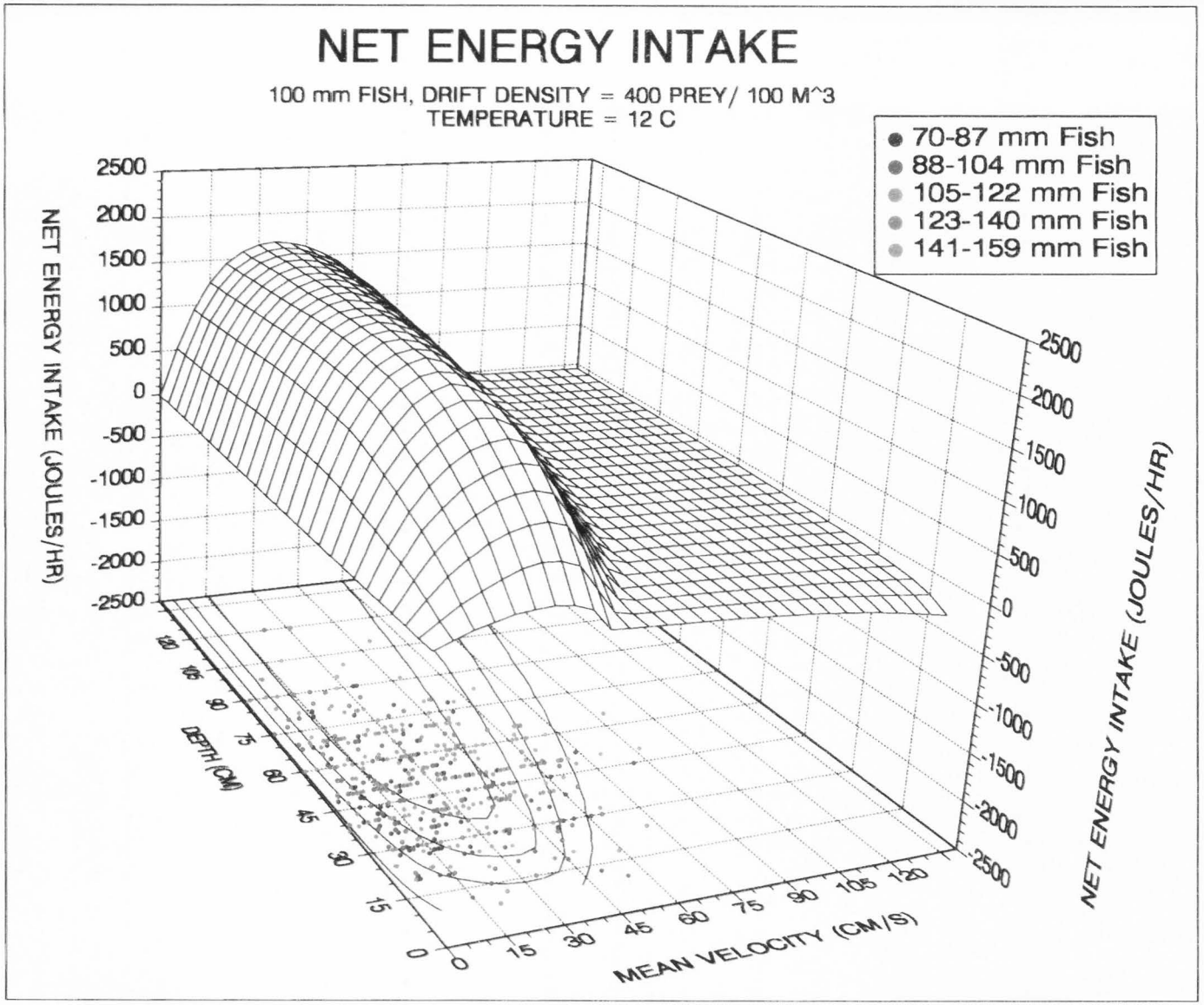
NET ENERGY INTAKE
100 mm FISH, DRIFT DENSITY = 400 PREY/ 100 M^3
TEMPERATURE = 12 C
70-87 mm Fish
88-104 mm Fish
105-122 mm Fish
123-140 mm Fish
141-159 mm Fish
NET ENERGY INTAKE (JOULES/HR)
2500
2000
1500
1000
500
0
-500
-1000
-1500
-2000
-2500
DEPTH (CM)
0
15
30
45
60
75
90
105
120
MEAN VELOCITY (CM/S)
NET ENERGY INTAKE (JOULES/HR)

Figure 23. NEI modeled at each total depth and mean column velocity combination for 200 mm trout at 12°C. Actual cutthroat trout depth/velocity locations from St. Charles Creek, Idaho, (Jacobsen, 1993, unpublished) are plotted as circles on the isoplot of the NEI surface. The total number of fish locations plotted is 249. The average size of the fish was 209 mm TL with a range from 160 to 490 mm. Note that this graph is oriented different than Figure 11.

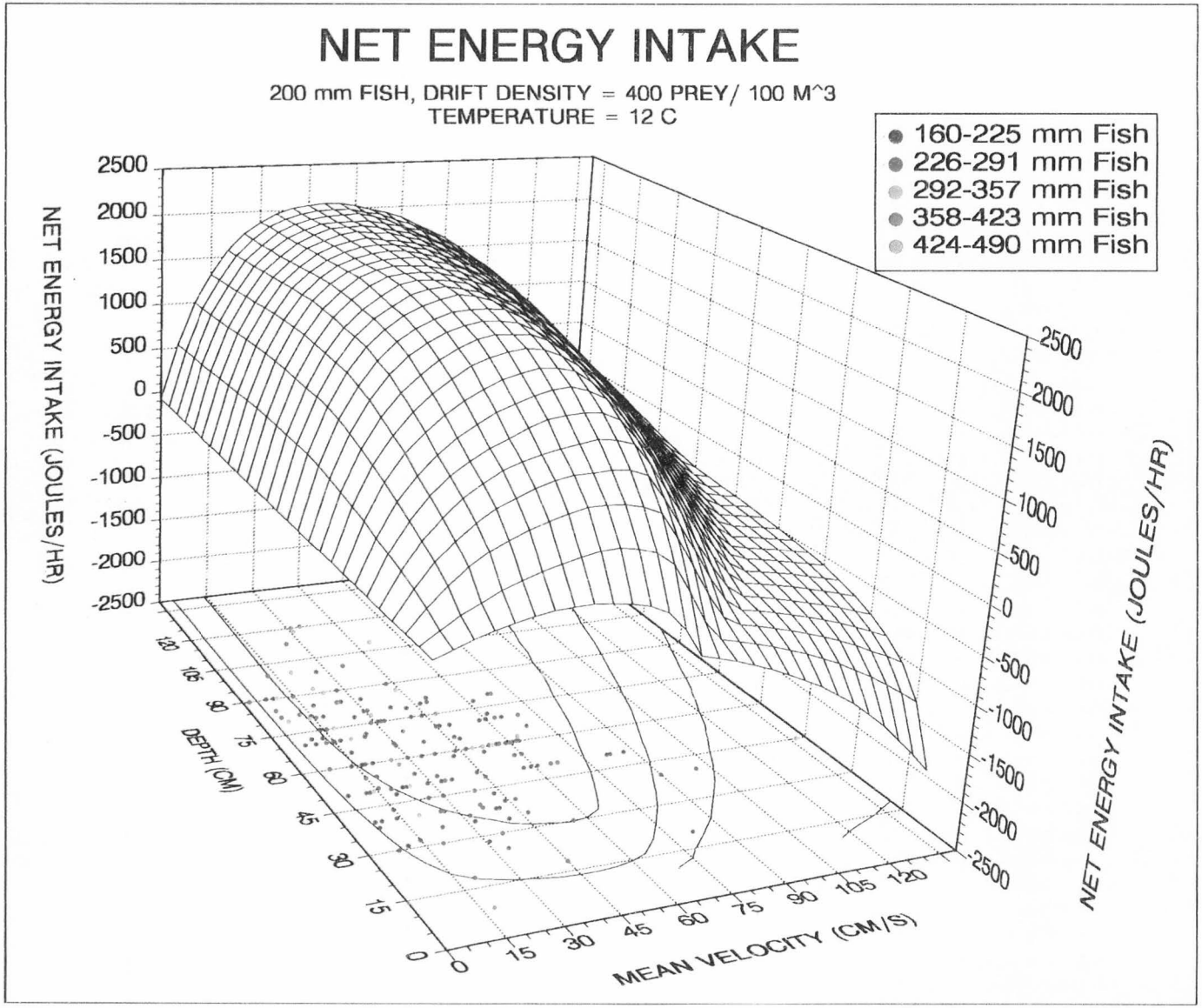
NET ENERGY INTAKE
200 mm FISH, DRIFT DENSITY = 400 PREY/ 100 M^3
TEMPERATURE = 12 C
160-225 mm Fish
226-291 mm Fish
292-357 mm Fish
358-423 mm Fish
424-490 mm Fish
NET ENERGY INTAKE (JOULES/HR)
2500
2000
1500
1000
500
0
-500
-1000
-1500
-2000
-2500
DEPTH (CM)
0
15
30
45
60
75
90
105
120
MEAN VELOCITY (CM/S)
NET ENERGY INTAKE (JOULES/HR)

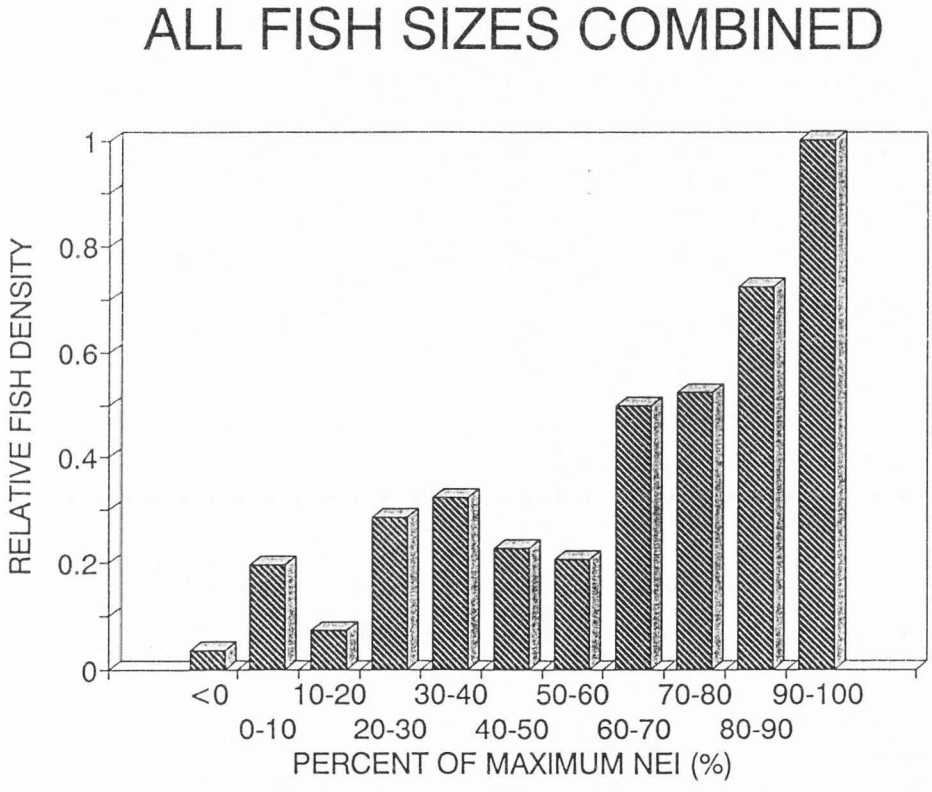

Figure 24. Correlation between relative fish preference (# fish/available habitat, scaled between 0 and 1.0) and percent of maximum NEI predicted by the NEI model (in 10% increments) for each of the different size classes of fish combined (10-39, 40-69, 70-159, 160-490 mm). Spearman's rank correlation coefficient $r_{s\ n=11} = 0.91$ ($P<0.01$).

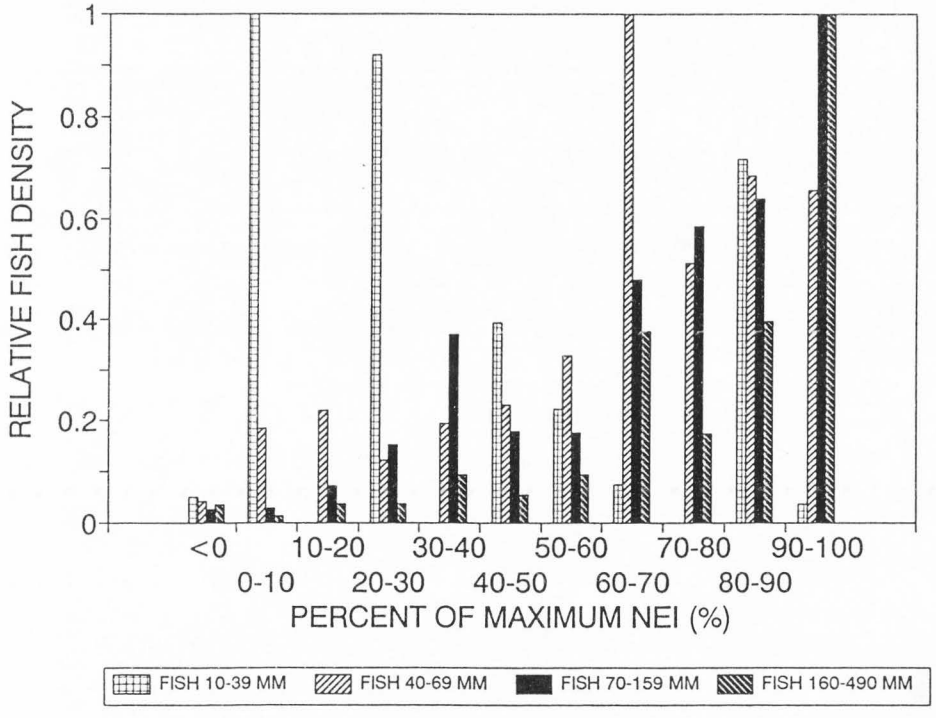

Figure 25. Correlation between relative fish preference (# fish/available habitat, scaled between 0 and 1.0) and percent of maximum NEI predicted by the NEI model (in 10% increments) for each of the different size classes of fish separately. Spearman's rank correlation coefficient from the smallest size class of fish to the largest is $r_{s\ n=11} = -0.14$ ($P<0.56$), $r_{s\ n=11} = 0.89$ ($P<0.01$), $r_{s\ n=11} = 0.96$ ($P<0.01$), $r_{s\ n=11} = 0.96$ ($P<0.01$).

The different NEI surfaces modeled for different sized fish show that as drift-feeding fish get larger, the model predicts they are able to obtain higher rates of NEI in progressively deeper and faster water. This results from increases in swimming speed and reaction distance as fish get larger (see the following Sensitivity Analysis section). The NEI model's pattern of predicting that fish should utilize deeper depths and faster velocities (also a wider range of velocities) as they get larger is closely followed by the actual habitat utilization of different sized fish in St. Charles Creek. This provides convincing evidence that in general fish in St. Charles Creek utilize habitats that provide high NEI, and that the size-dependent shifts of larger fish to deeper and faster water correspond to size-dependent shifts in the ability of fish to obtain NEI. The poorest fit of the model occurred for the smallest size class of fish (10-39 mm). The reason for the poor fit is unknown, but could possibly result from the model incorrectly predicting NEI for small fish and/or from small fish not utilizing high NEI sites because of predation or dominance threats of larger fish.

Results and discussion for
data set two (spatial data)

Detailed NEI modeling of four stations (two pools and two runs) on St. Charles Creek provides additional evidence that fish in St. Charles Creek generally utilize stream microhabitats that match the NEI model predictions of high NEI. Figures 26-30 show the modeled NEI and fish locations for each of the four stations.

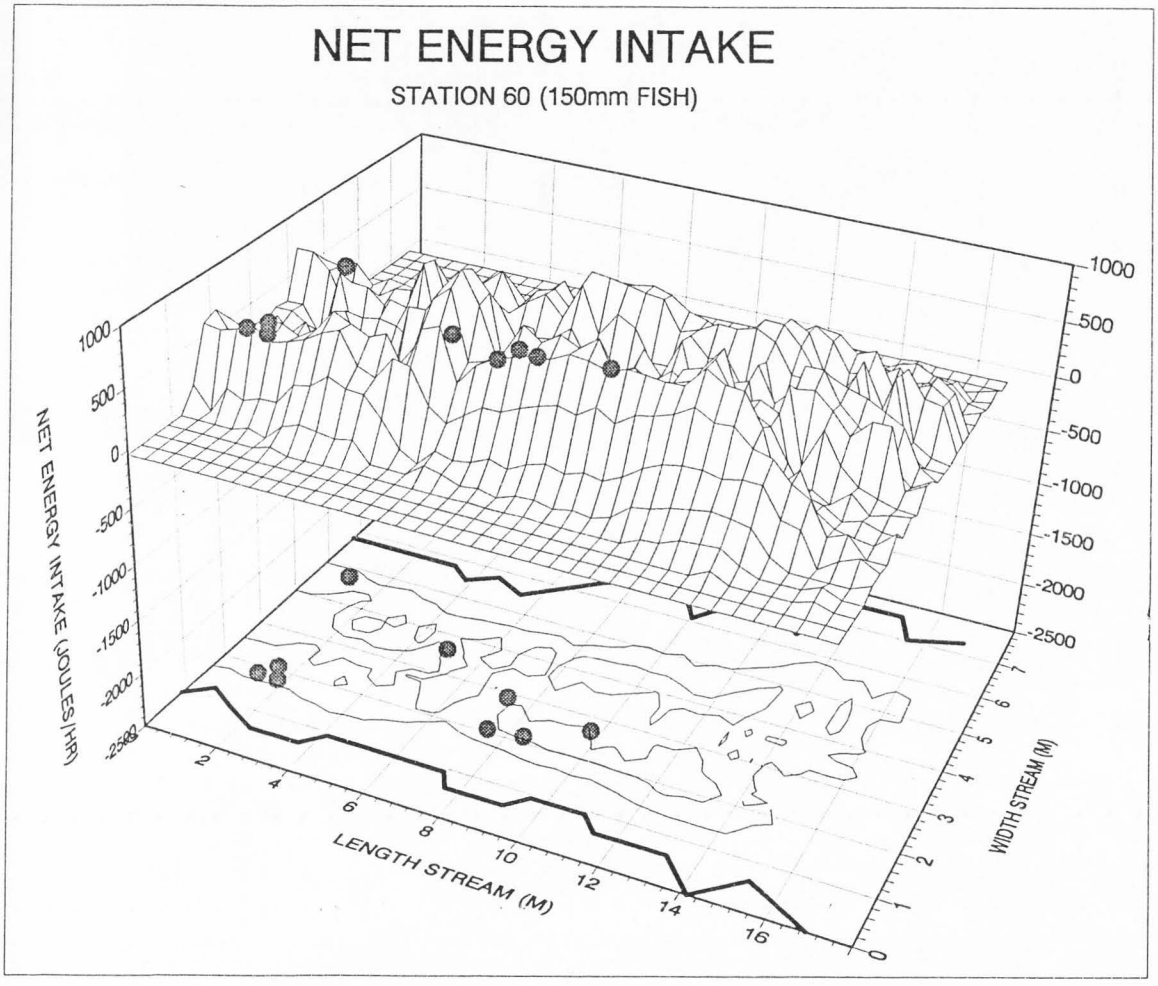

Figure 26. Modeled NEI and observed fish locations at Station 60 (a run) in St. Charles Creek. NEI was modeled for 150 mm fish and fish in this size class are plotted as darkened circles. Fish locations were recorded by snorkeling the station one time after which topography, depth, and velocity data were collected to model NEI. The temperature used in the model was 12°C and the drift rate was 209 prey/ 100 m^3. Bold black lines indicate the margins of the stream. Average NEI of the fish is 722 J/hr and average NEI in the stream is 378 J/hr.

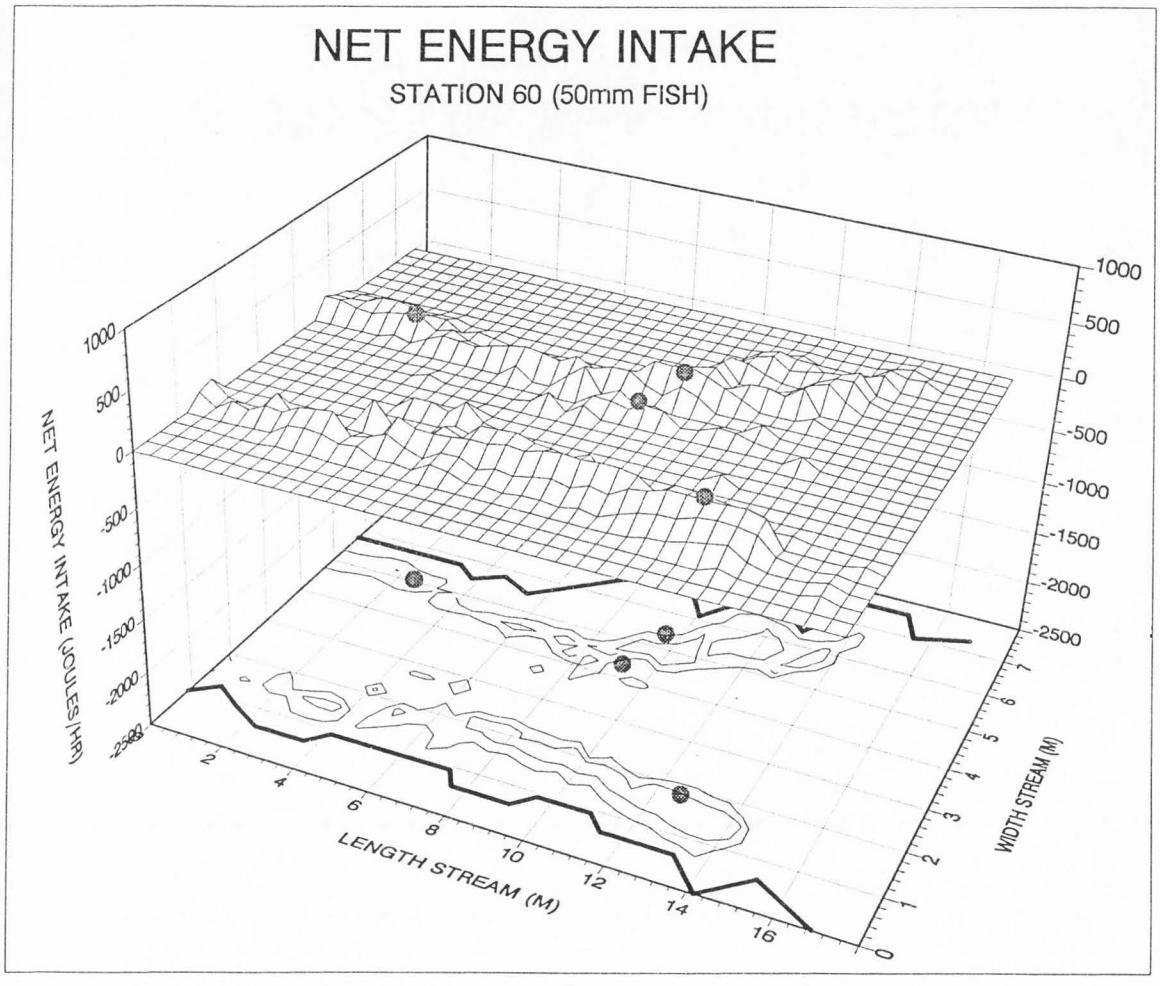

Figure 27. Modeled NEI and observed fish locations at Station 60 (a run) in St. Charles Creek. NEI was modeled for 50 mm fish and fish in this size class are plotted as darkened circles. Fish locations were recorded by snorkeling the station one time after which topography, depth, and velocity data were collected to model NEI. The temperature used in the model was 12°C and the drift rate was 209 prey/ 100 m^3. Bold black lines indicate the margins of the stream. Average NEI of the fish is 128 J/hr and average NEI in the stream is 36 J/hr.

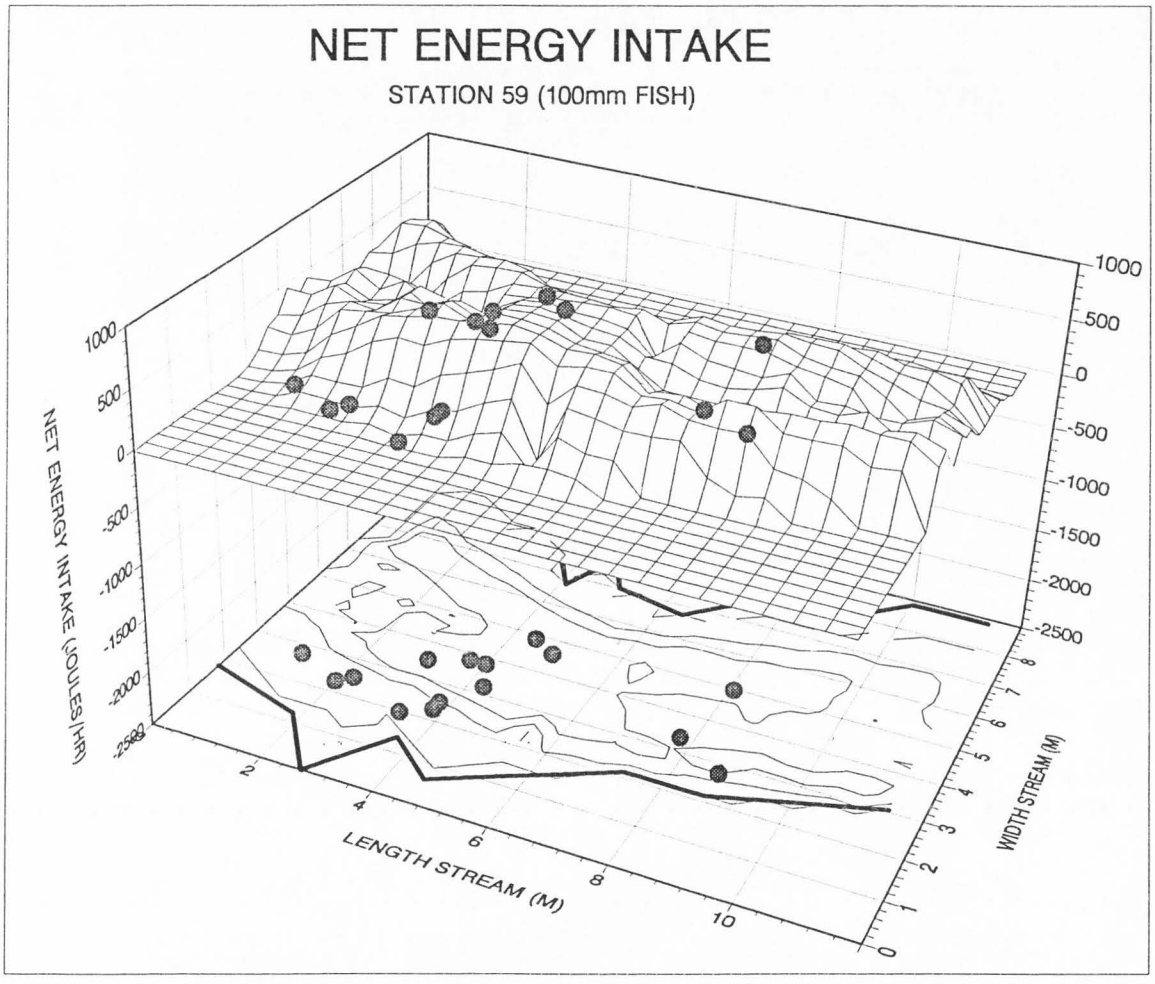

Figure 28. Modeled NEI and observed fish locations at Station 59 (a pool) in St. Charles Creek. NEI was modeled for 100 mm fish. Fish are plotted as darkened circles. Fish locations were recorded by snorkeling the station one time after which topography, depth, and velocity data were collected to model NEI. The temperature used in the model was 12°C and the drift rate was 149 prey/ 100 m^3. Bold black lines indicate the margins of the stream. Average NEI of the fish is 449 J/hr and average NEI in the stream is 355 J/hr.

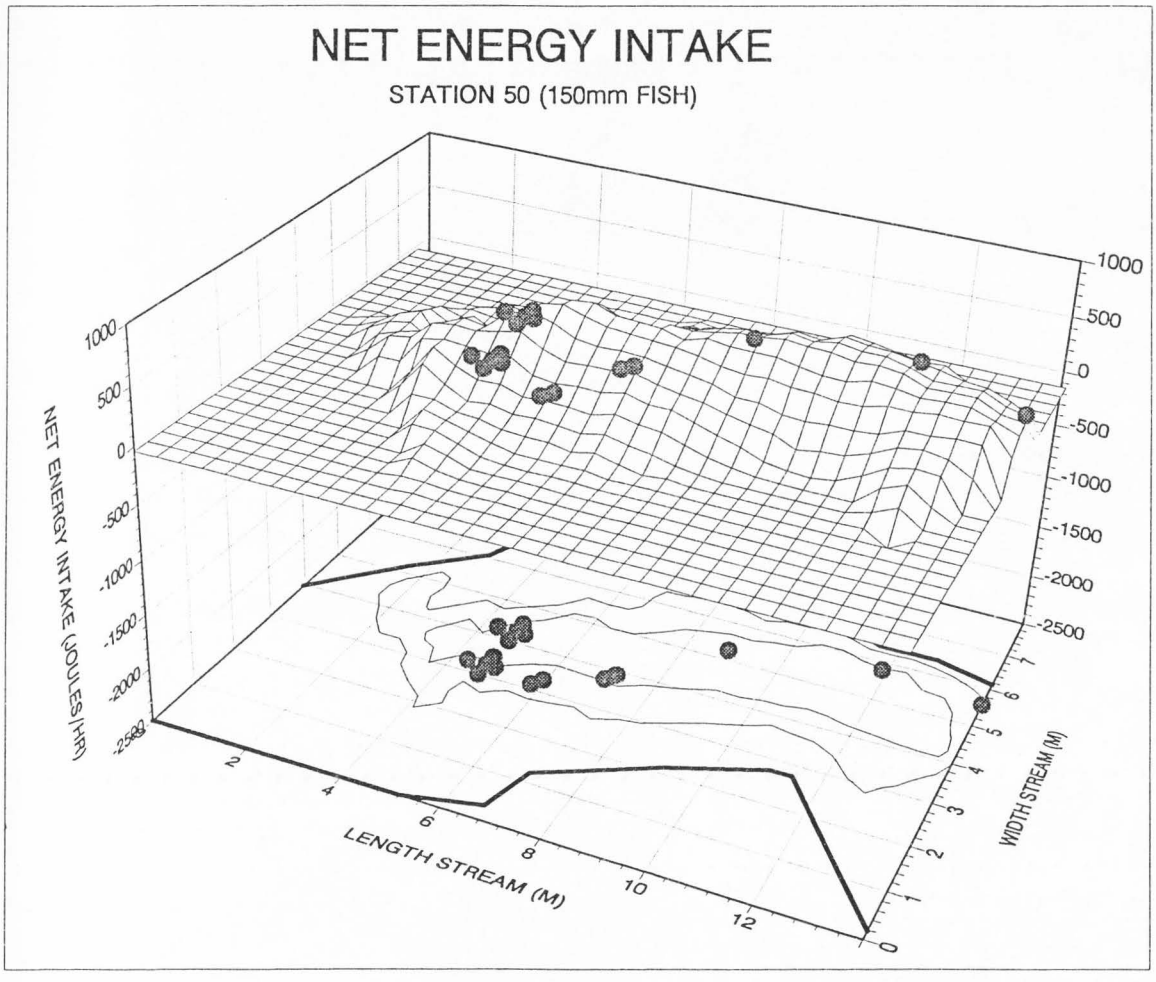

Figure 29. Modeled NEI and observed fish locations at Station 50 (a run) in St. Charles Creek. NEI was modeled for 150 mm fish. Fish are plotted as darkened circles. Fish locations were recorded by snorkeling the station one time after which topography, depth, and velocity data were collected to model NEI. The temperature used in the model was 12°C and the drift rate was 106 prey/ 100 m^3. Bold black lines indicate the margins of the stream. Average NEI of the fish is 412 J/hr and average NEI in the stream is 155 J/hr.

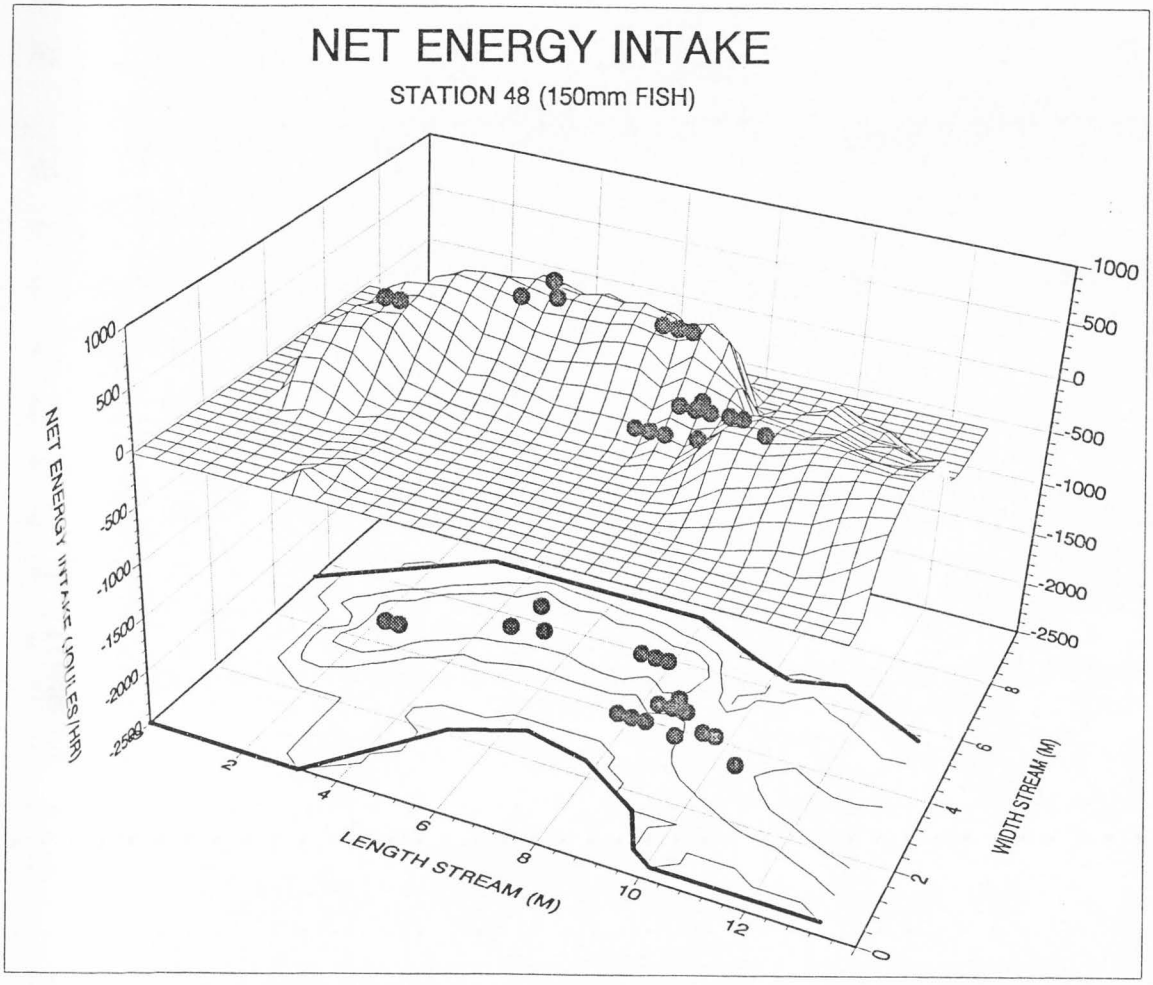

Figure 30. Modeled NEI and observed fish locations at Station 48 (a pool) in St. Charles Creek. NEI was modeled for 150 mm fish and fish in this size class are plotted as darkened circles. Fish locations were recorded by snorkeling the station one time after which topography, depth, and velocity data were collected to model NEI. The temperature used in the model was 12°C and the drift rate was 106 prey/ 100 m^3. Bold black lines indicate the margins of the stream. Average NEI of the fish is 418 J/hr and average NEI in the stream is 222 J/hr.

At each of the stream stations the average NEI of the locations fish utilized was higher (26 to 250% higher) than the average NEI available in the station (see figure captions for average NEI values). In each case except one (Station 59) the higher average NEI was significant ($P<0.05$). As a result, it appears that fish were selecting microhabitats with high NEI.

At Station 60 (a run) NEI was modeled for fish of two different sizes (150 and 50 mm) and the locations of fish of the corresponding sizes were overlaid on the appropriate NEI surface in Figures 26 and 27. All of the fish at this Station were located in areas of the stream that the NEI model predicted would provide high NEI. Stations 59, 50, and 48 (Figures 28-30) were also modeled in a similar manner, and in each case the majority of the fish locations were in or adjacent to areas of high NEI. In total, 45 of the 65 observed fish were located at or near the peak NEI locations in the stream. Rank correlation of relative fish habitat preference and modeled NEI shown in Figure 31 for the individual Stations 60, 59, 50, and 48, however, reveals a weaker relationship, Spearman's $r_{n=11} = 0.61$ ($P<0.03$), than would be expected if fish were strictly utilizing high NEI locations.

Several of the fish locations in Stations 59 and 48, particularly, were not located near peak NEI. In total, 9 fish were located at intermediate NEI and 11 fish were located in very low NEI areas (near zero NEI). Without exception, all of the fish at intermediate or low NEI locations were in areas with low velocities. The low velocities provide very little drift and consequently low NEI, but they result in low swimming costs and provide ideal resting locations for fish that are not feeding.

These results reveal a weakness in the data used to validate the NEI model. The optimum depth/velocity combination in terms of energetics depends on the activity fish are engaged in. High NEI locations should be utilized for feeding, but low swimming cost locations should be utilized for resting. To accurately assess the validity of the NEI model, the activity (e.g., resting or feeding) of the fish must be accurately assessed. Unfortunately, fish locations during this study were only observed once and for a short time period (a few minutes). As a result, the fish locations were not necessarily the locations that fish were utilizing as primary feeding locations. Future validation efforts of this sort should carefully address the activity states of fish (e.g., Hughes, 1991; Hill, 1989).

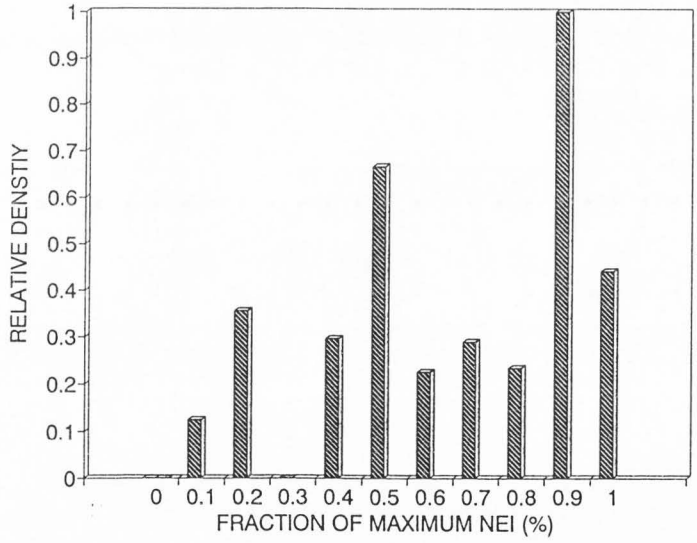

Figure 31. Correlation between relative fish preference (# fish/available habitat, scaled between 0 and 1.0) and percent of maximum NEI predicted by the NEI model (in 10% increments) for all stations combined (Station 60, 59, 50, and 48). Spearman's rank correlation coefficient $r_{s\ n=11} = 0.61$ ($P<0.03$).

SENSITIVITY ANALYSIS

Methods and assumptions

A single parameter perturbation analysis was used to determine the relative importance of each NEI model input parameter on NEI predictions and to determine which parameters in the model need additional research and refinement (Grant, 1986; Swartzman and Kaluzny, 1987). Analysis was accomplished by using baseline model input values to model NEI over a grid of depths and velocities (0-145 cm and 0-145 cm/s) and comparing baseline NEI output to the NEI output obtained by varying each input parameter by ±10%. For the baseline NEI output, a NEI surface was generated over the depth/velocity grid. A simple quantitative measure of the NEI surface was required to assess changes in the surface, so the volume under the surface was calculated along with its corresponding centroid. Then for each ±10% change in the input parameter, the percent change in the volume and centroid of the volume under the NEI surface was calculated to quantify the sensitivity (response) of the NEI surface. In addition, the perturbed NEI surface was subtracted from the baseline surface and the difference was plotted to show the actual change in NEI over the depth/velocity grid given a 10% perturbation. The input parameters that were varied are temperature, time required to make a feeding foray, capture cost, swimming cost, energy value of prey, drift density, depth off the bottom of the stream, power law coefficients, reaction distance, sustainable velocity of the fish, and maximum velocity of the fish.

The initial input values used to produce the baseline NEI surface were those used to validate the NEI model except that drift density was set to 120 prey/100 m^3 and the size of fish modeled was 120 mm, which is approximately the mean size of fish found in St. Charles Creek. All other input values are the same as those shown in Table 3 unless otherwise specified.

Results and discussion

Figure 32 shows the baseline NEI surface generated for the sensitivity analysis. The volume under the surface is 4,956,203 units and the coordinates of the centroid of the volume under the surface are depth = 89 cm, velocity = 41 cm/s, and NEI = 296 J/hr. Figures 33-36 show the response of the volume under the NEI surface and the depth, velocity, and NEI coordinates of the centroid, respectively, given ±10% changes in the input parameters. The volume under the NEI surface in conjunction with the centroid values gives a picture of how the NEI surface is changing (shifting) given changes in input values. In addition, the Appendix shows figures of each perturbed NEI surface subtracted from the baseline NEI surface.

The NEI surface was least sensitive to the time to make a feeding foray (time foraging), the capture cost, swimming cost, focal depth, and the maximum sustainable velocity of the fish. The NEI surface was most sensitive to changes in the maximum swimming velocity, reaction distance, and the power law.

Parameters that caused the largest upward shift in the NEI surface (i.e., increasing the NEI) were prey energy value, drift density, reaction distance, and maximum capture velocity. The parameters that caused the largest shifts in the NEI surface in

the depth direction were focal depth, the power law, and reaction distance. The parameters that caused the largest shifts in the velocity direction were temperature, focal depth, the power law, and maximum capture velocity.

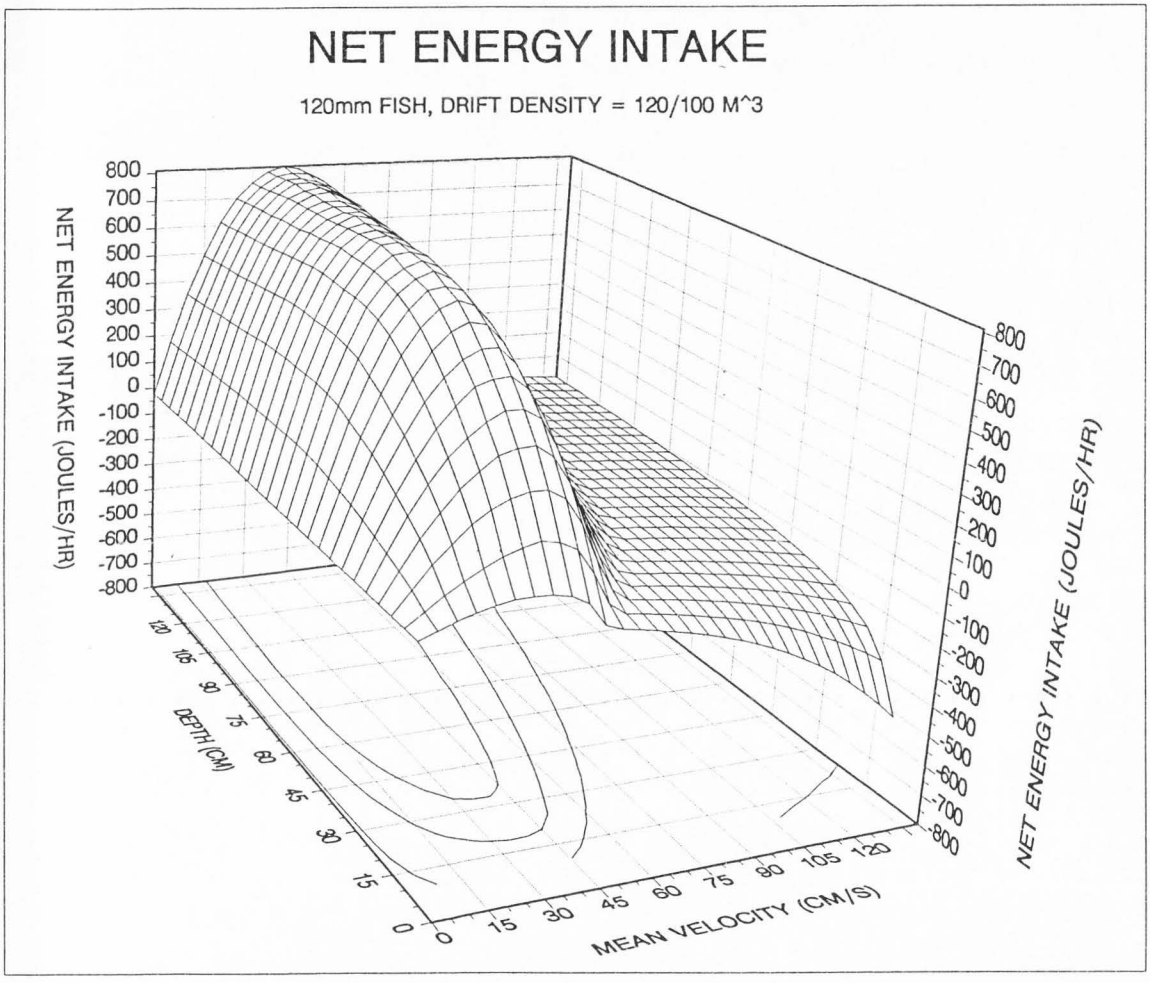

Figure 32. Baseline NEI surface used for sensitivity analysis. Modeled for 120 mm fish at temperature of 12°C and a drift rate of 120 prey/ 100 m^3. The volume under the NEI surface is 4,956,203 cubic units, the depth centroid of the volume is 89 cm, the velocity centroid is 41 cm/s, and the NEI centroid is 296 J/hr.

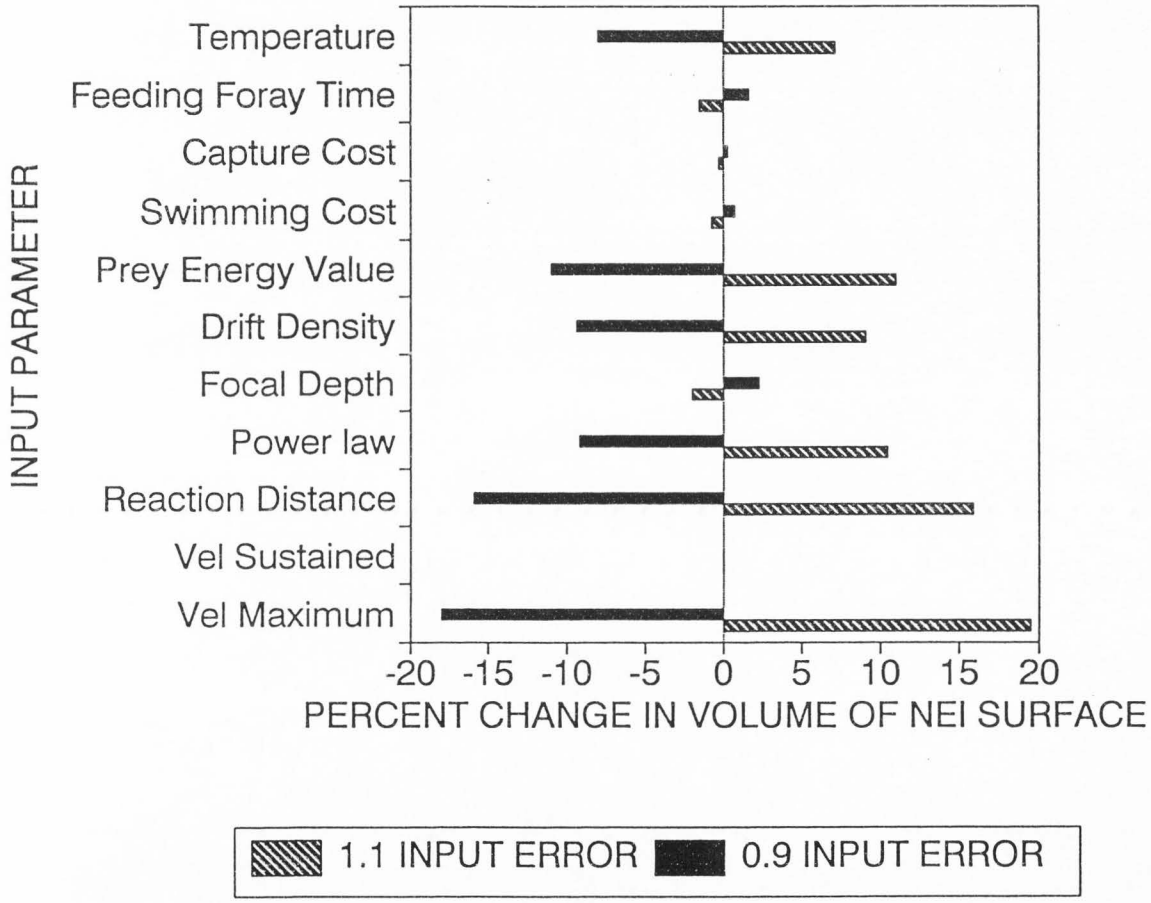

Figure 33. Percent change (sensitivity) of the volume under the NEI surface to 10% changes (1.1 X or 0.9 X nominal value) of each parameter used to model the NEI surface.

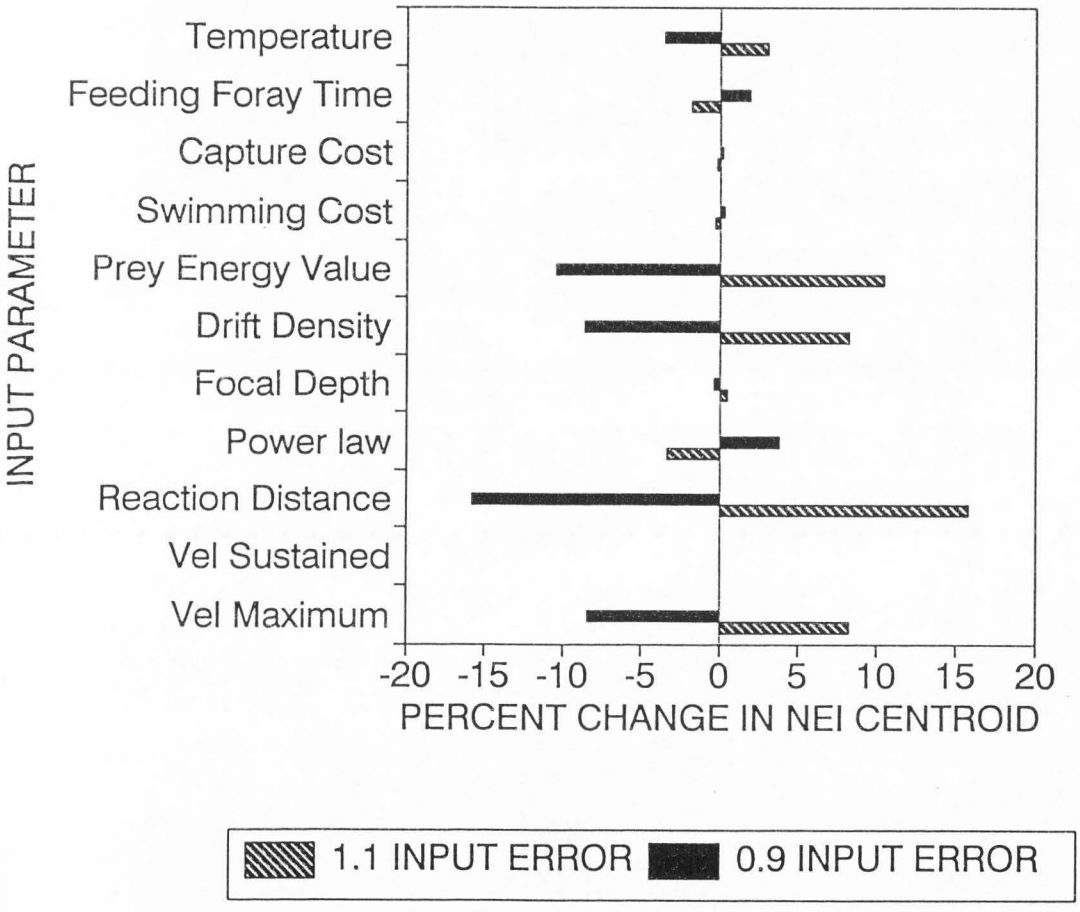

Figure 34. Percent change (sensitivity) of the NEI centroid for the volume under the NEI surface to 10% changes (1.1 X or 0.9 X nominal value) of each parameter used to model the NEI surface.

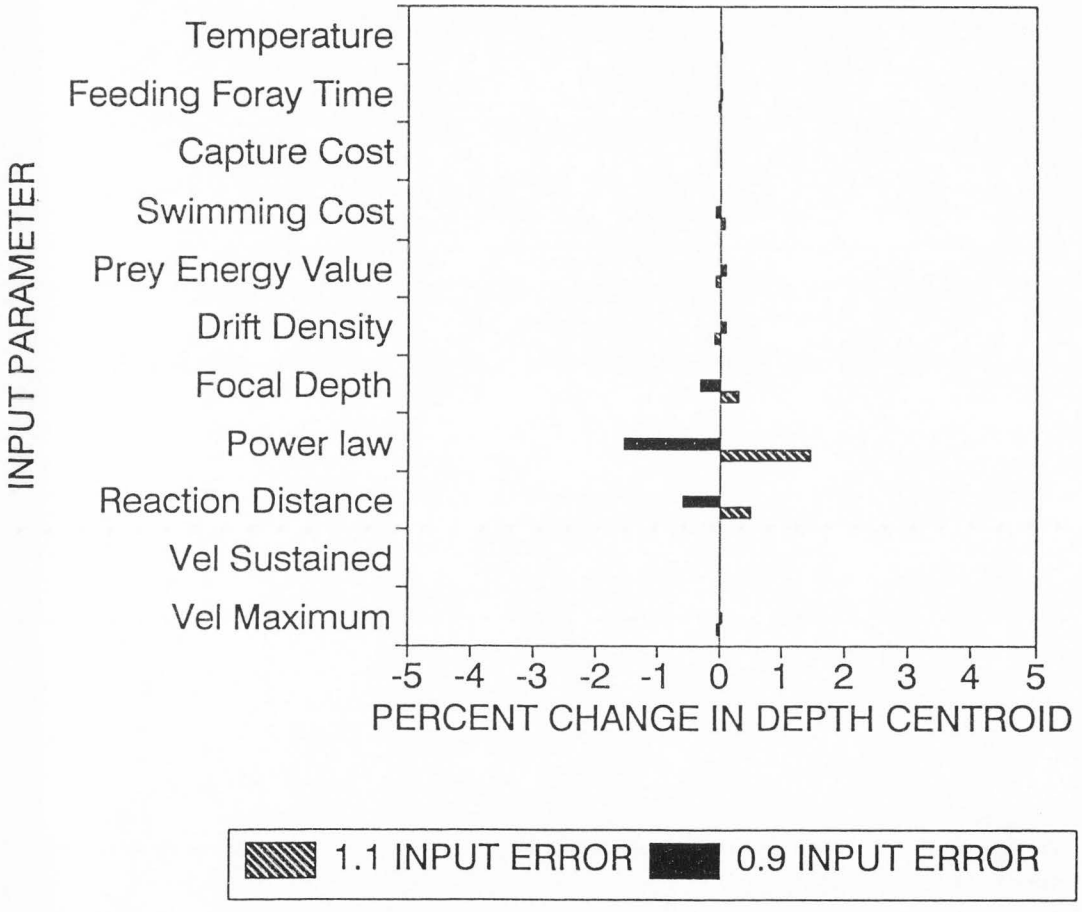

Figure 35. Percent change (sensitivity) of the depth centroid for the volume under the NEI surface to 10% changes (1.1 X or 0.9 X nominal value) of each parameter used to model the NEI surface.

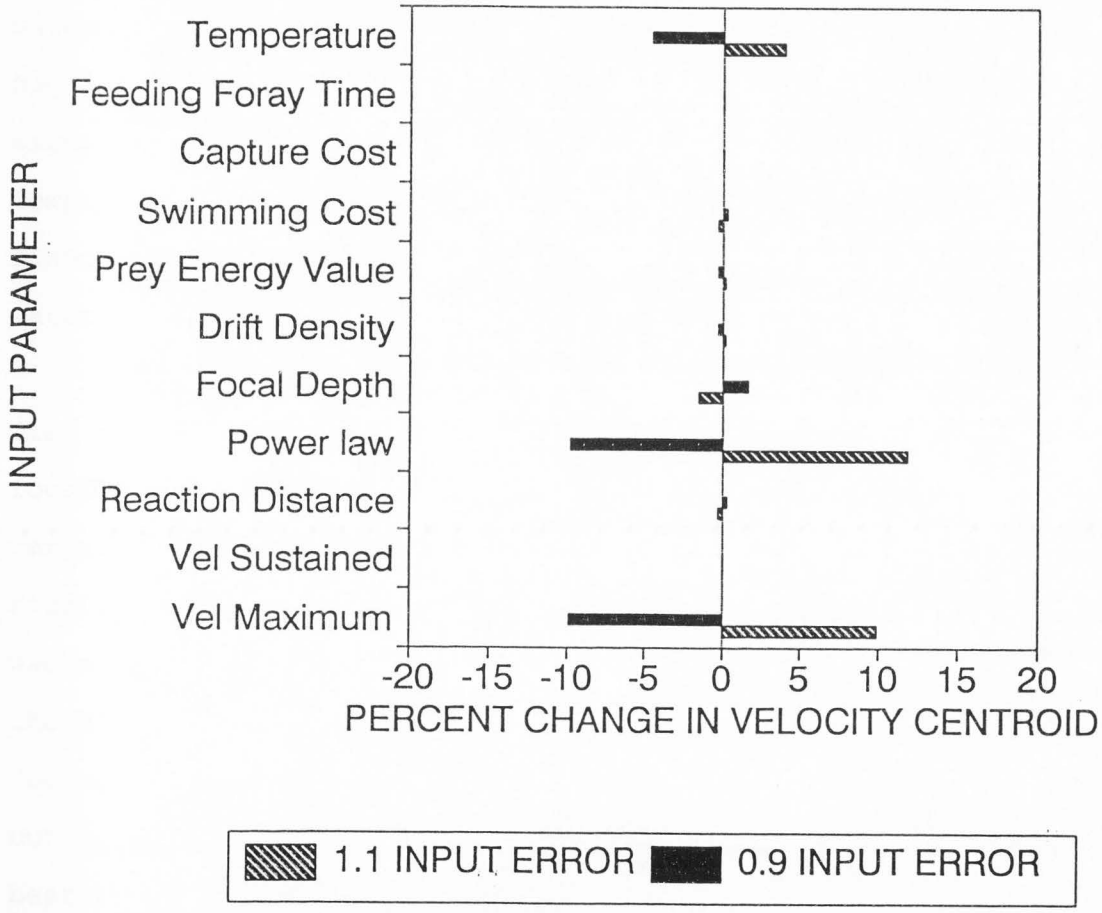

Figure 36. Percent change (sensitivity) of the velocity centroid for the volume under the NEI surface to 10% changes (1.1 X or 0.9 X nominal value) of each parameter used to model the NEI surface.

Temperature. Changing temperature changes the maximum velocity and the swimming cost of fish. In this instance a 10% increase in temperature caused a 4.2% increase in maximum velocity and approximately a 6% increase in swimming cost. The combined effects on the location of the NEI surface were primarily to shift the surface to higher velocities and increase the volume under the surface. The opposite effect occurred for a decrease in temperature. In each case, the change in the maximum velocity of the fish is the main driving force in shifting the NEI surface because the surface is relatively insensitive to swimming cost (see discussion below). Because temperature is a highly accurate (usually measured) input to the model, the main significance of these results is that changes in water temperature increase or decrease the maximum swimming velocity of fish and consequently increase or decrease the velocities of water at which fish can obtain positive NEI.

Feeding foray time. Although the amount of time it takes a fish to make a complete feeding foray (capture prey and return to focal position) is not accurately known and probably highly variable, it does not have much effect on the model. The only significant response to increasing or decreasing the foray time was a 2% decrease or increase, respectively, in the volume under the NEI surface. In essence, increasing the foray time slightly decreases the NEI available at a given depth/velocity combination but does not alter which depth/velocity combinations have the best NEI.

Capture cost. The cost of swimming (accelerating) to capture prey is probably the greatest unknown of the model input

parameters. Nevertheless, the NEI surface was insensitive to capture cost and it appears to be relatively unimportant in determining which depth and velocity combinations have the highest NEI. The cost of capturing prey, however, directly reduces the NEI gained from capturing prey and is a measure of the effort required to capture prey. As a result, it probably should not be discounted as being unimportant in terms of foraging behavior. For example, the cost of capture or the effort expended in capturing a prey item may affect a fish's decision about which prey items to pursue (e.g., small versus large prey and/or near versus distant prey).

Swimming cost. Like capture cost, the NEI surface is very insensitive to swimming cost. As a result, it appears swimming cost generally has little affect on NEI. This may not be true, however, when gross energy intake is very low, such as during resting periods, periods of very low drift densities, and cold temperature periods when maximum consumption is very low. These situations are addressed in a following section.

Prey energy value. The prey energy value, or the net amount of calories a fish is able to obtain from a prey item, had little effect on the depth or velocity centroid. Increasing the prey energy value did shift the NEI surface upward considerably with a 11% increase in the volume and a 10.5% increase in the NEI centroid. Decreasing prey energy value produced a similar magnitude of response but in the opposite direction.

Drift density. Changing drift density had nearly the exact same effect as did changing the prey energy value. Little shift in the depth or velocity centroid occurred but there was an 8 to

9% shift in the volume under the NEI surface and the NEI centroid. Altering drift density and prey energy value in the model alters the magnitude of NEI at a given depth/velocity combination but does not significantly change which depth/velocity combinations have the highest NEI in a relative sense.

Focal depth. Changing the focal depth of the fish produced relatively little response in the NEI surface. Increasing the focal depth increases the water velocity at the focal location. As a result, swimming cost is higher and the fish has to capture prey horizontally and upwards in higher velocity water. This causes the depth centroid to increase slightly (0.3%) and the velocity centroid to decrease slightly (1.5%). Decreasing the focal depth causes the opposite response.

Power law. The NEI surface was more sensitive to changing the coefficients of the power law than any other parameter. In part, this resulted from an anomaly in the way the analysis of the power law was handled. Changing the multiplicative constant of the power law by 10% actually results in a 30% change in the power constant when the power law is constrained as in equation 30. As a result, the 10% change in the power law most likely encompasses a majority of the range of input coefficients observed in the field for the power law. Therefore, the results definitely overestimate the sensitivity of the NEI surface to the power law compared to the other input parameters.

Increasing the power law coefficient (multiplicative constant) by 10% caused a 11.8% increase in the velocity centroid, a 10.4% increase in the volume centroid, a 3.4%

decrease in the NEI centroid, and a 1.5% increase in the depth centroid. Similar magnitude, but opposite direction changes resulted from a 10% decrease in the power law multiplicative constant. The velocity and depth centroid changes were the largest observed in the sensitivity analysis. Increasing the power law constants made faster and deeper water more energetically beneficial (see Figure A15-16 in the Appendix).

Changing the power law coefficients changes the shape of the velocity profile. Increasing the coefficients causes the velocity profile to have a greater difference between surface and bottom velocities. That is, the surface has much higher velocity than is found near the bottom. As a result, the foraging model allows fish to utilize faster mean velocities because the near bottom focal velocities are lower. Decreasing the coefficients causes the velocity profile to be more uniform (similar velocities surface and bottom) and makes high mean velocities less usable because the near bottom velocities are higher.

Reaction distance. Changing the reaction distance had a large impact on the volume under the surface and had the second largest change in the depth centroid. A 10% increase or decrease in reaction distance resulted in a 15.8% increase or decrease, respectively, in the volume under the surface. There was also a corresponding 0.5 - 0.6% increase and decrease, respectively, in the depth centroid. The velocity centroid was not sensitive to reaction distance.

Increasing the reaction distance allowed the capture of more prey in the model and made deeper water more advantageous. The converse occurred when the reaction distance was decreased.

Sustainable velocity. NEI was very insensitive to sustainable velocity. Practically no change in the NEI parameters was observed with a ±10% change in sustainable velocity. In the NEI model sustainable velocity is used to determine whether a focal position can be occupied by a fish or not. If the focal velocity is greater than the sustainable velocity of the fish, then the model assumes the fish will not occupy the focal position as a feeding site and the GEI is set to zero. The reason the NEI surface is insensitive to changes in the sustainable velocity is because changing the sustainable velocity changes the margins of the NEI surface where NEI is very low. As a result, the change is not significant as measured by the quantitative parameters of the NEI surface.

It must be understood, however, that the sustainable velocity defines the maximum water velocity at which a fish will maintain a focal site and as a result has an important impact on the shape of the NEI surface. To visualize this, Figures 20-23 show the NEI surfaces for different sized fish that have significantly different sustainable velocities.

Maximum capture velocity. Changing the maximum capture velocity caused the largest changes in the volume of the NEI surface. Increasing the maximum capture velocity caused a 19.5% increase in the volume under the NEI surface and decreasing the maximum capture velocity caused a 18% decrease in the volume under the NEI surface. Increasing the maximum capture velocity by 10% also caused a 9.9% increase in the velocity centroid and a 8.2% increase in the NEI centroid. The depth centroid decreased slightly, -0.05%, as the maximum capture velocity was increased.

Similar but opposite changes in the velocity, NEI, and depth centroids occurred with a 10% decrease in maximum capture velocity. Increasing the maximum capture velocity allows the fish to capture more prey at a given depth/velocity combination and allows the fish to take advantage of faster water.

SUPPLEMENTARY SENSITIVITY/SIMULATION ANALYSIS

Methods and assumptions

Supplementary NEI model simulations of various assumptions and ranges of input parameters in addition to the previous perturbation sensitivity analysis were used to provide in-depth insight into how the parameters affect profitable habitat location and how the NEI model compares with the observed habitat utilization of drift-feeding fish in the literature. All NEI model input parameters used in the simulation were identical to those used in the sensitivity analysis unless otherwise specified. The issues addressed in the simulation analysis were these: (1) the consequences of calculating NEI versus GEI, (2) the effect of different levels of drift density, (3) the effect of changing water temperature, (4) the effect of changing maximum capture velocity, (5) the effect of changing reaction distance, and (6) the amount of time required to reach maximum daily consumption.

Results and discussion

The consequences of calculating NEI versus GEI. The drift-feeding model incorporates basal and active metabolism, digestion costs, egestion, and excretion to provide a realistic measure of NEI instead of simply modeling GEI. To document the effect of modeling NEI versus GEI, both NEI and GEI were modeled for fish 25, 50, 100, 150, and 200 mm in length at high drift densities of 400 prey/100 m^3 and at low drift densities of 50 prey/100 m^3. Plots of NEI, GEI, and swimming cost where constructed over a

range of depths and velocities, and the optimum depth/velocity combinations according to GEI and NEI were compared.

Except in cases of very low energy intake, there is little difference in the optimum velocities predicted by NEI and GEI. Figures 37-40 show GEI, NEI, and swimming cost (includes basal metabolism) over a range of velocities from 0 - 140 cm/s for 25, 50, 100, and 200 mm fish, respectively. These values were calculated at stream depths of 45, 45, 50, and 65 cm, respectively. The difference between NEI and GEI in these figures is the result of swimming and capture costs, basal metabolism, digestion costs, egestion, and excretion being subtracted from the GEI. Swimming cost is plotted separately to give an idea of how relatively insignificant of a cost it is in most instances.

While there is considerable difference in the magnitudes of the GEI and NEI curves, the relative location of the peak of each curve is nearly identical. As a result it appears that the optimum velocity is the same whether GEI or NEI is calculated. The only significant difference occurs on the high velocity side of the NEI and GEI curves where the NEI curve predicts that higher velocities are less beneficial than the GEI curve predicts. This effect is more pronounced when low drift rates are encountered. Figure 41 shows a 150 mm fish modeled at a low drift rate of 50 prey/100 m^3. It is clear from the figure that high velocities (70^+ cm/s) are less beneficial in terms of NEI than GEI. This effect occurs because energy intake is relatively small at low drift rates and the swimming cost becomes significant.

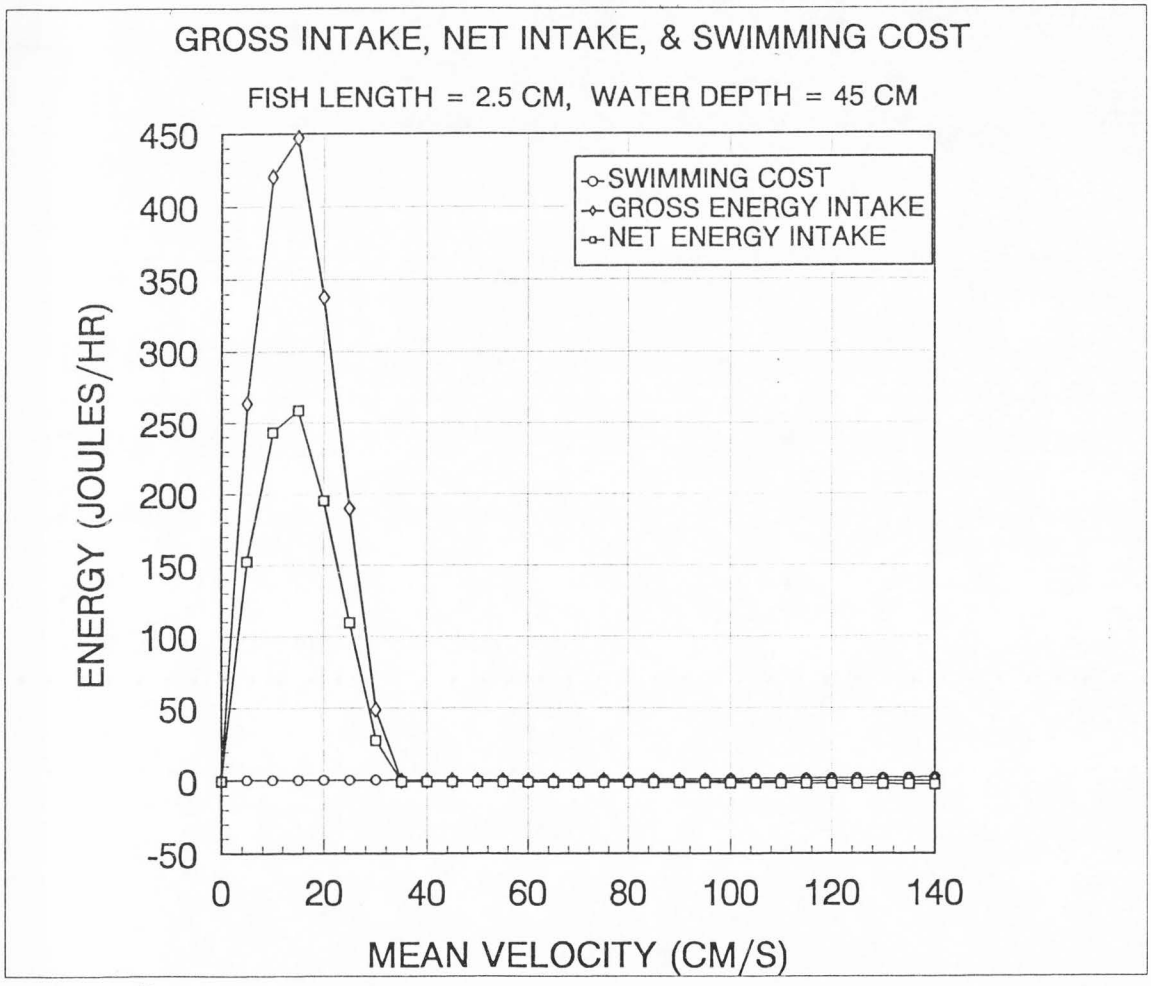

Figure 37. Plot of gross energy intake (GEI), NEI, and swimming cost (includes basal metabolism) for a 25 mm fish over a range of mean velocities at a total depth of 45 cm. The data are modeled at a temperature of 12°C and a drift rate of 400 prey/ 100 m^3.

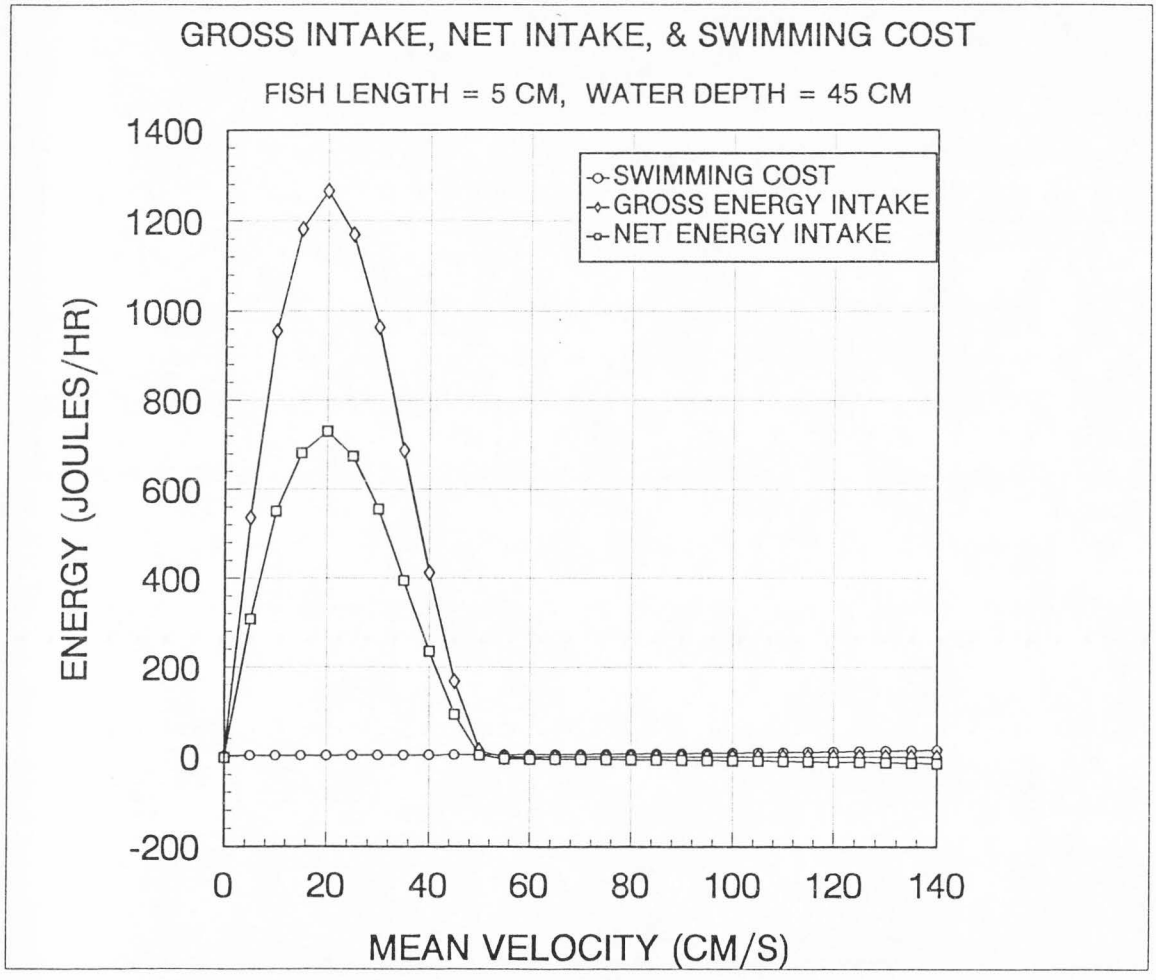

Figure 38. Plot of gross energy intake (GEI), NEI, and swimming cost (includes basal metabolism) for a 50 mm fish over a range of mean velocities at a total depth of 45 cm. The data are modeled at a temperature of 12°C and a drift rate of 400 prey/ 100 m^3.

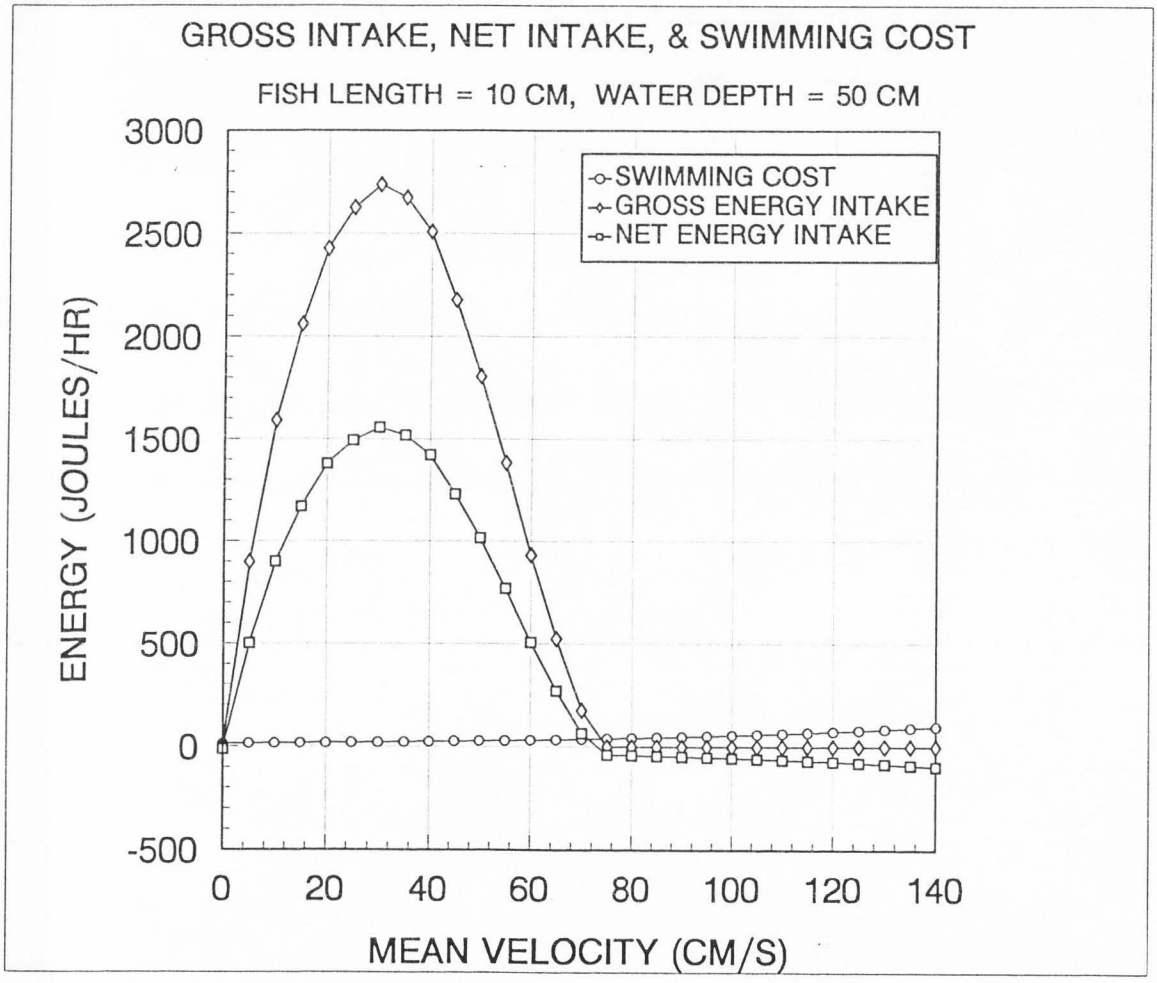

Figure 39. Plot of gross energy intake (GEI), NEI, and swimming cost (includes basal metabolism) for a 100 mm fish over a range of mean velocities at a total depth of 50 cm. The data are modeled at a temperature of 12°C and a drift rate of 400 prey/ 100 m^3.

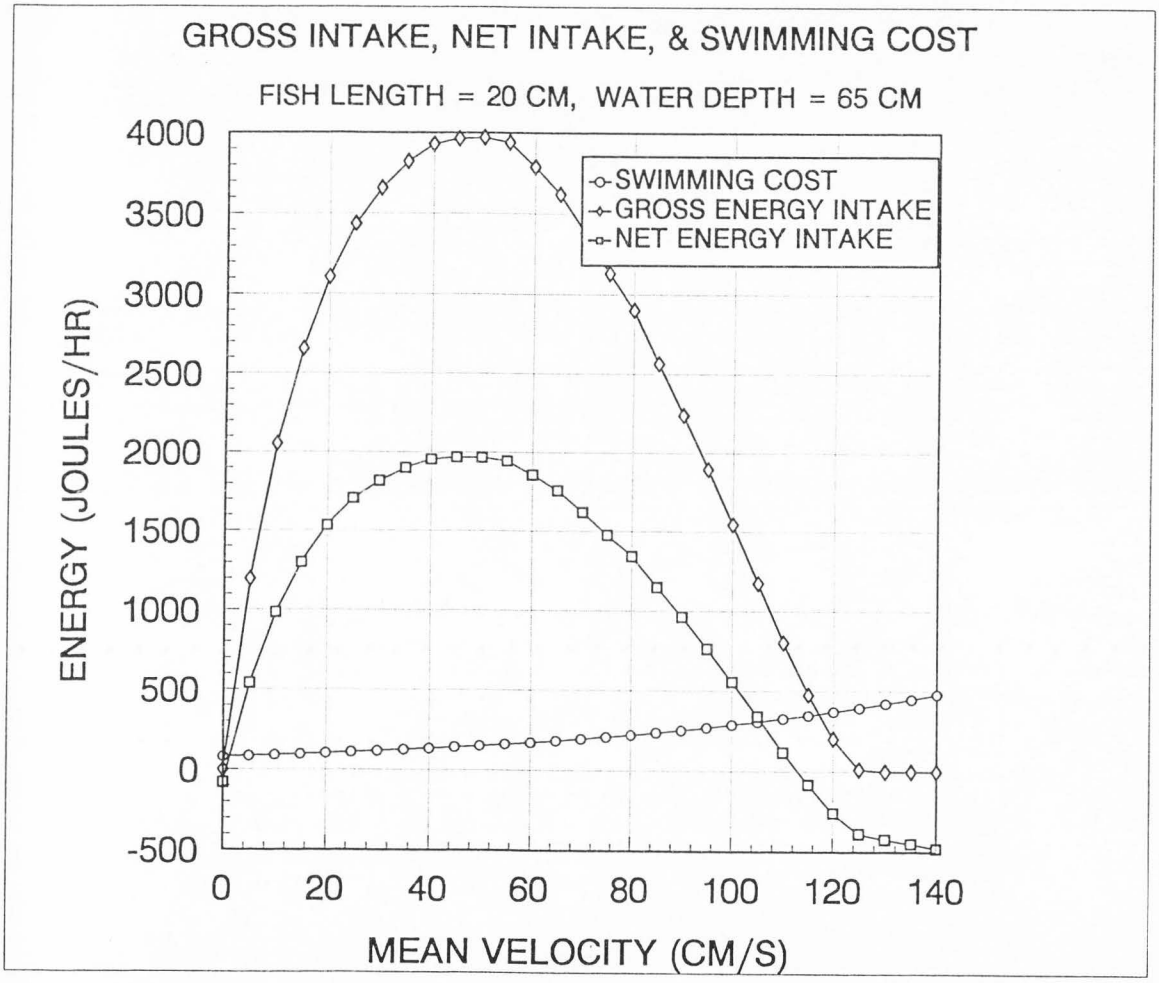

Figure 40. Plot of gross energy intake (GEI), NEI, and swimming cost (includes basal metabolism) for a 200 mm fish over a range of mean velocities at a total depth of 65 cm. The data are modeled at a temperature of 12°C and a drift rate of 400 prey/ 100 m^3.

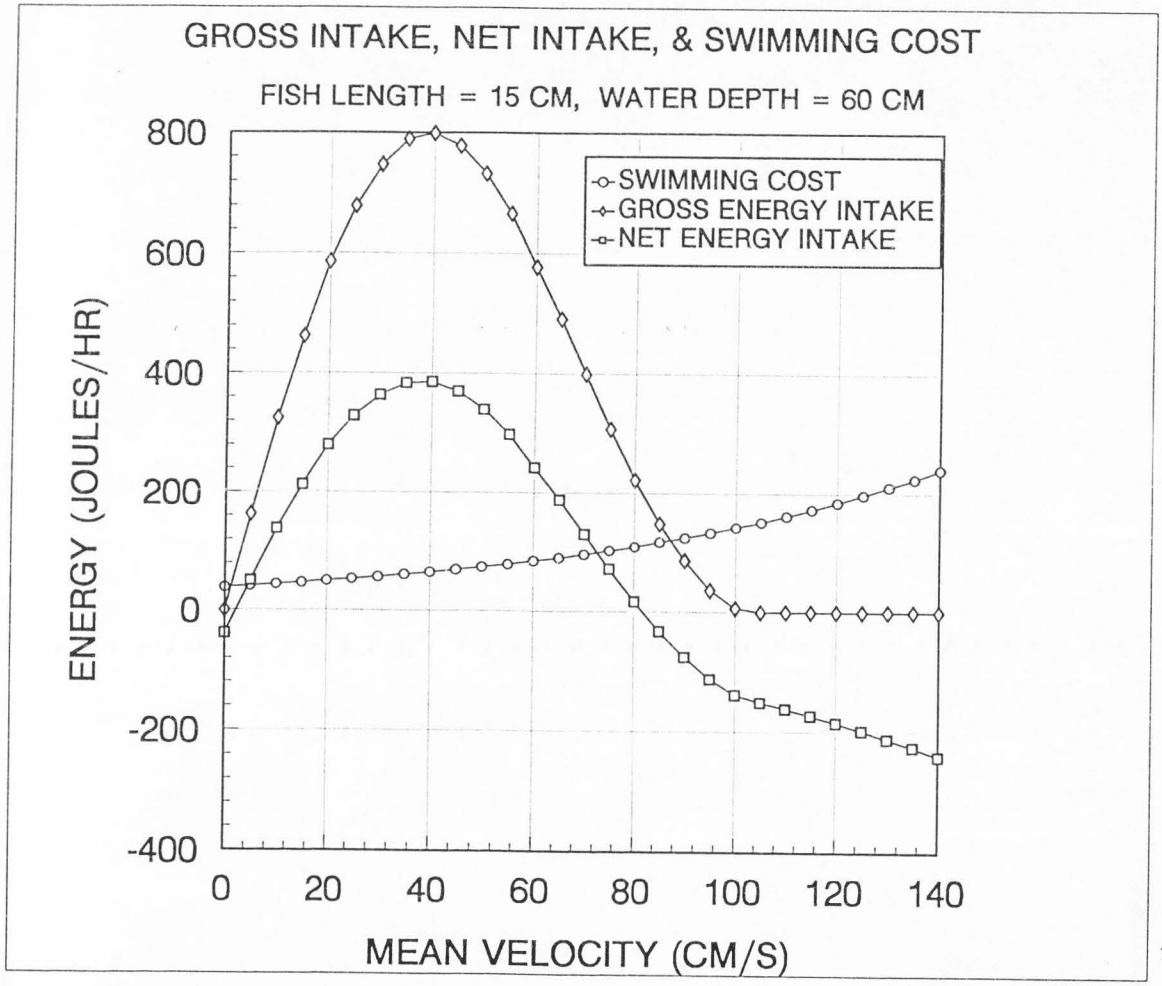

Figure 41. Plot of gross energy intake (GEI), NEI, and swimming cost (includes basal metabolism) for a 150 mm fish over a range of mean velocities at a total depth of 60 cm. The data are modeled at a temperature of 12°C and a drift rate of 50 prey/ 100 m^3.

Figure 42 shows NEI, GEI, and swimming cost for a 200 mm fish (same data modeled as that in Figure 40) over a range of *depths* from 0 to 140 cm. In a similar manner as occurred with respect to velocities, the NEI and GEI curves predict similar optimal depths. Only where energy intake is very small, at the shallow depths, is there any deviation between NEI and GEI.

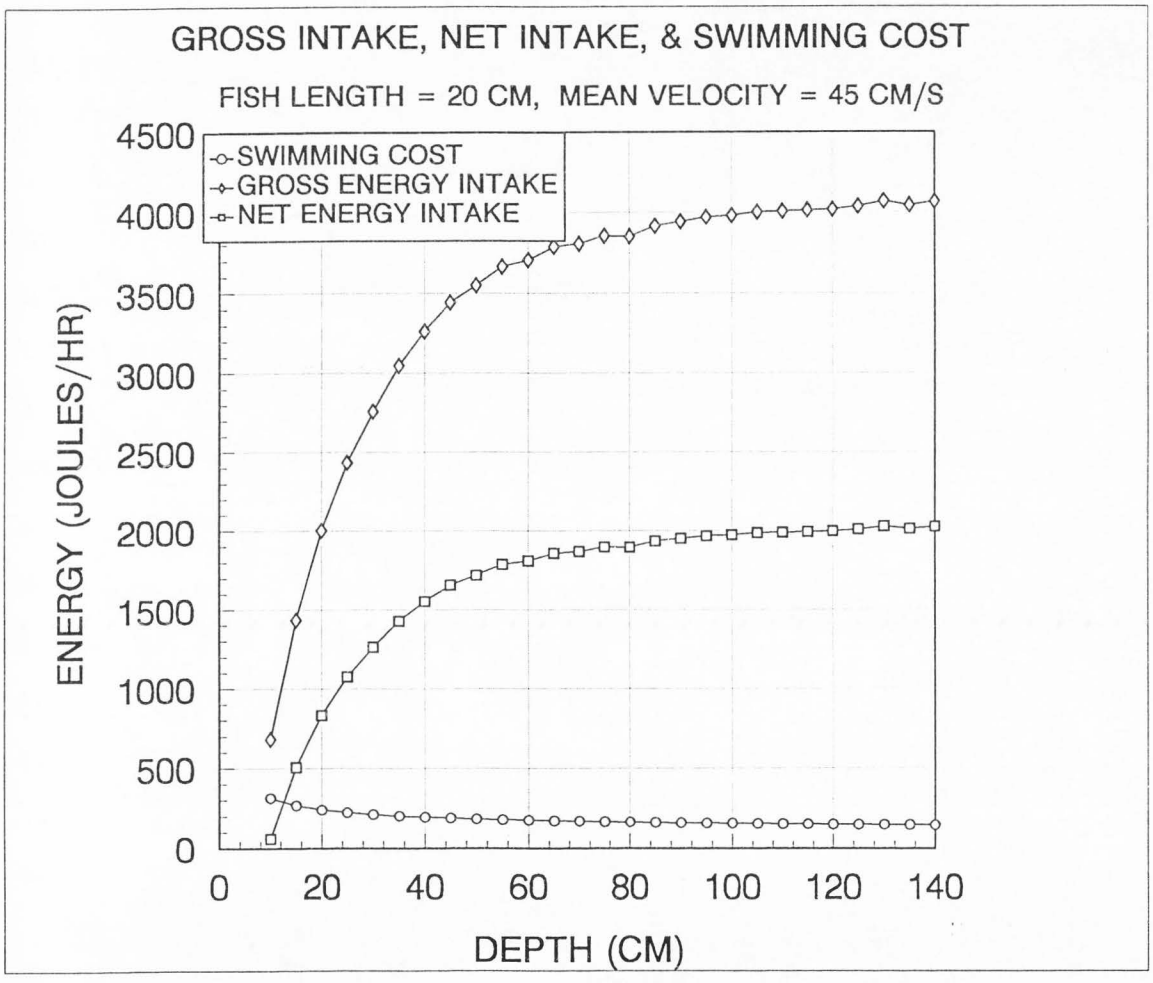

Figure 42. Plot of gross energy intake (GEI), NEI, and swimming cost (includes basal metabolism) for a 200 mm fish over a range of total depths at a mean velocity of 45 cm/s. The data are modeled at a temperature of 12°C and a drift rate of 400 prey/ 100 m^3.

The effect of different levels of drift density. The effect of different levels of drift density was addressed by modeling NEI over a range of drift densities from 0 to 1000 prey/100 m^3. NEI was modeled for 150 mm fish at 12°C and plotted on a grid of water depths and mean velocities.

Changing drift density had very little effect on the orientation of the NEI surface on the depth and velocity axes; however, increasing or decreasing the drift density does increase or decrease the magnitude of the NEI surface as shown in Figures 43-47. As a result the optimum depth and velocity combinations do not change with changes in drift density (except when no drift is available, see below). What does change, however, is the quantity of depth and velocity combinations that provide sufficient NEI to sustain fish. A 150 mm (22.3 grams) fish can consume approximately 5000 J of energy at 12°C (equation 22). As a result it would take a fish over 5 hours of feeding to satiate at a GEI of 1000 J/hr (approximately 500 J/hr NEI). As can be seen in Figure 44, at a drift rate of 50 prey/100 M^3, very few depth and velocity combinations approach a NEI of 500 J/hr; however, with a drift rate of 400 prey/100 M^3, a vast majority of the depth and velocity combinations have an NEI of 500 J/hr or more (Figure 46). As a result it appears that more stream habitat can sustain fish when drift rates are high than when drift rates are lower.

The only time the model predicts that the optimum depth/velocity combinations change with changes in drift density is when drift is approximately zero. When energy intake is zero, it is obviously most advantageous, as can be seen from Figure 43,

for fish to utilize velocities that minimize swimming costs. Fish should also minimize swimming costs when poor visibility (caused by darkness or turbidity) precludes fish from being able to capture prey or when fish are resting and not actively capturing prey.

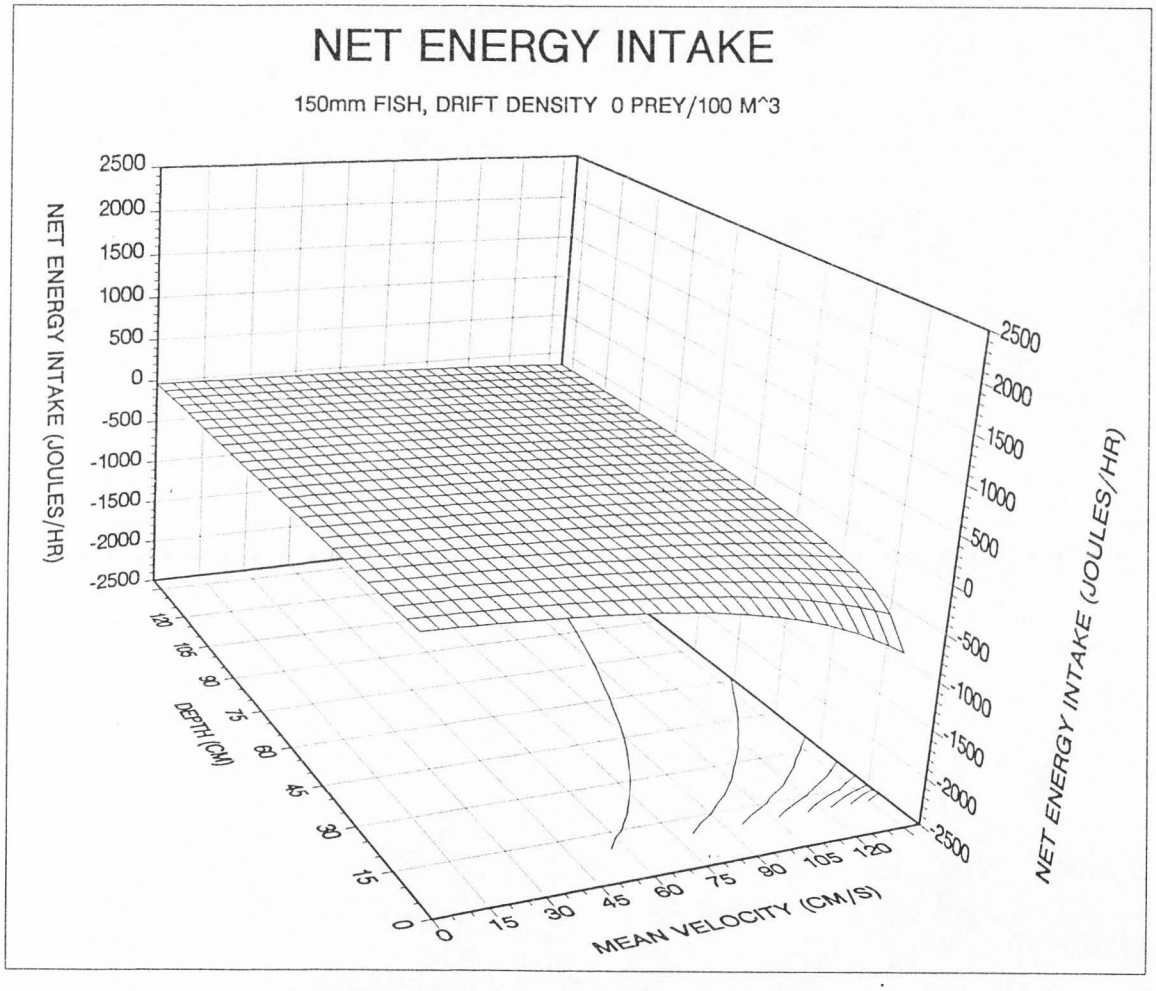

Figure 43. Modeled NEI for a 150 mm fish at a drift density of 0 prey/ 100 m^3 and a temperature of 12°C.

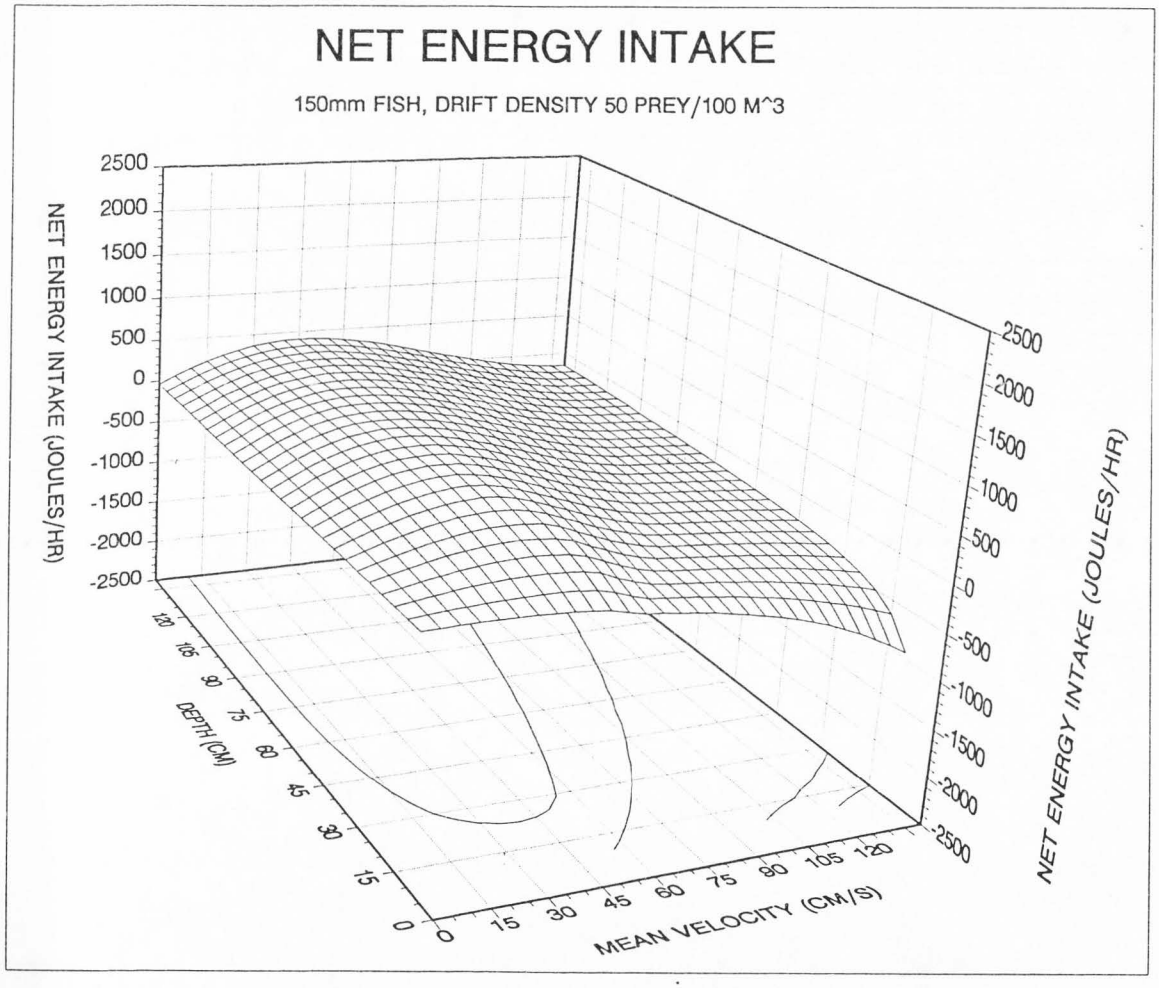

Figure 44. Modeled NEI for a 150 mm fish at a drift density of 50 prey/ 100 m^3 and a temperature of 12°C.

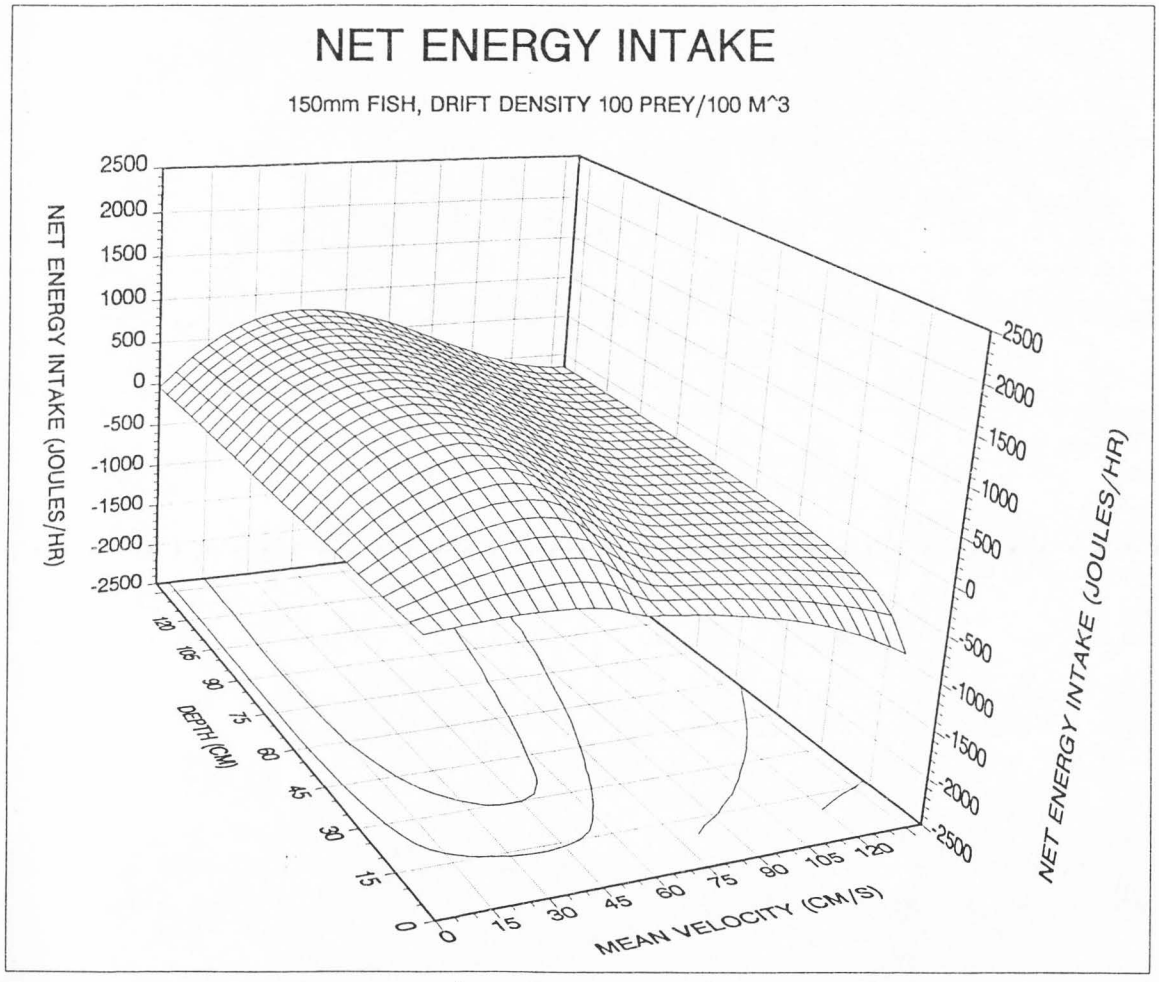

Figure 45. Modeled NEI for a 150 mm fish at a drift density of 100 prey/ 100 m^3 and a temperature of 12°C.

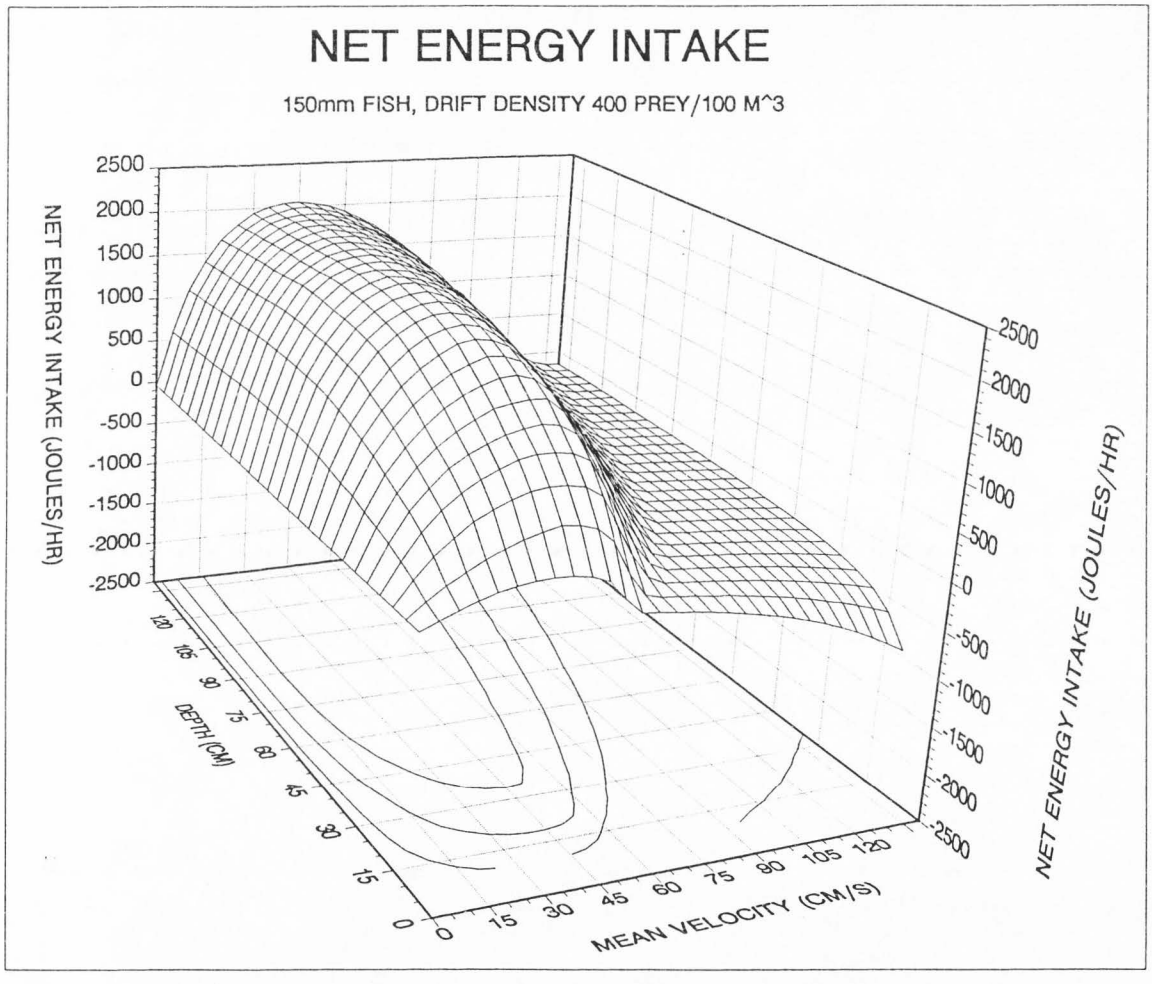

Figure 46. Modeled NEI for a 150 mm fish at a drift density of 400 prey/ 100 m^3 and a temperature of 12°C.

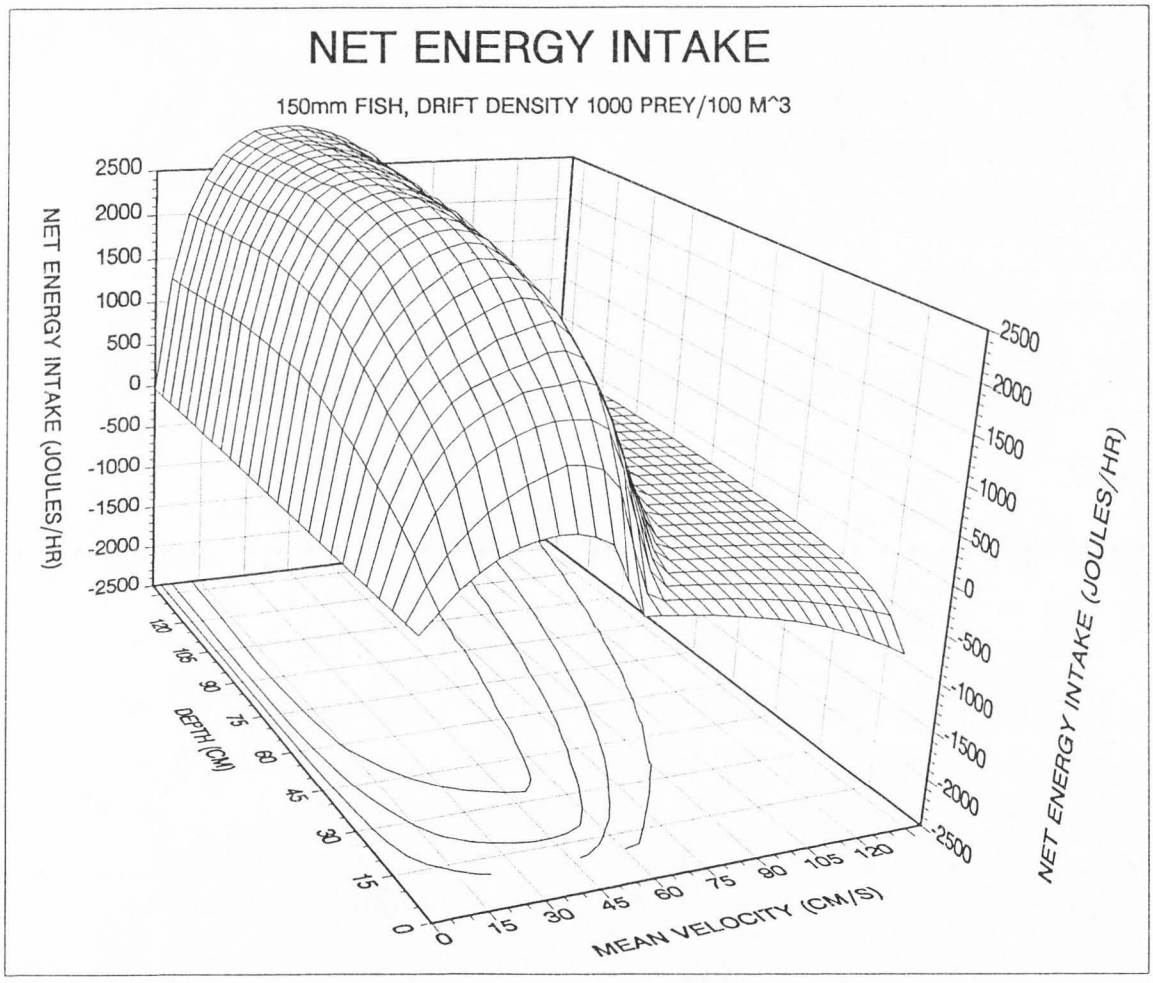

Figure 47. Modeled NEI for a 150 mm fish at a drift density of 1000 prey/ 100 m^3 and a temperature of 12°C.

The effect of changing temperature. Changing temperature changes the maximum velocity and the swimming cost of fish. To address the effect of changing temperatures on NEI, the results of model runs for a 200 mm fish were plotted for four different temperatures (3, 9, 12, and 17°C).

Because swimming velocity increases when temperature increases, the model predicts that as temperatures rise from 3 to 17°C that the optimum mean water velocity increases and the quantity of depth/velocity combinations suitable for fish increases. Figures 48-50 in conjunction with Figure 23 show the NEI surface for a 200 mm fish at 3, 9, 12, and 17°C. The optimum velocity increases from approximately 35 cm/s at 3°C to 55 cm/s at 17°C. In addition, the range of velocities with high NEI is considerably broader at the higher temperatures.

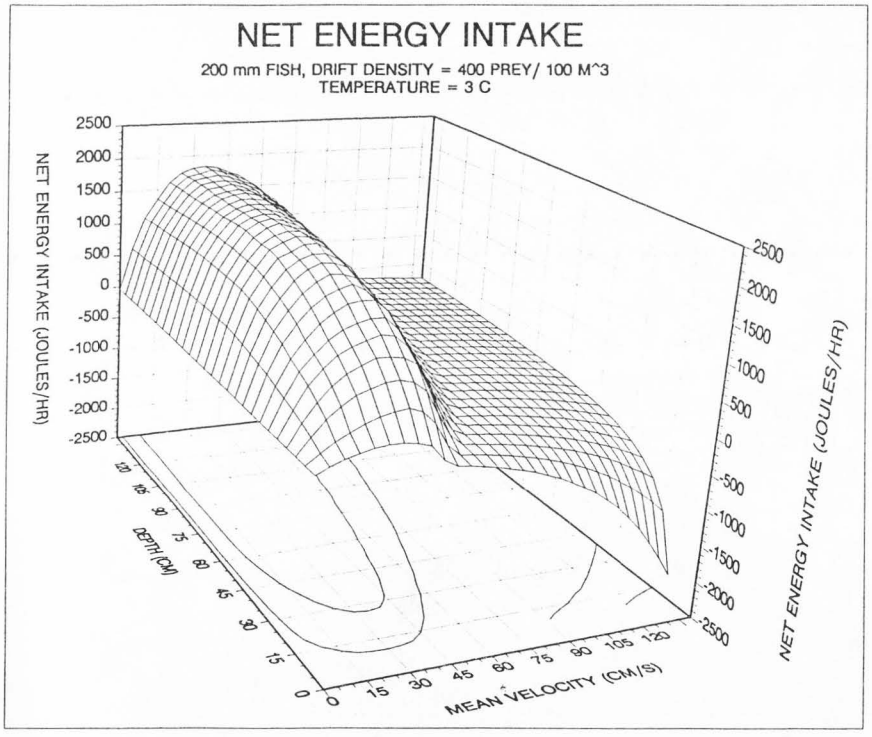

Figure 48. Modeled NEI for a 200 mm fish at a temperature of 3°C and a drift density of 400 prey/ 100 m^3.

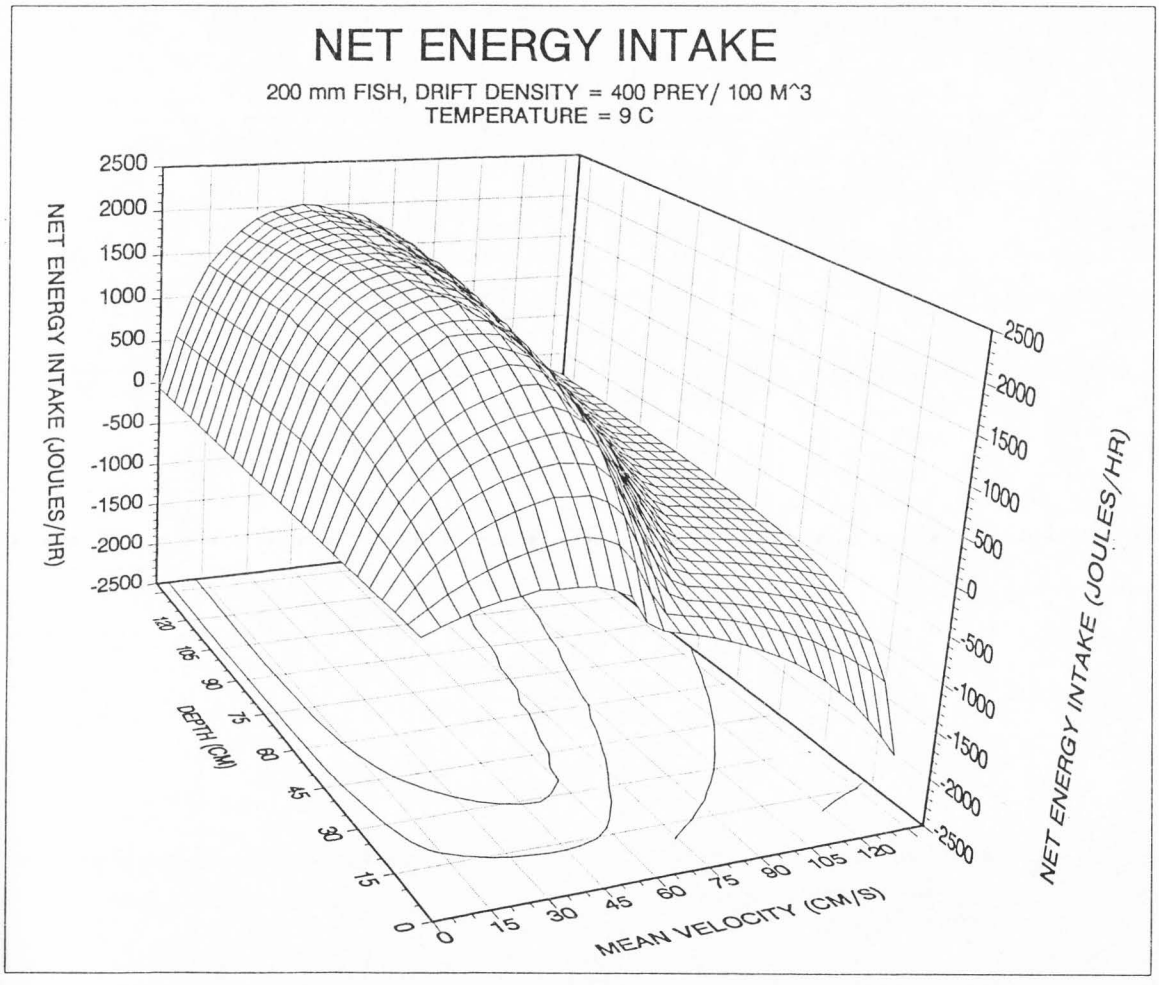

Figure 49. Modeled NEI for a 200 mm fish at a temperature of 9°C and a drift density of 400 prey/ 100 m^3.

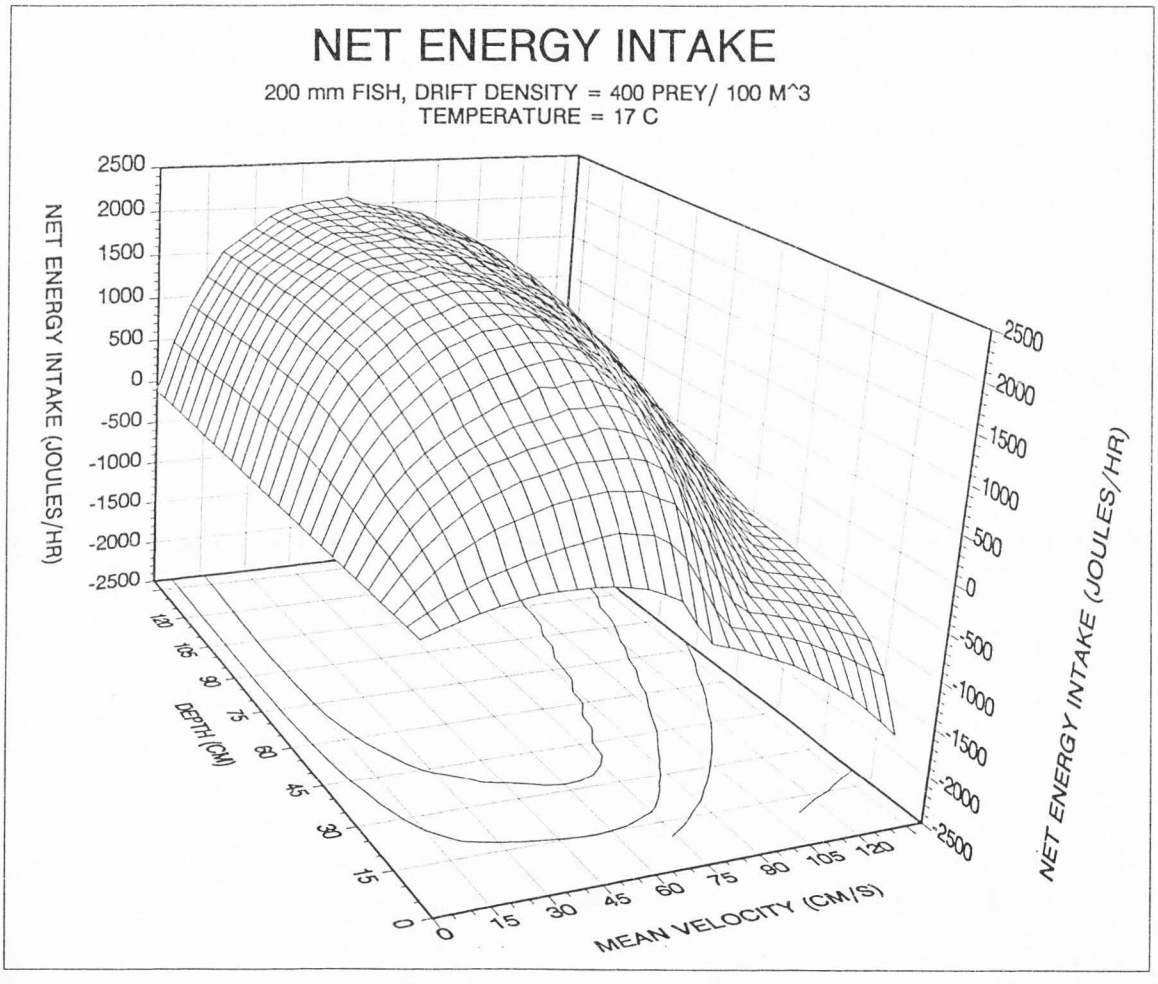

Figure 50. Modeled NEI for a 200 mm fish at a temperature of 17°C and a drift density of 400 prey/ 100 m^3.

The effect of changing maximum capture velocity. Swimming velocity increases as fish get larger and generally increases as temperature increases (see Figure 5). The effect of maximum capture velocity on NEI was addressed by using data already modeled for fish ranging in size from 25 to 200 mm (i.e., different maximum capture velocities) and for fish 200 mm at temperatures from 3 to 17°C (i.e., different maximum capture velocities).

With an increase in swimming velocity, the model predicts that fish are able to increase NEI at each habitable depth/velocity combination and they are able to utilize faster and deeper water more efficiently (note: deeper water only if the reaction distance is large enough; see reaction distance section below). This effect can be seen in model results already shown. Figures 20-23 show NEI for fish at 25, 50, 100, and 200 mm and Figures 48-50 and Figure 23 show 200 mm fish at 3, 9, 12, and 17°.

The effect of changing the reaction distance. Reaction distance increases as fish get larger and as prey size increases (Figure 3). The effect of changing reaction distances was addressed by modeling NEI for a 150 mm fish with three different reaction distances to a mean prey size of 3.5 mm. In addition, data already modeled for fish ranging from 25 to 200 mm (i.e., different reaction distances) were used to look at the effect of reaction distance.

The results of increasing reaction distance are that fish are able to capture larger prey farther away and that fish with larger reaction distances (larger fish) are able to capture more prey and take greater advantage of deeper water. For example,

small 25 mm fish have a reaction distance of 35 cm to large prey (6 mm long) and they obtain maximum NEI in water about 40 cm deep (Figure 20). Because the fish cannot see most prey at longer distances, deeper water does not provide additional foraging area. Larger fish have larger reaction distances and can take advantage of deeper water. A 200 mm fish has a reaction distance of 79 cm to 6 mm prey and obtains maximum NEI at a depth of approximately 75 cm (see Figure 23).

To clearly show the effect of reaction distance on NEI without the complicating factors of swimming speed and cost, a 150 mm fish was modeled with three different reaction distances. Figures 51-53 show clearly that increasing reaction distance increases NEI and increases the optimum depth.

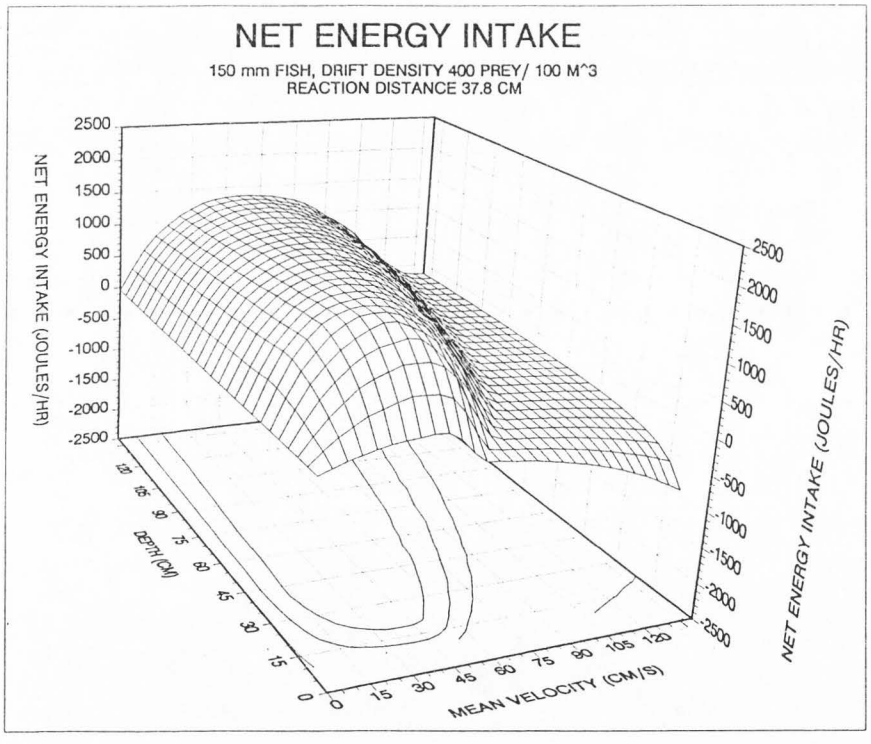

Figure 51. Modeled NEI for a 150 mm fish at a reaction distance of 37.8 cm, a temperature of 12°C, and a drift density of 400 prey/ 100 m^3.

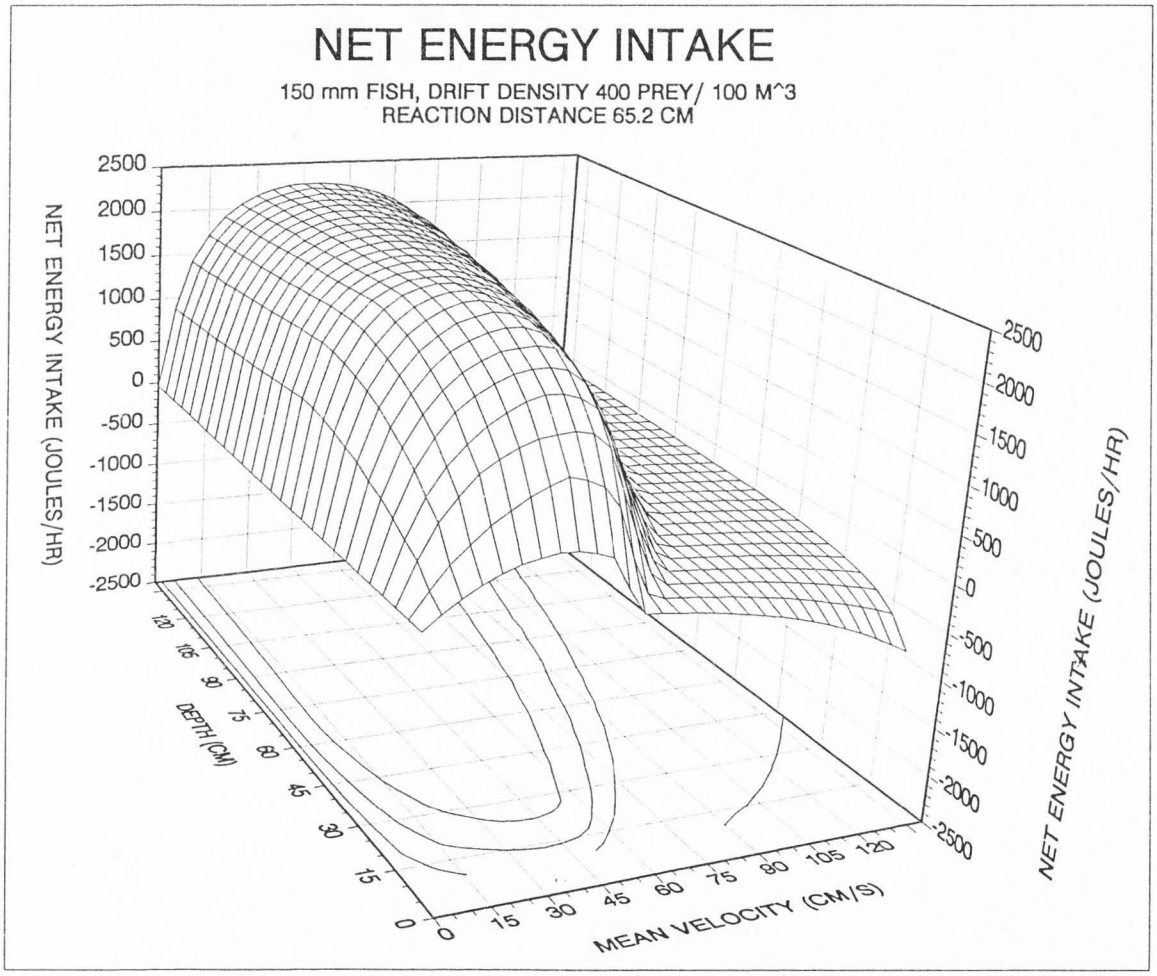

Figure 52. Modeled NEI for a 150 mm fish at a reaction distance of 65.2 cm, a temperature of 12°C, and a drift density of 400 prey/ 100 m^3.

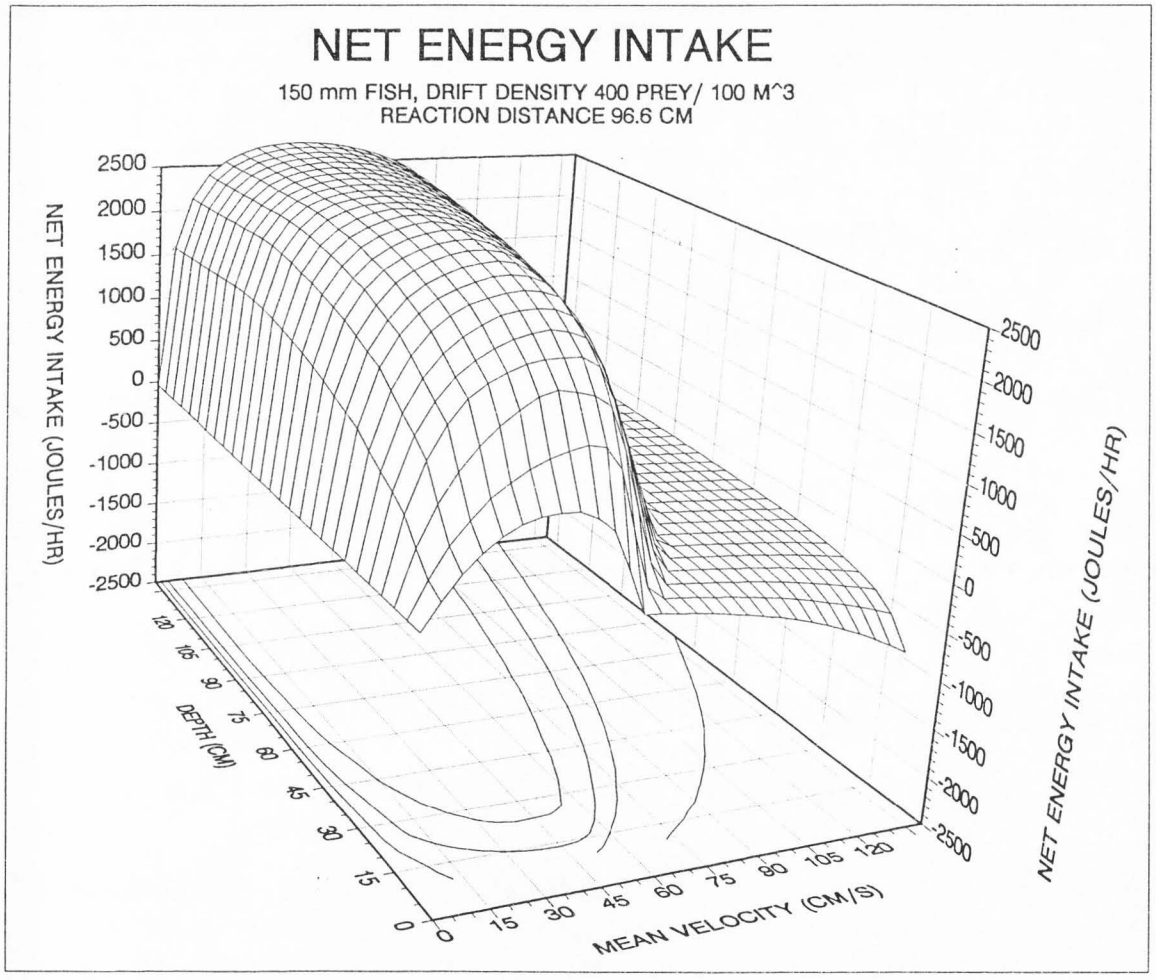

Figure 53. Modeled NEI for a 150 mm fish at a reaction distance of 96.6 cm, a temperature of 12°C, and a drift density of 400 prey/ 100 m^3.

Incorporation of the time required to reach maximum daily consumption. To address the effect that incorporation of the time required to reach maximum daily consumption (satiation) in the NEI model would have on the interpretation of habitat suitability, several plots of satiation time were derived for different fish sizes and different water temperatures.

A plot of satiation time versus consumption rate was derived for fish ranging from 25 to 200 mm at various temperatures using equation 22 (also see Figure 7). The results of these plots, Figures 54-57, show the amount of time it takes a drift-feeding fish to satiate given the hourly consumption rates (GEI) ranging from 0 to 4,000 joules/hr and temperatures ranging from 4 to 17.8°C. These figures can be used in conjunction with the hourly GEI rates calculated for St. Charles Creek to get an idea of how long it takes fish to satiate. NEI is roughly one half of GEI (see Figures 37-40) so any data presented thus far in NEI can be used with the time-to-satiation figures to obtain satiation time by doubling the NEI to get a consumption rate. For example, most of the maximum NEI in the field validation for the two pools and two runs in St. Charles Creek is less than 500 J/hr NEI or 1000 J/hr GEI (See Figures 26-30). Given a GEI of 1000 J/hr at 12°, it takes a 100 mm fish 2 hr to reach satiation and a 200 mm fish 10.5 hr. Note, however, that modeled GEI would be slightly higher for 200 mm fish due to their faster capture velocities and larger reaction distances.

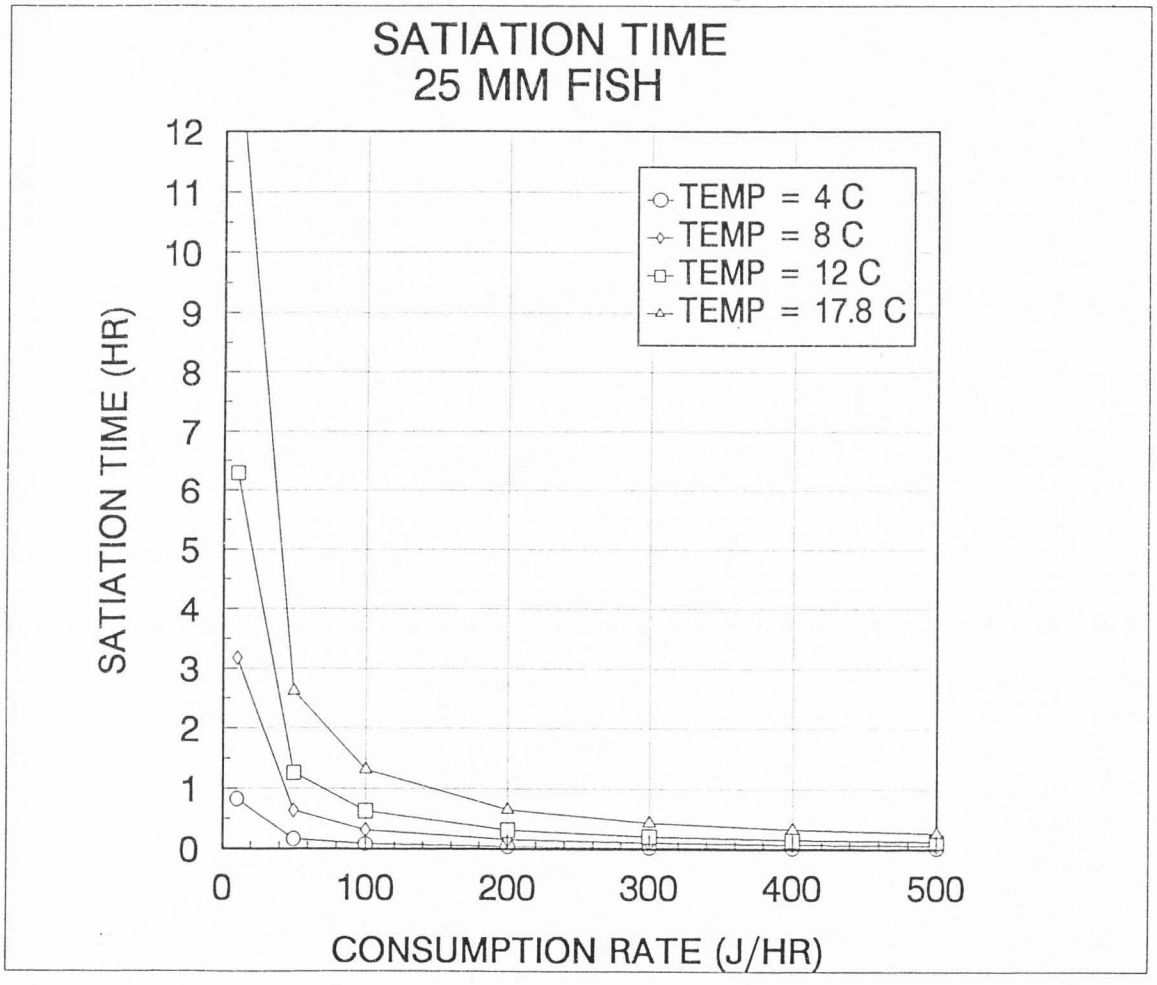

Figure 54. Satiation time versus hourly consumption rate (GEI) for 25 mm fish at temperatures of 4, 8, 12, and 17.8°C. Differences in satiation time result from the differences in maximum daily consumption of fish at different temperatures (equation 22).

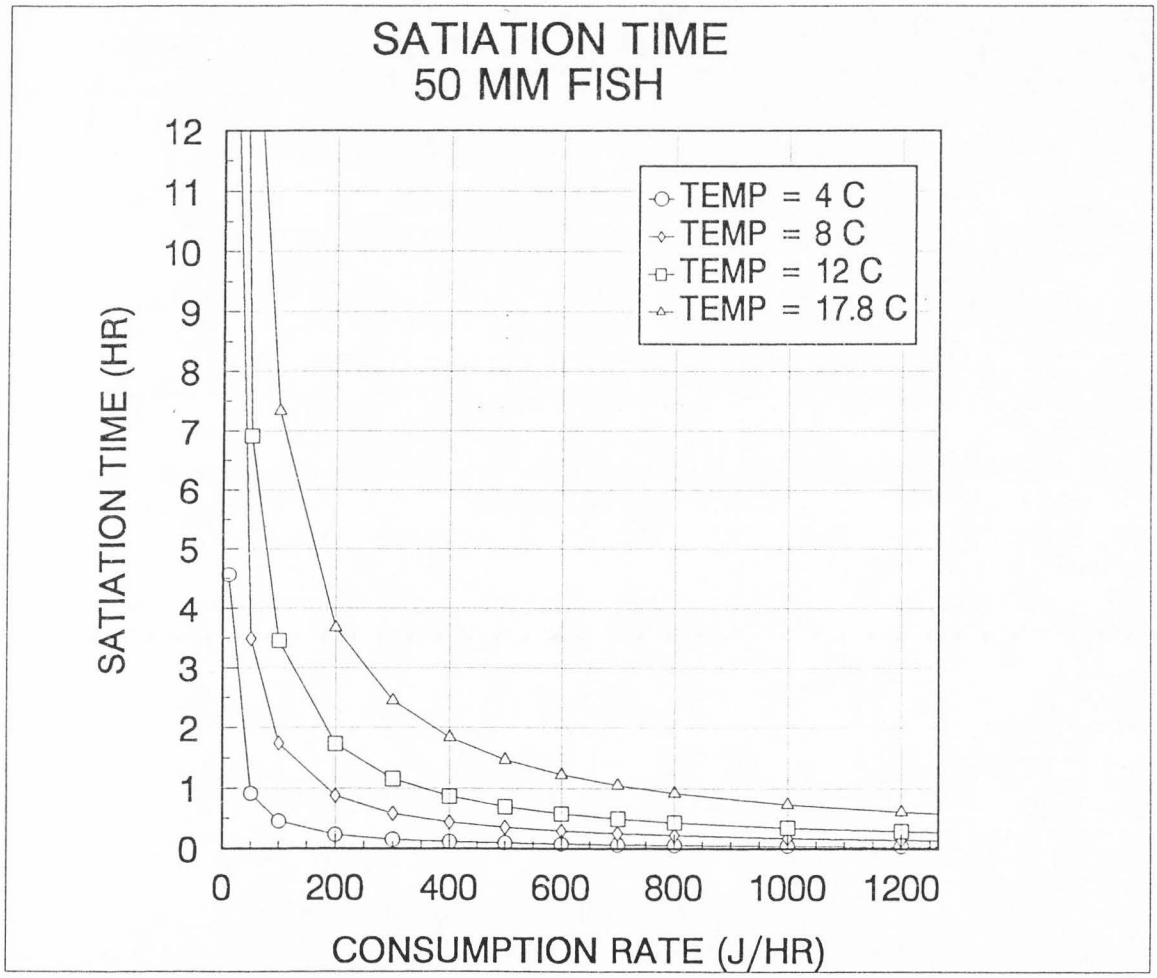

Figure 55. Satiation time versus hourly consumption rate (GEI) for 50 mm fish at temperatures of 4, 8, 12, and 17.8°C. Differences in satiation time result from the differences in maximum daily consumption of fish at different temperatures (equation 22).

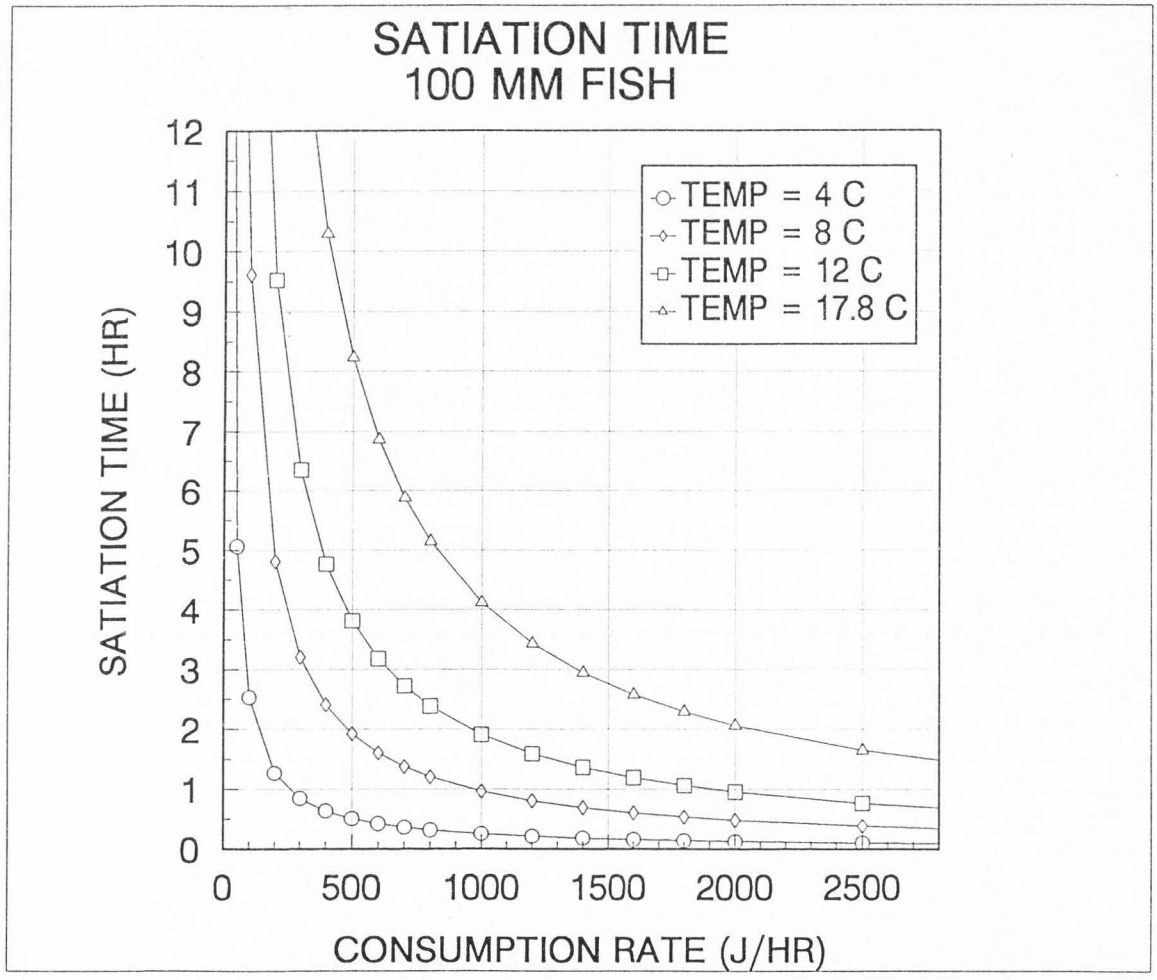

Figure 56. Satiation time versus hourly consumption rate (GEI) for 100 mm fish at temperatures of 4, 8, 12, and 17.8°C. Differences in satiation time result from the differences in maximum daily consumption of fish at different temperatures (equation 22).

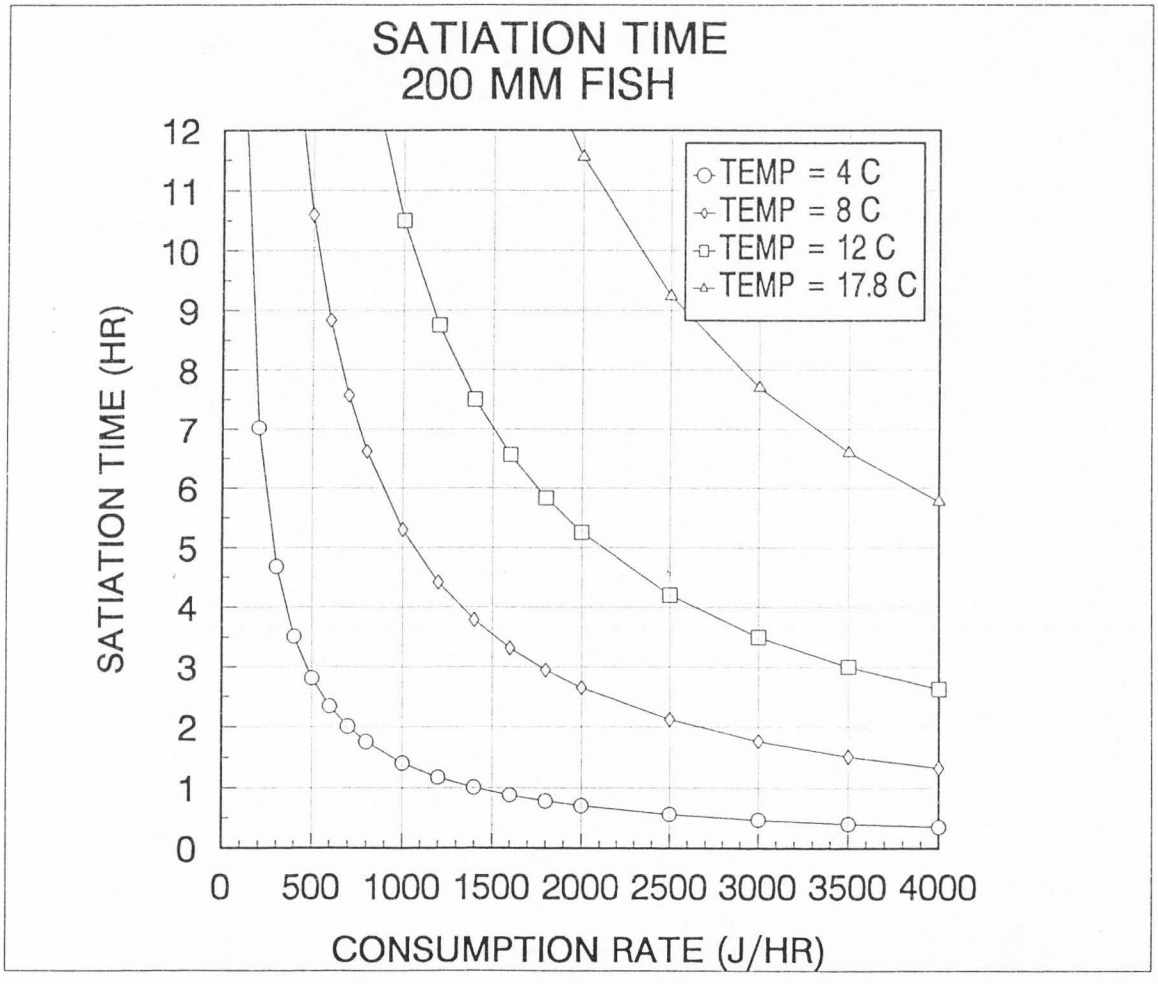

Figure 57. Satiation time versus hourly consumption rate (GEI) for 200 mm fish at temperatures of 4, 8, 12, and 17.8°C. Differences in satiation time result from the differences in maximum daily consumption of fish at different temperatures (equation 22).

To show clearly how fish size affects satiation time, a plot of satiation time versus fish length was developed at a temperature of 12°C using the maximum GEI calculated for each fish size at a drift density of 400 prey/100 m^3 (see Figures 37-40 or 20-23). The plot shown in Figure 58 illustrates that the model predicts small fish take considerably less time to satiate than large fish (0.14 versus 2.65 hr) and that the time increases exponentially as fish get larger.

To show the effect of temperature on satiation time, a plot of satiation time versus temperature for a 200 mm fish was developed using the maximum GEI rates modeled for a 200 mm fish at temperatures ranging from 3 to 17°C and a drift rate of 400 prey/100 m^3 (see Figures 23 and 48-50). The plot of satiation time versus temperature shows that as temperature increases, satiation time increases very rapidly (Figure 59). At low temperatures (3-6°C) only fractions of an hour are required for satiation while at 17°C nearly 5 hr are required for satiation.

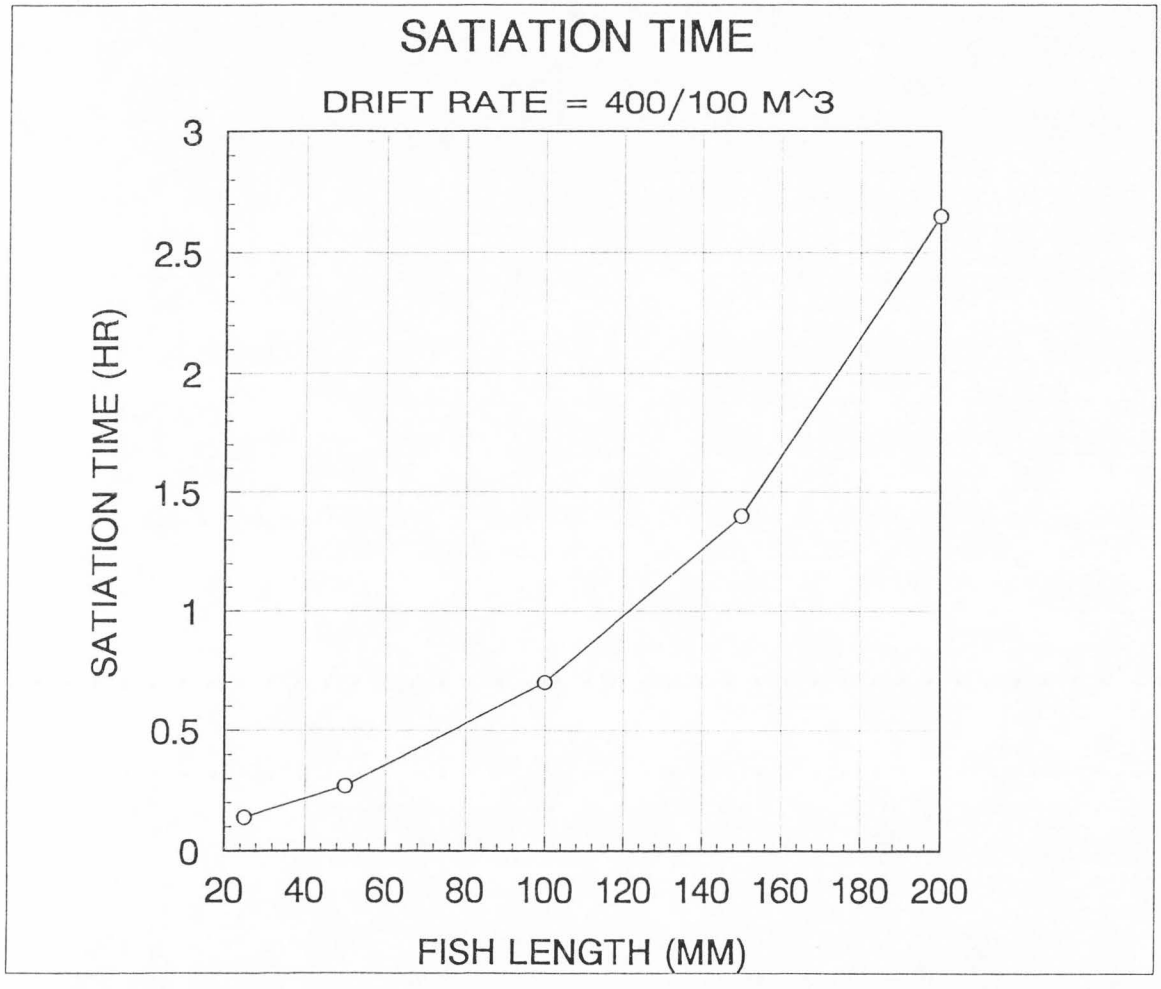

Figure 58. The effect of fish size on satiation time. Satiation time is calculated from maximum daily consumption (equation 22) and the maximum GEI rates calculated for a drift rate of 400 prey/ 100 m^3 and temperature of 12°C (e.g., Figures 33 - 36).

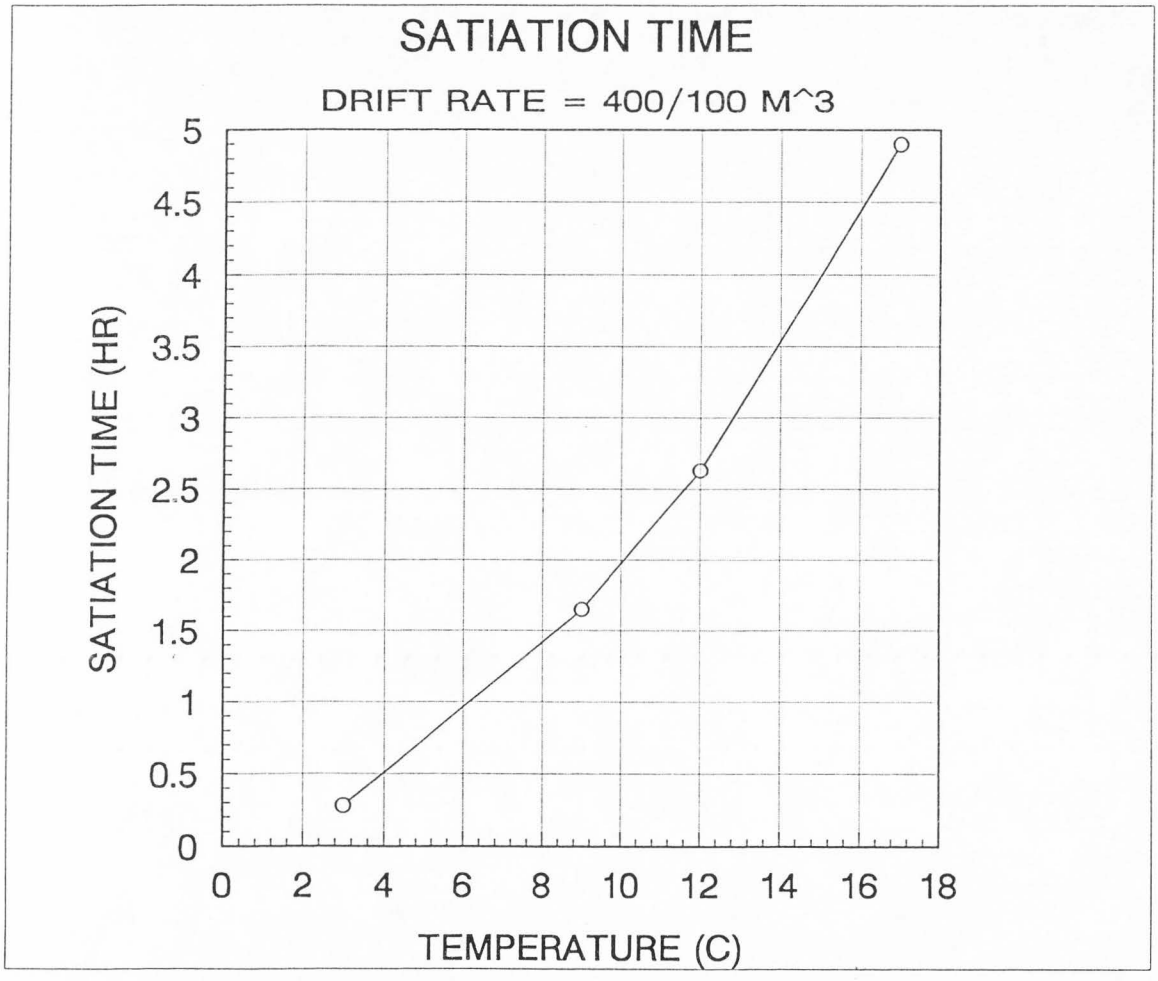

Figure 59. The effect of temperature on satiation time for a 200 mm fish. Satiation time is calculated from maximum daily consumption (equation 22) and the maximum GEI rates calculated for a drift rate of 400 prey/ 100 m^3 (e.g., Figure 37).

DISCUSSION

General discussion

The model. Frequently salmonid habitat models rely on simplistic assumptions and/or correlative data that do not allow them to provide cause-and-effect results or predictions. This NEI model attempts to rectify some of that problem by developing an individual-based, mechanistic model for lotic systems that incorporates many of the factors that affect energy intake by sit-and-wait, drift-feeding salmonids. The model is in part a combination of a basic predation model described by Holling (1959; 1966) and the prey capture model of Hughes and Dill (1990). The model appears to provide a conceptually sound method of quantifying NEI and provides a mechanistic basis of understanding how many abiotic variables (e.g., depth, velocity, temperature, stream morphology) and biotic variables (e.g., swimming speed and cost, invertebrate drift, energy assimilation) affect the net energy intake of drift-feeding fish. This mechanistic understanding in turn provides a method of determining stream habitat suitability in terms of NEI and consequently the energetic fitness attained by fish in various types of habitat.

As a result of its design, however, the NEI model fails to address a number of factors that can affect stream habitat utilization. Because the model is individual-based, it fails to account for the results of intra- and interspecific competition and predation on habitat choice. In addition, because the model addresses NEI, the effects of behaviors other than feeding and resting behavior on habitat utilization are not addressed.

Nevertheless, the NEI model provides accurate predictions of the habitat utilized in St. Charles Creek by drift-feeding salmonids.

The validation. The results from the NEI modeling of fish locations in St. Charles Creek add to the growing set of data that supports the idea that drift-feeding salmonids utilize habitats that provide high rates of net energy intake (NEI) (e.g., Fausch, 1984; Hill, 1989; Hughes and Dill, 1990; Hughes, 1991; Hill and Grossman, 1993). Validation of the NEI model in this research was based on the premise that fish choose habitats when feeding that provide high NEI; therefore, if the NEI output closely matches the habitat (depths and velocities and stream profile) that fish are utilizing, then the model is accurate (valid) or at least has not been shown to be invalid. Generally, the NEI model accurately predicted the habitat that trout (mostly cutthroat trout) in St. Charles Creek were utilizing. Depth and velocity data collected in St. Charles Creek by Lee Jacobsen (1993, unpublished) showed that as fish increased in size, they utilized deeper and faster water. The NEI model accurately predicted the shift to deeper and faster water for the larger fish, and the optimum NEI depths and velocities predicted by the model were similar to the depths and velocities actually being utilized by all sizes of fish except fish in the very smallest size class (10-39 mm). The smallest fish may have been using depths and velocities with low NEI due to predation and/or linear dominance threats of larger fish or the NEI model may have been inaccurately calculating NEI for very small fish.

The detailed mapping of physical habitat and fish locations in two pools and two runs in St. Charles Creek provided

additional evidence that cutthroat trout in St. Charles Creek are generally utilizing habitat that the NEI model predicts will provide optimum NEI. These data also highlight one of the difficulties of validating the NEI model in the field. Several of the fish observed were utilizing low velocity water where the model predicted low NEI values. If the fish were actually feeding, then they were feeding in areas that disagreed with the NEI model predictions; however, if the fish were engaging in some other activity, such as resting or avoiding predation, then the fish were utilizing habitat that minimizes energy costs as the NEI model predicts they should. With respect to energetics, fish should utilize a combination of high NEI habitat when feeding and low cost (typically low NEI) habitat when they are not feeding. Unfortunately, it is often difficult to determine the type of activity fish are engaged in from brief field observations.

Predictions and insights from the model

Deeper and faster water. As fish grow larger, their sustainable swimming speed and reaction distance both increase. Increased swimming speed increases both the depth and velocity for optimum NEI, while increased reaction distance increases the optimum depth. As a result, the NEI model predicts larger fish should utilize deeper and faster water to optimize their NEI. This corresponds to a large body of data, including this thesis, that show that salmonids do utilize deeper and faster water as they grow larger (e.g., Chapman and Bjornn, 1969; Everest and Chapman, 1972; Wankowski and Thorpe, 1979; Smith and Li, 1983; Baltz and Moyle, 1984; Baltz et al., 1991)

The NEI model explains why larger fish in St. Charles Creek and other studies were found in faster and deeper water and conversely why small fish are found in slower water. However, it does not explain why the smaller fish are found primarily in shallow water. Small fish can attain their maximum NEI in shallower water than large fish because they have smaller reaction distances and slower swimming speeds; nevertheless, NEI remains high in deep water for small fish according to the model. It is possible and perhaps most probable that small fish are being excluded from the deeper water by more dominate large fish (e.g., Fausch, 1984; Hughes, 1991).

Water temperature. The NEI model predicts that water temperature should have a profound effect on habitat choice. Given cold water temperatures, the model predicts that optimum NEI occurs in lower velocity water, whereas at higher temperatures optimum NEI is predicted in faster velocities. This primarily occurs because of the slower swimming velocities of fish at low temperatures and faster swimming velocities at warmer temperatures. Numerous studies that show salmonids utilize slower and often deeper water in the winter support the predictions of the NEI model (e.g., Chapman and Bjornn, 1969; Smith and Li, 1983; Campbell and Neuner, 1985; Cunjak and Power, 1986; Baltz et al., 1991).

The NEI model explains energetically why fish should utilize slower velocities in the winter; however, it does not necessarily provide an energetic reason for fish moving to deeper water where NEI is similar to that at intermediate depths. Some possible explanations for the move to deeper water include: (1)

because deeper water and slow velocities are correlated, fish utilize deeper water as a byproduct of selecting for slower velocities, (2) decreased aggressiveness by large dominate fish in colder water allows smaller fish to utilize deeper water habitats they are typically excluded from in warmer water (e.g., Cunjak and Power, 1986), and/or (3) some other factor not related to NEI such as safety is provided by deep water habitats.

Satiation time. The model predicts that given optimum stream habitat and typical drift densities, larger fish take a significantly longer time to satiate than smaller fish because of their larger consumption capacities. As a result, as fish get larger the ability to continue growing may become limited by the ability to obtain enough NEI. This could limit the size of fish in particular habitats (e.g., small streams) and/or produce a stimulus for emigration. The model also predicts that as temperatures increase, fish should require significantly more time to satiate because their daily consumption capacity increases with increased temperature up to roughly 18°C.

GEI versus NEI. The model predictions of which habitats fish should utilize are nearly identical for GEI or NEI. The only difference occurs when energy intake is very low and swimming cost becomes significant. In general, however, swimming costs are insignificant to the model predictions of optimum habitat except at very low NEI. The primary advantage of calculating NEI is that it can provide a more precise measure of the amount of energy available for growth and reproduction. One of the areas of the NEI model that was not validated in this study and that is very important is whether the model is

predicting the magnitude of NEI accurately. This needs to be done by actually measuring intake of drift-feeding fish and determining whether or not the model accurately predicts the number of drifting prey captured. If the magnitude of NEI can be predicted accurately, then the important ability to actually predict growth is possible.

Drift density. The model predicts that drift density in a stream does not alter which depth/velocity habitats provide optimum habitat; however, it does predict that the range of depth/velocity combinations that provide suitable NEI increases substantially when drift density increases. In addition, as drift increases, the magnitude of NEI increases and it takes less time for fish to satiate. This means that a given stream will provide more habitat with suitable NEI given increased drift density. The model also predicts that when drift density is nearly zero or when feeding is not occurring due to poor visibility (e.g., darkness or turbidity) or because fish are resting, that fish should utilize the lowest velocity water available.

Engineering significance (applications of the model)

The most profound applications of the NEI model are that it could be utilized to explain many of the empirical observations of fish habitat utilization and be used as a predictive tool to accurately assess/predict the impacts of natural and anthropogenic habitat alteration. Assuming that NEI can accurately be modeled, then it would be possible to quantify energetic fitness of fish in given habitats. As a result the

effects of changes in stream flow, water temperature, and stream productivity on drift-feeding salmonids could be modeled and predicted from direct cause-and-effect principles. In addition, the importance of other factors such as predation and competition on habitat utilization could be assessed in terms of their effect on NEI.

Currently, IFIM is the most widely used method of quantifying the impacts of stream flow and habitat alteration on fisheries resources. IFIM is frequently used as a tool to assess environmental impacts associated with water development projects (e.g., hydropower plants and irrigation). IFIM utilizes empirically derived suitability curves (SI curves) for depth, velocity, and substrate/cover to rate the suitability of stream habitat. Unfortunately the biological meaning of SI curves and the transferability of SI curves between different streams or stream flows are not well understood. As a result, IFIM analyses provide ambiguous results.

Many SI curves that have been developed for salmonids (e.g., Bovee, 1978) predict similar and sometimes identical habitats as are predicted by the NEI model (unpublished data). This should be expected if drift-feeding salmonids are utilizing high net energy locations in streams because SI curves are simply an empirical measure of the habitats that fish are utilizing (i.e., empirical measures of NEI). Unfortunately, there currently is a lack of understanding about the mechanisms that produce given SI curves, so when SI curves differ among streams, investigators, and/or fish populations, it is difficult to reconcile or understand the differences. In addition, because SI

curves are not explicitly based on a biological measure of fitness such as NEI, it is difficult to assess the meaning of SI curves. It appears that NEI modeling could provide a superior and more interpretable method of determining the suitability of stream habitat in drift-feeding salmonids by assessing habitat in terms of energetics, which in turn can be directly related to fish fitness.

Recommendations

The most pressing need in terms of NEI modeling is the need for future research comparing the NEI model predictions of net energy intake with actual empirical measures of net energy intake by drift-feeding salmonids at different depths, velocities, and drift densities. The comparison would allow direct validation of the model as a measure of NEI and/or suggest ways in which the NEI model could mechanistically be improved. For instance, there are numerous factors that might need to be incorporated into the model to make it a more accurate predictor of NEI. The model may need to incorporate fish acceleration into the prey capture phase, or capture probability, or different directions of capture instead of lateral and vertical (e.g., forward or backwards slightly), and/or the effects of low light levels on reaction distances (e.g., shading and light attenuation in deep water). In addition, feeding motivation at different satiation states might be important in predicting NEI. Nevertheless, if the NEI model can be shown to accurately predict NEI or can be modified to accurately predict NEI, then it can be used with confidence to assess the energetic (fitness) potential of stream habitats.

REFERENCES

Allan, J.D. 1987. Macroinvertebrate drift in a Rocky Mountain stream. Hydrobiol. 144:261-268.

Bachman, R.A. 1984. Foraging behavior of free-ranging wild and hatchery brown trout in a Stream. Trans. Am. Fish. Soc. 113(1):1-36.

Bainbridge, R. 1960. Speed and stamina in three fish. J. Exp. Biol. 37:129-153.

Baltz, D. M. and P. B. Moyle. 1984. Segregation by species and size classes of rainbow trout, *Salmo Gairdneri*, and Sacramento sucker, *Catostomus occidentalis*, in three California streams. Environ. Biol. Fishes. The Hague: Dr. W. Junk Publishers 10:101-110.

Baltz, D.M., B. Vondracek, L.R. Brown, and P.B. Moyle. 1991. Seasonal changes in microhabitat selection by rainbow trout in a small stream. Trans. Am. Fish. Soc. 120:166-176.

Bannon, E. and N.H. Ringler. 1986. Optimal prey size for stream resident brown trout (*Salmo trutta*): Tests of predictive models. Can. J. Zool. 64:704-713.

Beamish, F. W. H. 1978. Swimming capacity, p. 101-187. *In* W. S. Hoar and D. J. Randal (Eds.). Fish Physiology, Vol. VII: Locomotion. Academic Press, New York.

Bisson, P.A. 1978. Diel food selection by two sizes of rainbow trout (*Salmo gairdneri*) in an experimental stream. J. Fish. Res. Board Canada 35:971-975

Bovee, K. D., 1978. Probability-of-use criteria for the family salmonidae: Instream flow information paper No. 4, U.S. Fish and Wildlife Service, FWS/OBS-78/07, Ft. Collins, Colorado.

Bres, M. 1986. A new look at optimal foraging behaviour; rule of thumb in the rainbow trout. J. Fish Biol. 29:25-36.

Brett, J.R. 1964. The Respiratory metabolism and swimming performance of young sockeye salmon. J. Fish. Res. Board Canada 21(5):1183-1226.

Brett, J.R. 1970. Fish-the energy cost of living, p. 37-52. *In* W. J. McNeil (Ed.). Marine aquaculture. Oregon State University Press, Corvallis, Oregon.

Brett, J.R. and N.R. Glass. 1973. Metabolic rates and critical swimming speeds of sockeye salmon (*Oncorhynchus nerka*) in relation to size and temperature. J. Fish. Res. Board Canada 30:379-387.

Brett, J.R. and T.D.D. Groves. 1979. Physiological energetics, p. 279-352. *In* W.S. Hoar, D.J., Randal and J.R. Brett (Eds.). Fish physiology, Vol. 8, Bioenergetics and growth, Academic Press, New York.

Brett, J.R., M. Hollands, and D.F. Alderdice. 1958. The effect of temperature on the cruising speed of young sockeye and coho salmon. J. Fish. Res. Board Canada 15(4):587-605.

Brett, J.R., J.E. Shelbourn, and C.T. Shoop. 1969. Growth rate and body composition of fingerling sockeye salmon, *Oncorhynchus nerka*, in relation to temperature and ration size. J. Fish. Res. Board Canada 26:2363-2394.

Campbell, R.F. and J.H. Neuner. 1985. Seasonal and diurnal shifts in habitat utilized by resident rainbow trout in western Washington Cascade Mountain streams, p. 39-48. *In* F. W. Olson, R. G. White, and R. H. Hamre (Eds.). Proceedings of the symposium on small hydropower and fisheries. American Fisheries Society, Bethesda, Maryland.

Chapman, D.W. and T.C. Bjornn. 1969. Distribution of salmonids in streams, with special reference to food and feeding, p. 153-176. *In* T.G. Northcote (Ed.). Salmon and trout in streams. H. R. MacMillan Lectures in Fisheries, University of British Columbia, Vancouver.

Confer, J.L. and P.L. Blades. 1975. Omnivorous zooplankton and planktivorous fish. Limnol. & Oceanogr. 20(4):571-579.

Confer, J.L., G.L. Howick, M.H. Corzette, S.L. Kramer, S. Fitzgibbon, and R. Landesberg. 1978. Visual predation by planktivores. Oikos 31:27-37.

Cummins, K.W. and J.C. Wuycheck. 1971. Caloric equivalents for investigations in ecological energetics. Mitt. int. Ver. Theor. Angew. Limnol. 18:1-158.

Cunjak, R. A. and G. Power. 1986. Winter habitat utilization by stream resident brook trout (*Salvelinus fontinalis*) and brown trout (*Salmo trutta*). Can. J. Fish. Aquat. Sci. 43:1970-1981.

Dunbrack, R.L. and L.M. Dill. 1983. A model of size dependent surface feeding in a stream dwelling salmonid. Environ. Biol. Fishes 8:203-216.

Dunbrack, R.L. and L.M. Dill. 1984. Three-dimensional prey reaction field of the juvenile coho salmon (Oncorhynchus kisutch). Can. J. Fish. Aquat. Sci. 41:1176-1182.

Dunbrack, R. L. and L. A. Giguere. 1987. Adaptive responses to accelerating costs of movement: A bioenergetic basis for the type-III functional response. Am. Nat. 130(1):147-160.

EA Engineering, Science, and Technology, Inc. 1986. Instream flow methodologies. Research project 2194-2, Completion report, Electric Power Research Institute, Palo Alto, California.

Edmundson, E., F. E. Everest, and D. W. Chapman. 1968. Permanence of station in juvenile chinook salmon and steelhead trout. J. Fish. Res. Board Canada 25:1453-1464.

Edsall, T.A., E.H. Brown Jr., T.G. Yocom and R.S.C. Wolcott Jr. 1974. Utilization of alewives by coho salmon in Lake Michigan. Great Lakes Fishery Laboratory, Administrative Report. 14 p.

Eggers, D. M. 1975. A synthesis of the feeding behavior and growth of juvenile sockeye salmon in the limnetic environment. Unpublished Ph.D. thesis. Univ. Washington, Seattle. 217 p.

Eggers, D.M. 1977. The nature of prey selection by planktivorous fish. Ecology 58:46-59.

Elliott, J.M. 1970. Methods of sampling invertebrate drift in running water. Ann. Limnol. 1(5):133-159.

Elliott, J.M. 1975a. Number of meals in a day, maximum weight of food consumed in a day and maximum rate of feeding for brown trout, Salmo trutta L. Freshw. Biol. 5:287-303.

Elliott, J.M. 1975b. Weight of food and time required to satiate brown trout, Salmo trutta L. Freshw. Biol. 5:51-64.

Elliott, J. M. 1976. Energy losses in the waste products of brown trout (Salmo trutta L.). J. Animal Ecol. 45:561-580.

Elliott, J.M. 1979. Energetics of freshwater teleosts. Symp. Zool. Soc. Lond. 44:29-61.

Everest, F. H. and D. W. Chapman. 1972. Habitat selection and spatial interactions by juvenile chinook salmon and steelhead trout in two Idaho streams. J. Fish. Res. Board Canada 29:91-100.

Fry, F. E. and E. T. Cox. 1970. A relation of size to swimming speed in rainbow trout. J. Fish. Res. Board Canada 27:976-978.

Fausch, K.D. 1984. Profitable stream position for salmonids: relating specific growth rate to net energy gain. Can. J. Zool. 62:441-451.

Gendron, R.P. and J.E.R. Staddon. 1983. Searching for cryptic prey: the effect of search rate. Am. Nat. 121(2):172-186.

Glova, G.J. and J.E. McInerney. 1977. Critical swimming speeds of coho salmon (*Oncorhynchus kisutch*) fry to smolt stages in relation to salinity and temperature. J. Fish. Res. Board Canada 34:151-154.

Godin, J.G.J. and R. W. Rangeley. 1989. Living in the fast lane: effects of cost of locomotion on foraging behaviour in juvenile Atlantic salmon. Anim. Behav. 37:943-954.

Grant, W.E. 1986. Systems analysis and simulation in wildlife and fisheries science. Wiley, New York, 338 p.

Griffiths, J.S. and D.F. Alderdice. 1972. Effects of acclimation and acute temperature experience on the swimming speed of juvenile coho salmon. J. Fish. Res. Board Canada 29:251-264.

Heggenes, J., T.G. Northcote, and A. Peter. 1991. Spatial stability of cutthroat trout (*Oncorhynchys clarki*) in a small, coastal stream. Can. J. Fish. Aquatic Sci. 48:757-762.

Henderson, M. A. 1982. An analysis of prey detection in cutthroat trout (*Salmo clarki clarki*) and dolly varden charr (*Salvelinus malma*). Unpublished Ph.D. Dissertation. The University of British Columbia, Vancouver, Canada, 152 p.

Hill, J. 1989. The energetic significance of microhabitat use in two stream fishes. Unpublished Ph.D. Dissertation. University of Georgia, Georgia, 125 p.

Hill, J. and G.D. Grossman. 1993. An energetic model for microhabitat use for rainbow trout and rosyside dace. Ecology, 74:685-698.

Holling, C. S. 1959. Some characteristics of simple types of predation and parasitism. Canad. Ent. 91:385-398.

Holling, C. S. 1966. The functional response of invertebrate predators to prey density. Mem. Entomol. Soc. Can. 48.1-86.

Hughes, N.F. 1991. The behavioral ecology of arctic grayling distribution in interior Alaskan streams. Draft Ph.D. Dissertation. University of Alaska Fairbanks, Alaska.

Hughes, N.F. and L.M. Dill. 1990. Position choice by drift-feeding salmonids: Model and test for Arctic grayling (Thymallus arcticus) in subarctic mountain streams, interior Alaska. Can. J. Fish. Aquatic Sci. 47(10):2039-2048.

Irvine, J.R. and T.G. Northcote. 1982. Significance of sequential feeding patterns of juvenile rainbow trout in a large lake-fed river. Trans. Amer. Fish. Soc. 111:446-452.

Jenkins, T.M. Jr. 1969. Social structure, position choice and micro-distribution of two trout species (*Salmo trutta* and *Salmo gairdneri*) resident in mountain streams. Anim. Behav. Monogr. 2(2):57-123.

Jobling, M. 1987. Influences of food particle size and dietary energy content on patterns of gastric evacuation in fish: test of a physiological model of gastric emptying. J. Fish Biol. 30:299-314.

Jones, D.R. 1971. The effect of hypoxia and anaemia on the swimming performance of rainbow trout (*Salmo gairdneri*). J. Exp, Biol. 55:541-551.

Jones, D.R., J.W. Kiceniuk, and O.S. Bamford. 1974. Evaluation of the swimming performance of several fish species from the Mackenzie River. J. Fish. Res. Board Canada 31:1641-1647.

Kettle, D. and W.J. O'Brien 1978. Vulnerability of Arctic zooplankton species to predation by small lake trout (*Salvelinus namaycush*). Fish. Res. Board Canada 35:1495-1500.

Kitchell, J. F. 1983. Energetics, p. 312-338. *In* P.W. Webb and D. Weihs (Eds.). Fish Biomechanics. Praeger Publishers, New York.

Kitchell, J.F., J.F. Koonce, R.V. O'Neill, H.H. Shugart, Jr., J.J. Magnuson, and R.S. Booth. 1974. Model of fish biomass dynamics. Trans. Am. Fish. Soc. 103:786-798.

Krebs, C.J. 1989. Ecological methodology. Harper & Row, New York. 654 p.

Lazzaro, X. 1987. A review of planktivorous fishes: their evolution, feeding behaviour, selectivities, and impacts. Hydrobiol. 146:97-167.

Leopold, L.B, M.G. Wolman, and J.P. Miller. 1964. Fluvial Processes in Geomorphology. W. H. Freeman and Company, San Francisco. 521 p.

Levine, J.S., P.S. Lobel, and E.F. McNichol Jr. 1979. Visual communication in fishes, p. 447-475. *In* M.A. Ali (ed.), Environmental physiology of fishes. Plenum Press, New York and London. 723 p.

Luecke, C. and W.J. O'Brien. 1981. Prey location volume of a planktivorous fish: A new measure of prey vulnerability. Can. J. Fish. Aquatic Sci. 38:1264-1270.

Manly, B.F.J. 1991. Randomization and Monte Carlo methods in biology. Chapman and Hall, New York. 281 p.

Matter, W.J. and A.J. Hopwood. 1980. Vertical distribution of invertebrate drift in a large river. Limnol. & Oceanogr. 25(6):1117-1121.

Milhouse, R.T. 1990. User's guide to the physical habitat simulation system-version II. U.S. Fish Wildlife Service Draft Biological Report.

Ney, J. J. 1990. Trophic economics in fisheries: assessment of demand-supply relationships between predators and prey. Reviews in Aquatic Sciences 2(1):55-81.

Orth, D.J. and O.E. Maughan. 1982. Evaluation of the incremental methodology for recommending instream flows for fishes. Trans. Amer. Fish. Soc. 111:413-445.

Platts, W.S., W.F. Megahan, and G.W. Minshall. 1983. Methods for evaluating stream, riparian, and biotic conditions. Gen. Tech. Rep. INT-138. Ogden, Utah: U.S. Department of Agriculture, Forest Service, Intermountain Forest and Range Experiment Station. 70 p.

Power, M.E., R.J. Stout, C.E. Cushing, P.P. Harper, F.R. Hauer, W.J. Matthews, P.B. Moyle, and B. Statzner. 1988. Biotic and abiotic controls in river and stream communities. J. N. Am. Benthol. Soc. 7(4):456-479.

Puckett, K.J. and L.M. Dill. 1984. Cost of sustained and burst swimming to juvenile coho salmon (*Oncorhynchus kisutch*). Can. J. Fish. Aquatic Sci. 41:1546-1551.

Rantz, S. E. and others. 1982. Measurement and computation of streamflow: Volume 1. Measurement of stage and dischanrge. Volume 2. Computation of discharge. U.S. Geological Survey Water-Supply Paper 2175, U.S. Government Printing Office, Washington, D.C. 631 p.

Rao, G.M.M. 1968. Oxygen consumption of rainbow trout (*Salmo gairdneri*) in relation to activity and salinity. Can. J. Zool. 46:781-786.

Reiser, D.W., T.A. Wesche, and C. Estes. 1989. Status of instream flow legislation and practices in North America. Fisheries 14(2):22-29.

Ringler, N.H. and D.F. Brodowski. 1983. Functional responses of brown trout (*Salmo trutta* L.) to invertebrate drift. J. Freshw. Ecol. 2:45-57.

Romesburg, C. H. and K. Marshall. 1985. CHITEST: a Monte-Carlo computer program for contingency table tests. Comput. & Geosci. 2(1):69-78.

Schmidt, D. and W. J. O'Brien. 1982. Planktivorous feeding ecology of Arctic grayling (*Thymallus arcticus*). Can. J. Fish. Aquatic Sci. 39:475-482.

Scott, D. and C.S. Shirvell. 1987. A critique of the Instream Flow Incremental Methodology and observations on flow determination in New Zealand. p. 27-43. *In* J.F. Craig and J.B. Kemper (Eds.). Regulated streams: Advances in ecology, Proceedings of the Third International Symposium on Regulated Streams. Plenum Press, New York.

Skinner, W.D. 1985. Size selection of food by cutthroat trout, *Salmo clarki*, in an Idaho stream. Great Basin Nat. 45(2):327-331.

Smith, J.J. and H.W. Li. 1983. Energetic factors influencing foraging tactics of juvenile steelhead trout, *Salmo gairdneri*, p. 173-180. *In* D.L.G. Noakes, D.G. Lingquist, G.S. Helfman and J.A. Ward, (Eds.). Predators and prey in fishes. Dr W. Junk Publishers, The Hague, Netherlands.

Smock, L.A. 1980. Relationships between body size and biomass of aquatic insects. Freshw. Biol. 10:375-383.

Stephens, D.W., and J.R. Krebs. 1986. Foraging theory. Princeton University Press, Princeton, New Jersey. 247 p.

Stewart, D. J. 1980. Salmonid predators and their forage base in Lake Michigan: a bioenergetics-modelling synthesis. Unpublished Ph.D. Dissertation, University of Wisconsin, Madison, Wisconsin.

Swartzman, G.L. and S.P. Kaluzny. 1987. Ecological simulation primer. MacMillan Publishing Company, New York. 370 p.

Townsend, C.R. and I.J. Winfield. 1985. The application of optimal foraging theory to feeding behaviour in fish, p. 67-98. *In* P. Tytler, and P. Calow (Eds.). Fish energetics: New perspectives. Johns Hopkins University Press, Baltimore.

Vinyard, G.L. and W.J. O'Brien. 1976. Effects of light and turbidity on the reactive distance of bluegill (*Lepomis macrochirus*). J. Fish. Res. Board Canada 33:2845-2849.

Wankowski, J.W.J. 1979. Morphological limitations, prey size selectivity, and growth response of juvenile atlantic salmon, *Salmo salar*. J. Fish Biol. 14:89-100.

Wankowski, J.W.J. 1981. Behavioural aspects of predation by juvenile Atlantic Salmon (*Salmo salar* L.) on particulate, drifting prey. Animal Behav. 29:557-571.

Wankowski, J.W.J. and J.E. Thorpe. 1979. Spatial distribution and feeding in Atlantic salmon, *Salmo salar* L., juveniles. J. Fish Biol. 14:239-247.

Ware, D.M. 1973. Risk of epibenthic prey to predation by rainbow trout (*Salmo gairdneri*). J. Fish. Res. Board Canada 30(6):787-797.

Ware, D.M. 1982. Power and evolutionary fitness of teleosts. Can. J. Fish. Aquatic Sci. 39:3-13.

Waters, T.F. 1965. Interpretation of invertebrate drift in streams. Ecology 46(3):327-333.

Webb, P.W. 1975. Hydrodynamics and energetics of fish propulsion. Bull. Fish. Res. Board Canada, 190:1-158.

Webb, P.W. 1982. Fast-start resistance of trout. J. Exp. Biol. 96:93-106.

Wilzbach, M.A. 1985. Relative roles of food abundance and cover in determining the habitat distribution of stream-dwelling cutthroat trout (*Salmo clarki*). Can. J. Fish. Aquatic Sci. 42:1668-1672.

Wilzbach, M.A., K.W. Cummins, and J.D. Hall. 1986. Influence of habitat manipulations on interactions between cutthroat trout and invertebrate drift. Ecology 76(4):898-911.

Wright, D. L. and W. J. O'Brien. 1984. The development and field test of a tactical model of the planktivorous feeding of white crappie (*Pomoxis annularis*). Ecol. Monogr. 54(1):65-98.

APPENDIX

SENSITIVITY ANALYSIS GRAPHS

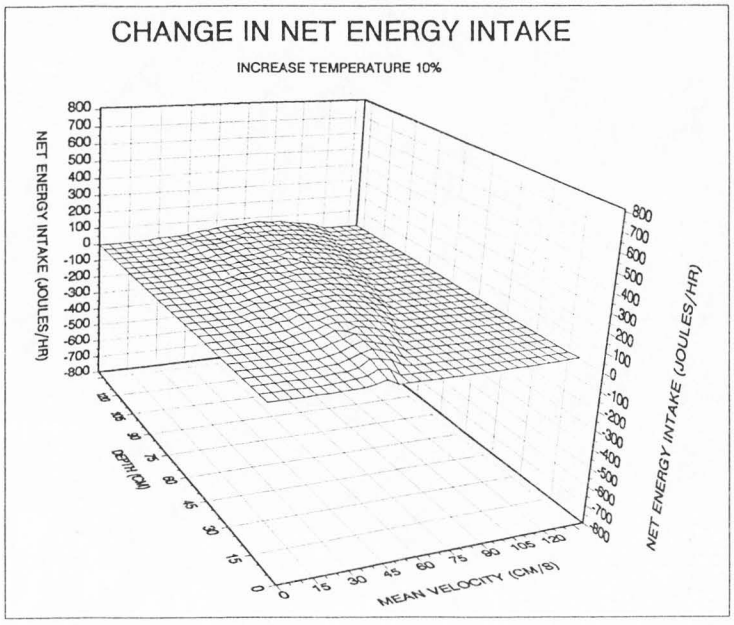

Figure A1. Graphic of the change (sensitivity) of net energy intake to a 10% increase (perturbation) in temperature. The surface presented was derived by subtracting the perturbed NEI surface from the baseline NEI surface.

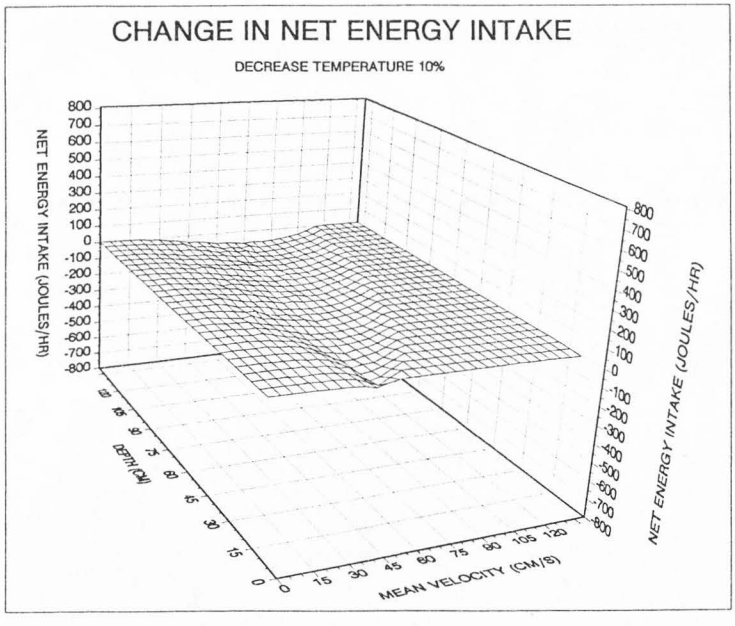

Figure A2. Graphic of the change (sensitivity) of net energy intake to a 10% decrease (perturbation) in temperature. The surface presented was derived by subtracting the perturbed NEI surface from the baseline NEI surface.

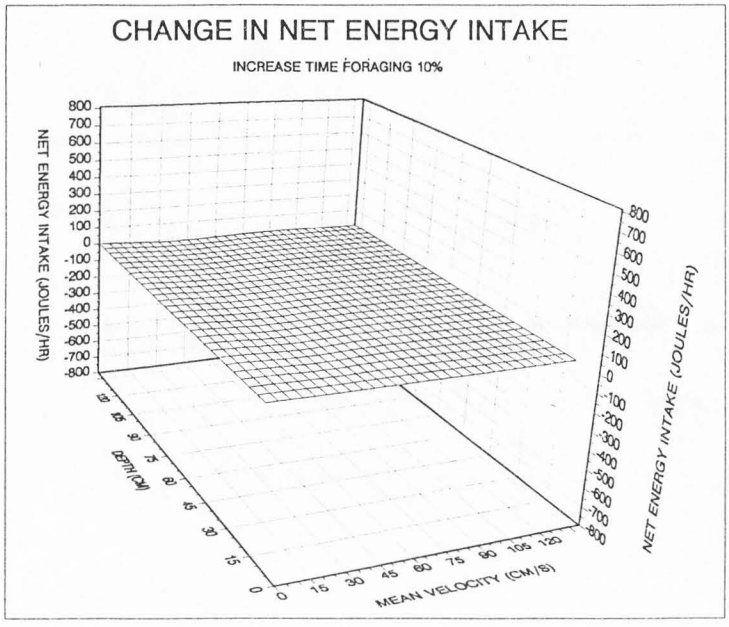

Figure A3. Graphic of the change (sensitivity) of net energy intake to a 10% increase (perturbation) in feeding foray time. The surface presented was derived by subtracting the perturbed NEI surface from the baseline NEI surface.

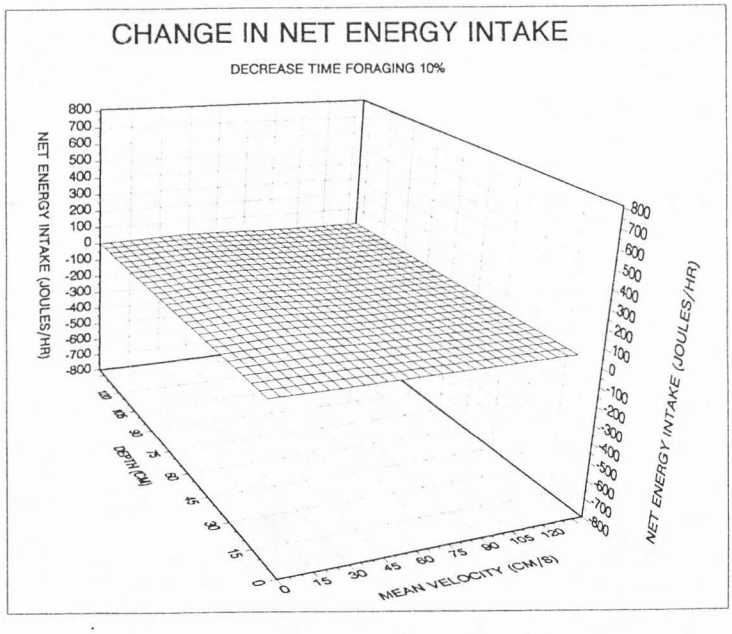

Figure A4. Graphic of the change (sensitivity) of net energy intake to a 10% decrease (perturbation) in feeding foray time. The surface presented was derived by subtracting the perturbed NEI surface from the baseline NEI surface.

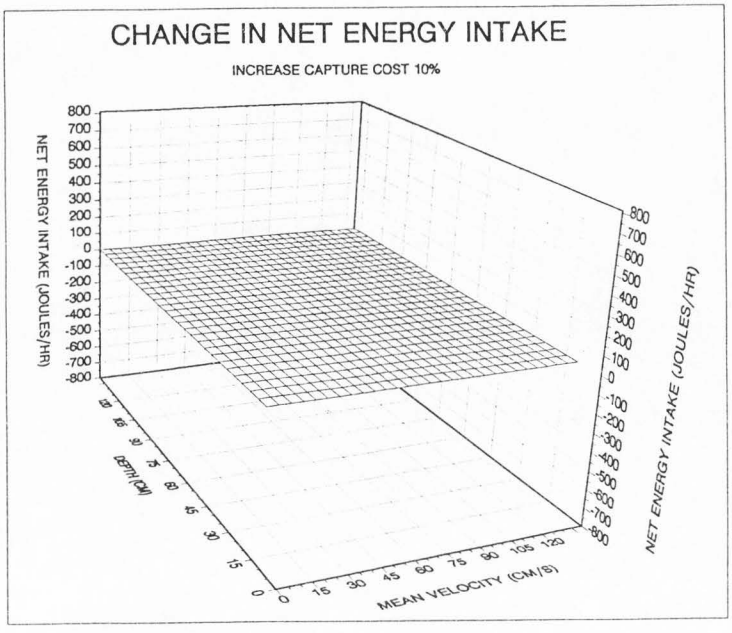

Figure A5. Graphic of the change (sensitivity) of net energy intake to a 10% increase (perturbation) in capture cost. The surface presented was derived by subtracting the perturbed NEI surface from the baseline NEI surface.

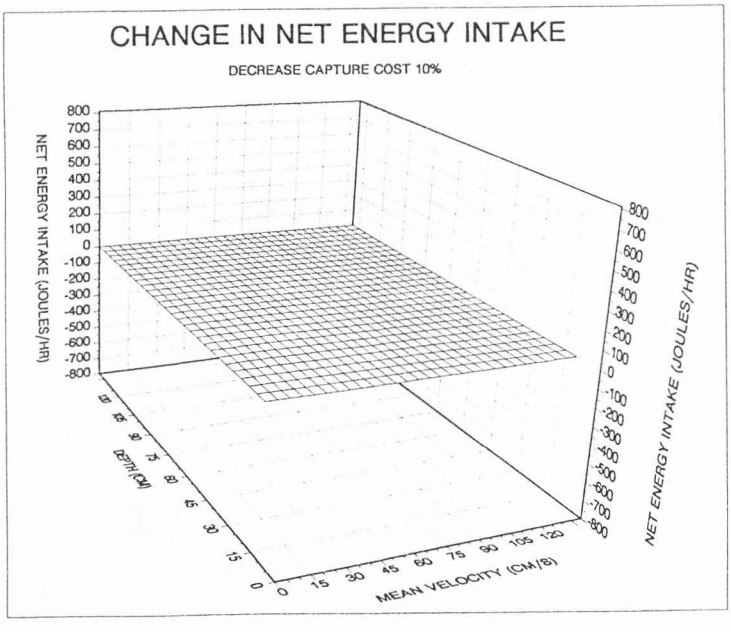

Figure A6. Graphic of the change (sensitivity) of net energy intake to a 10% decrease (perturbation) in capture cost. The surface presented was derived by subtracting the perturbed NEI surface from the baseline NEI surface.

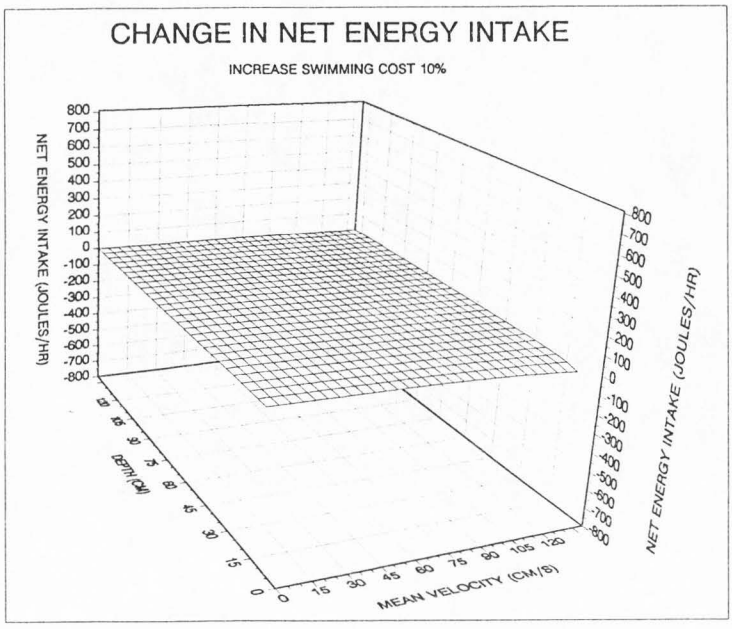

Figure A7. Graphic of the change (sensitivity) of net energy intake to a 10% increase (perturbation) in swimming cost. The surface presented was derived by subtracting the perturbed NEI surface from the baseline NEI surface.

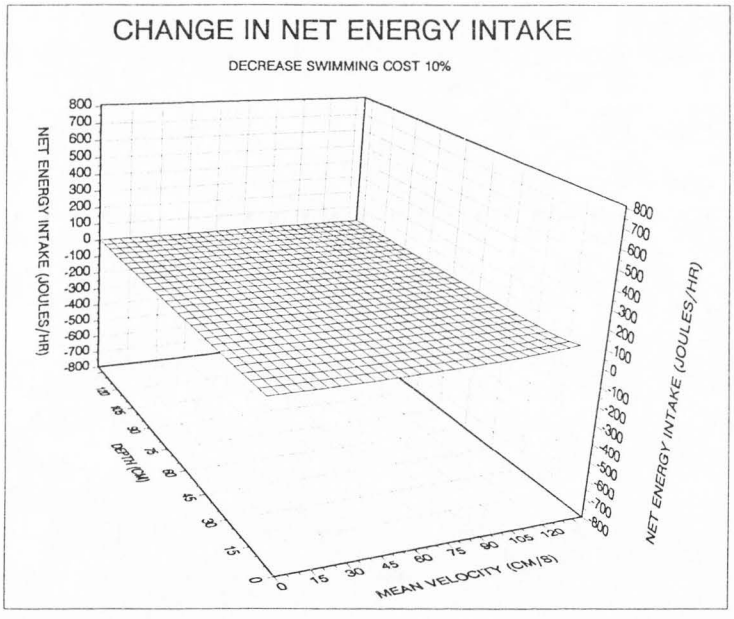

Figure A8. Graphic of the change (sensitivity) of net energy intake to a 10% decrease (perturbation) in swimming cost. The surface presented was derived by subtracting the perturbed NEI surface from the baseline NEI surface.

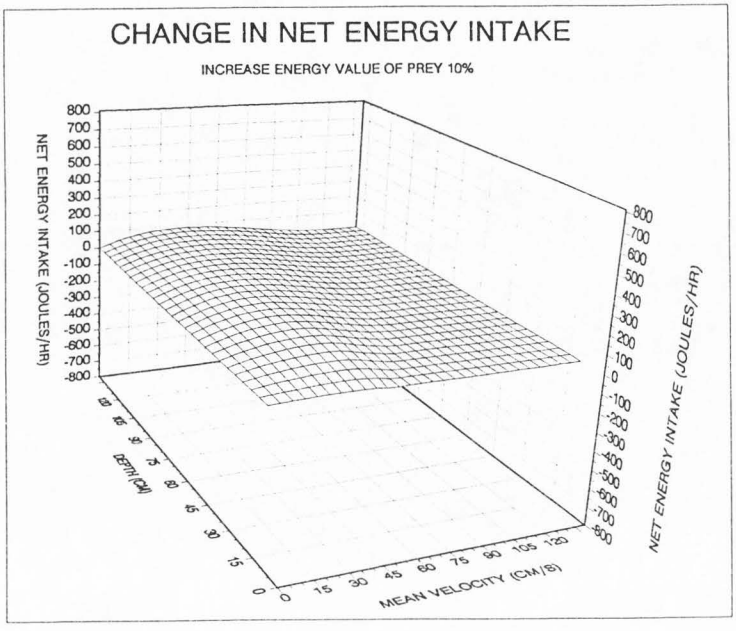

Figure A9. Graphic of the change (sensitivity) of net energy intake to a 10% increase (perturbation) in prey energy value. The surface presented was derived by subtracting the perturbed NEI surface from the baseline NEI surface.

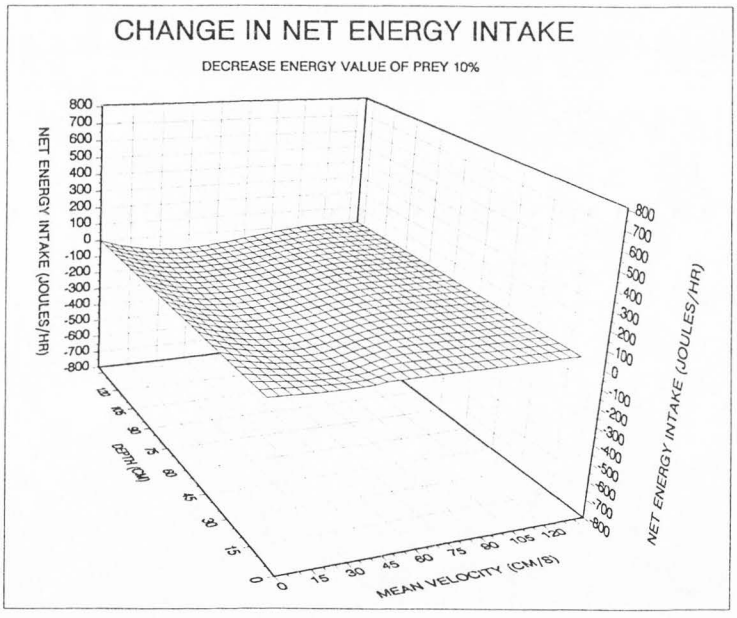

Figure A10. Graphic of the change (sensitivity) of net energy intake to a 10% decrease (perturbation) in prey energy value. The surface presented was derived by subtracting the perturbed NEI surface from the baseline NEI surface.

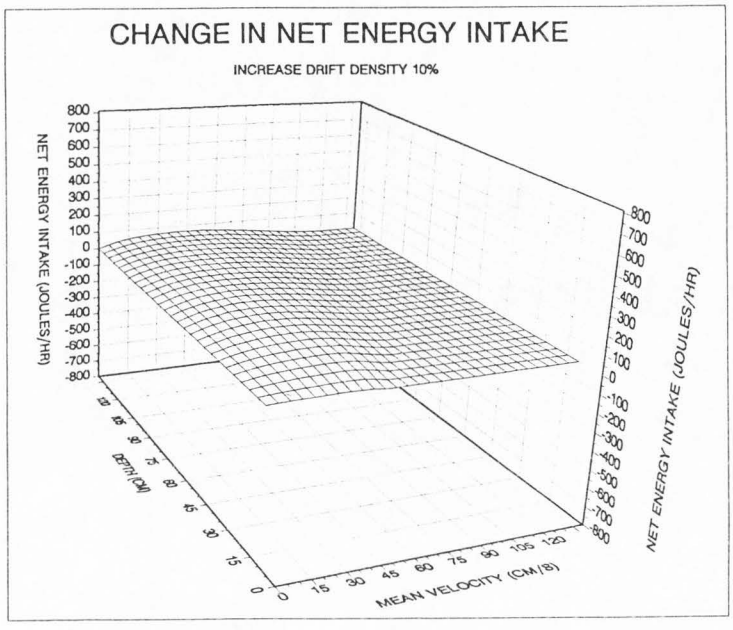

Figure A11. Graphic of the change (sensitivity) of net energy intake to a 10% increase (perturbation) in drift density. The surface presented was derived by subtracting the perturbed NEI surface from the baseline NEI surface.

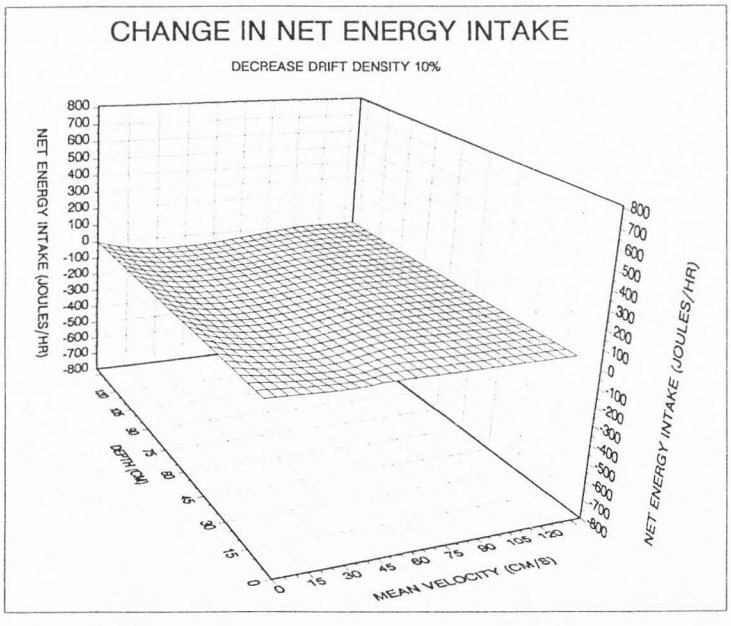

Figure A12. Graphic of the change (sensitivity) of net energy intake to a 10% decrease (perturbation) in drift density. The surface presented was derived by subtracting the perturbed NEI surface from the baseline NEI surface.

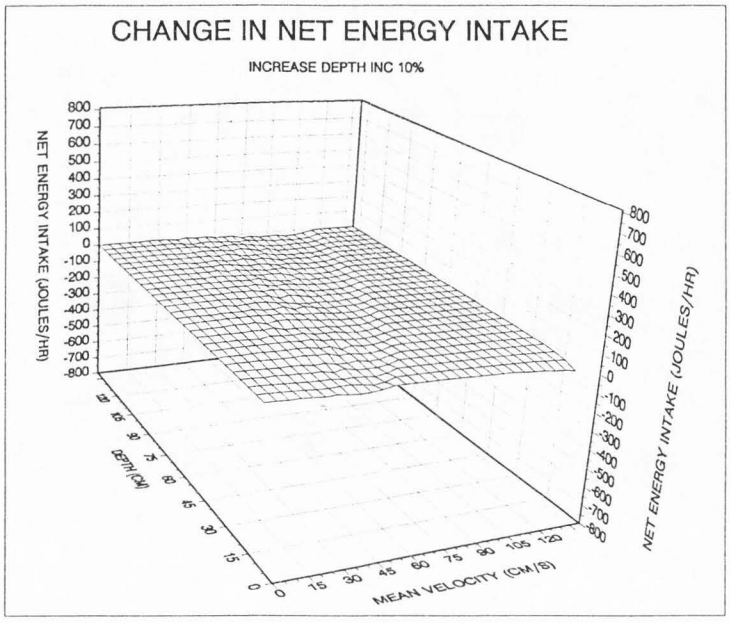

Figure A13. Graphic of the change (sensitivity) of net energy intake to a 10% increase (perturbation) in focal depth. The surface presented was derived by subtracting the perturbed NEI surface from the baseline NEI surface.

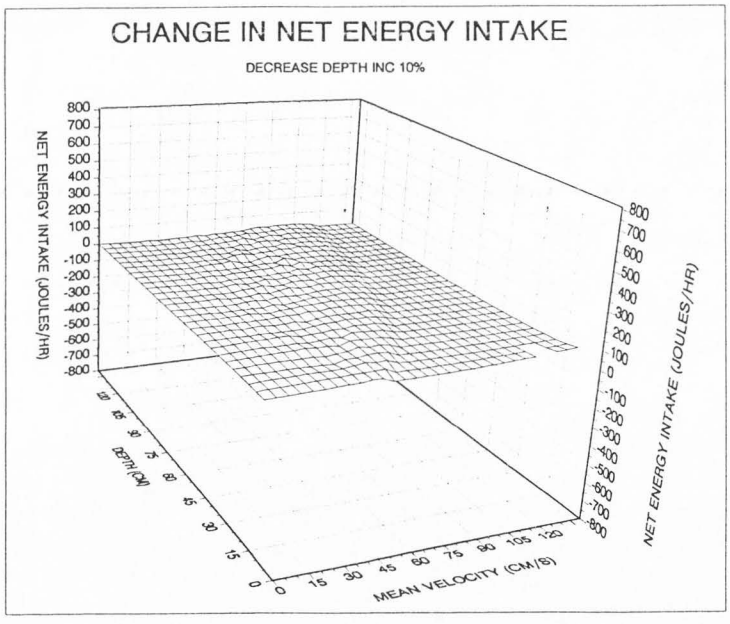

Figure A14. Graphic of the change (sensitivity) of net energy intake to a 10% decrease (perturbation) in focal depth. The surface presented was derived by subtracting the perturbed NEI surface from the baseline NEI surface.

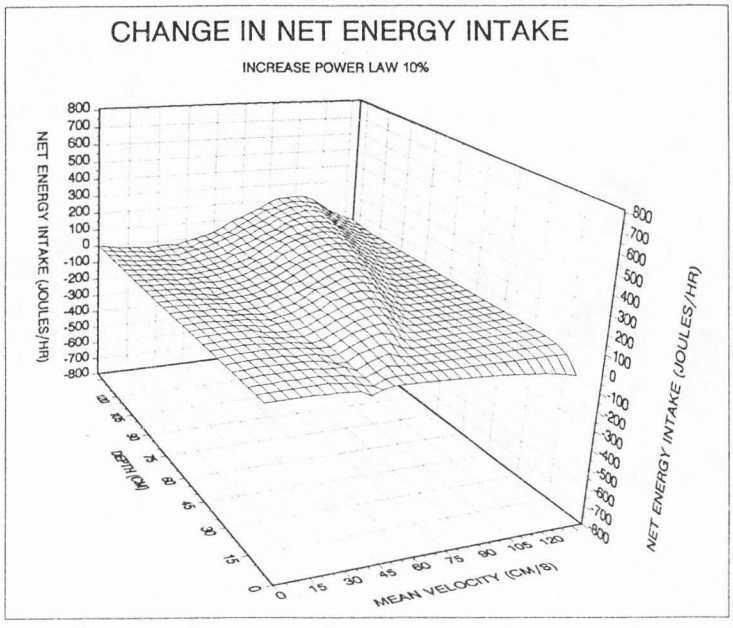

Figure A15. Graphic of the change (sensitivity) of net energy intake to a 10% increase (perturbation) in the power law constant. The surface presented was derived by subtracting the perturbed NEI surface from the baseline NEI surface.

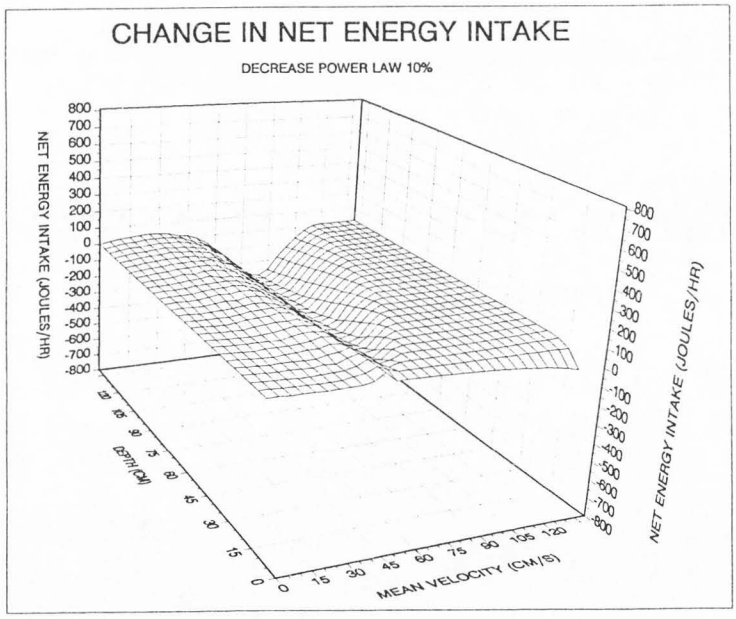

Figure A16. Graphic of the change (sensitivity) of net energy intake to a 10% decrease (perturbation) in the power law constant. The surface presented was derived by subtracting the perturbed NEI surface from the baseline NEI surface.

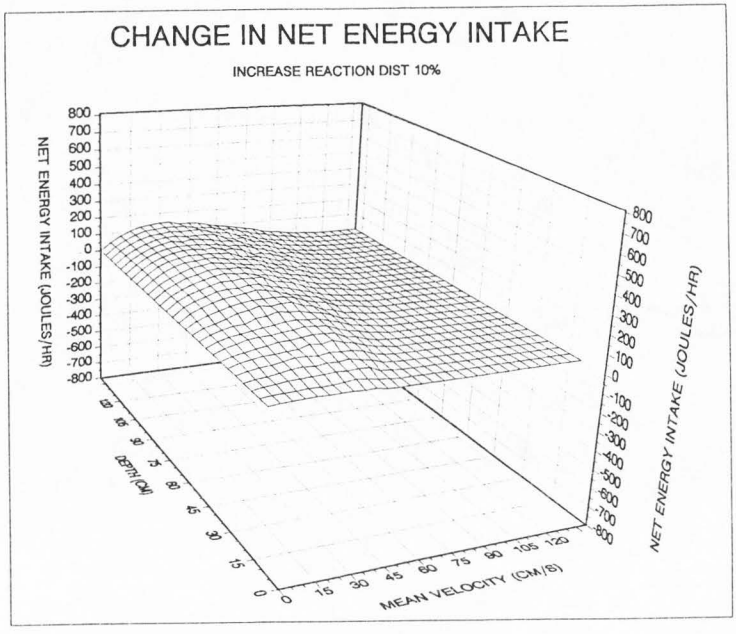

Figure A17. Graphic of the change (sensitivity) of net energy intake to a 10% increase (perturbation) in reaction distance. The surface presented was derived by subtracting the perturbed NEI surface from the baseline NEI surface.

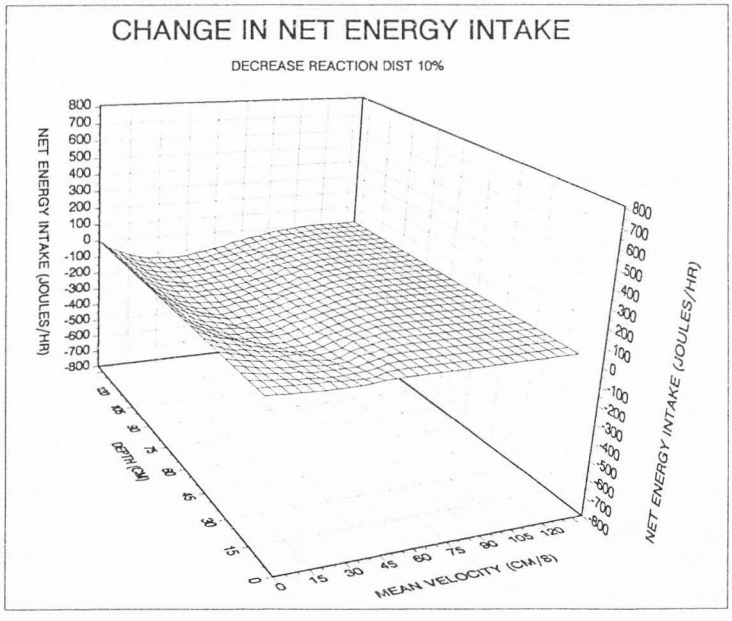

Figure A18. Graphic of the change (sensitivity) of net energy intake to a 10% decrease (perturbation) in reaction distance. The surface presented was derived by subtracting the perturbed NEI surface from the baseline NEI surface.

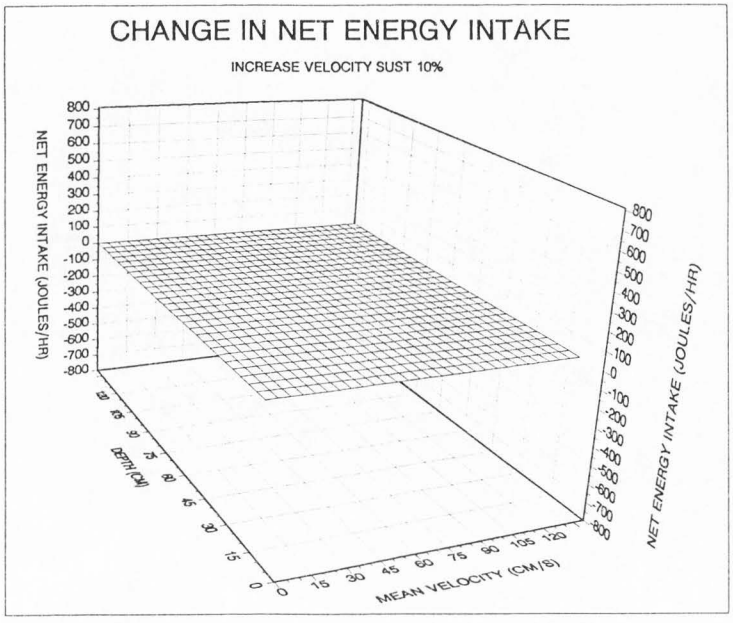

Figure A19. Graphic of the change (sensitivity) of net energy intake to a 10% increase (perturbation) in the sustained velocity. The surface presented was derived by subtracting the perturbed NEI surface from the baseline NEI surface.

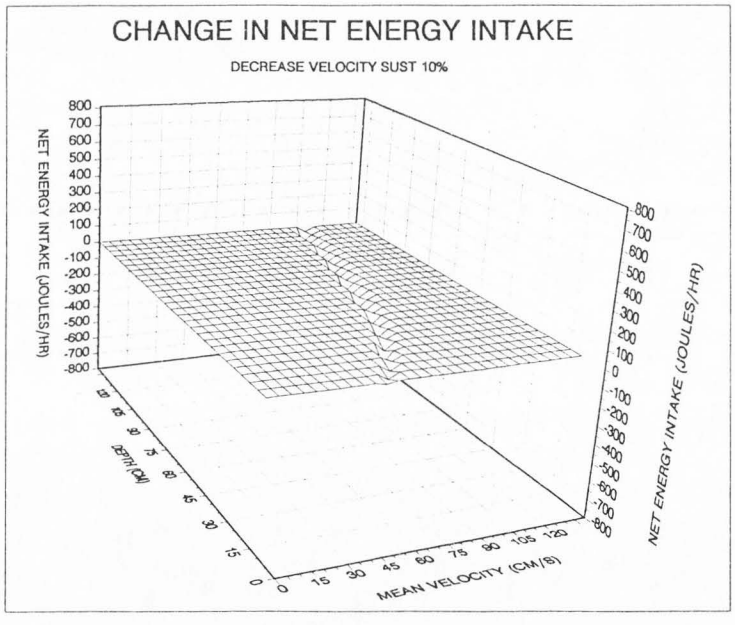

Figure A20. Graphic of the change (sensitivity) of net energy intake to a 10% decrease (perturbation) in the sustained velocity. The surface presented was derived by subtracting the perturbed NEI surface from the baseline NEI surface.

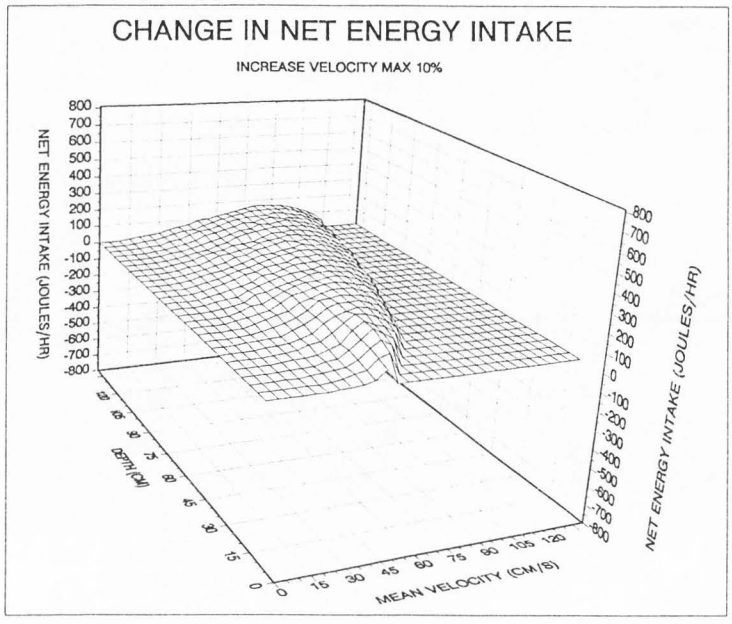

Figure A21. Graphic of the change (sensitivity) of net energy intake to a 10% increase (perturbation) in the maximum capture velocity. The surface presented was derived by subtracting the perturbed NEI surface from the baseline NEI surface.

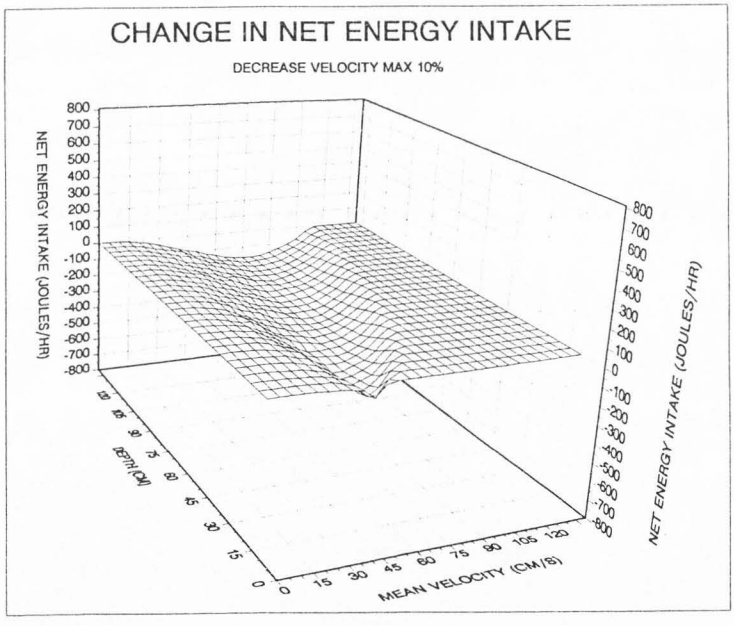

Figure A22. Graphic of the change (sensitivity) of net energy intake to a 10% decrease (perturbation) in the maximum capture velocity. The surface presented was derived by subtracting the perturbed NEI surface from the baseline NEI surface.